Application of FTLOADDS to Simulate Flow, Salinity, and Surface-Water Stage in the Southern Everglades, Florida

By John D. Wang, Eric D. Swain, Melinda A. Wolfert, Christian D. Langevin, Dawn E. James, and Pamela A. Telis

Prepared in cooperation with the South Florida Water Management District as part of the Comprehensive Everglades Restoration Plan

Scientific Investigations Report 2007–5010

U.S. Department of the Interior
U.S. Geological Survey

U.S. Department of the Interior
DIRK KEMPTHORNE, Secretary

U.S. Geological Survey
Mark D. Myers, Director

U.S. Geological Survey, Reston, Virginia: 2007

For product and ordering information:
World Wide Web: *http://www.usgs.gov/pubprod*
Telephone: 1-888-ASK-USGS

For more information on the USGS--the Federal source for science about the Earth, its natural and living resources, natural hazards, and the environment:
World Wide Web: http://www.usgs.gov
Telephone: 1-888-ASK-USGS

Suggested citation:

Wang, J.D., Swain, E.D., Wolfert, M.A., Langevin, C.D., James, D.E., and Telis, P.A., 2007, Application of FTLOADDS to Simulate Flow, Salinity, and Surface-Water Stage in the Southern Everglades, Florida: U.S. Geological Survey Scientific Investigations Report 2007–5010, 114 p.

Contents

Figures

Appendix Figures

Tables

Conversion Factors, Acronyms, and Abbreviations

Multiply	By	To Obtain
centimeter (cm)	0.3937	inch (in.)
meter (m)	3.281	foot (ft)
meter per day (m/d)	3.281	foot per day (ft/d)
meter per second (m/s)	3.281	foot per second (ft/s)
meter per year (m/yr)	3.281	foot per year (ft/yr)
kilometer (km)	0.6214	mile (mi)
square kilometer (km^2)	0.3861	square mile (mi^2)
cubic meter (m^3)	264.2	gallon (gal)
cubic meter per second (m^3/s)	264.2	gallon per second (gal/s)
cubic meter per day (m^3/d)	264.2	gallon per day (gal/d)

Acronyms

ADAPS	Automated Data Processing System
ADI	Alternating Direct Implicit
CERP	Comprehensive Everglades Restoration Plan
DIFMEAN	difference in means
DTPM	Dynamic Thiessen polygon method
EFDC	Environmental Fluid Dynamics Code
ESICS	Embedded Southern Inland and Coastal Systems application
ET	evapotranspiration
FBFKFS	Florida Bay Florida Keys Feasibility Study
FTLOADDS	Flow and Transport in a Linked Overland/Aquifer Density Dependent System
GHB	general-head boundary
JBWS	Joe Bay Weather Station
MAE	mean absolute error
MB	Manatee Bay
NOAA	National Oceanic and Atmospheric Administration
OIH	Old Ingraham Highway
PET	potential evapotranspiration
PEV	percentage of explained variance
PM	Penman-Monteith evapotranspiration equation
ppt	parts per thousand
psu	practical salinity units
PT	Priestley-Taylor evapotranspiration equation
SDP	standard data period

SFNRC	South Florida Natural Resources Center
SFWMD	South Florida Water Management District
SFWMM	South Florida Water Management Model
SICS	Southern Inland and Coastal Systems
SOFIA	South Florida Information Access
SWIFT2D	Surface-Water Integrated Flow and Transport in Two Dimensions
s/m	seconds per meter
TIME	Tides and Inflows in the Mangroves of the Everglades
TSB	Taylor Slough Bridge
USACE	U.S. Army Corps of Engineers
USGS	U.S. Geological Survey
UTM	Universal Transverse Mercator

Vertical coordinate information is referenced to the North American Vertical Datum of 1988 (NAVD 88); horizontal coordinate information is referenced to the North American Datums of 1927 and 1983 (NAD 27 and NAD 83).

Application of FTLOADDS to Simulate Flow, Salinity, and Surface-Water Stage in the Southern Everglades, Florida

By John D. Wang, Eric D. Swain, Melinda A. Wolfert, Christian D. Langevin, Dawn E. James, and Pamela A. Telis

Abstract

The Comprehensive Everglades Restoration Plan requires numerical modeling to achieve a sufficient understanding of coastal freshwater flows, nutrient sources, and the evaluation of management alternatives to restore the ecosystem of southern Florida. Numerical models include a regional water-management model to represent restoration changes to the hydrology of southern Florida and a hydrodynamic model to represent the southern and western offshore waters. The coastal interface between these two systems, however, has complex surface-water/ground-water and freshwater/saltwater interactions and requires a specialized modeling effort. The Flow and Transport in a Linked Overland/Aquifer Density Dependent System (FTLOADDS) code was developed to represent connected surface- and ground-water systems with variable-density flow.

The first use of FTLOADDS is the Southern Inland and Coastal Systems (SICS) application to the southeastern part of the Everglades/Florida Bay coastal region. The need to (1) expand the domain of the numerical modeling into most of Everglades National Park and the western coastal area, and (2) better represent the effect of water-delivery control structures, led to the application of the FTLOADDS code to the Tides and Inflows in the Mangroves of the Everglades (TIME) domain. This application allows the model to address a broader range of hydrologic issues and incorporate new code modifications. The surface-water hydrology is of primary interest to water managers, and is the main focus of this study. The coupling to ground water, however, was necessary to accurately represent leakage exchange between the surface water and ground water, which transfers substantial volumes of water and salt.

Initial calibration and analysis of the TIME application produced simulated results that compare well statistically with field-measured values. A comparison of TIME simulation results to previous SICS results shows improved capabilities, particularly in the representation of coastal flows. This improvement most likely is due to a more stable numerical representation of the coastal creek outlets.

Sensitivity analyses were performed by varying frictional resistance, leakage, barriers to flow, and topography. Changing frictional resistance values in inland areas was shown to improve water-level representation locally, but to have a negligible effect on area-wide values. These changes have only local effects and are not physically based (as are the unchanged values), and thus have limited validity. Sensitivity tests indicate that the overall accuracy of the simulation is diminished if leakage between surface water and ground water is not simulated. The inclusion of a major road as a complete barrier to surface-water flow influenced the local distribution and timing of flow; however, the changes in total flow and individual creekflows were negligible. The model land-surface altitude was lowered by 0.1 meter to determine the sensitivity to topographic variation. This topographic sensitivity test produced mixed results in matching field data. Overall, the representation of stage did not improve definitively.

A final calibration utilized the results of the sensitivity analysis to refine the TIME application. To accomplish this calibration, the friction coefficient was reduced at the northern boundary inflow and increased in the southwestern corner of the model, the evapotranspiration function was varied, additional data were used for the ground-water head boundary along the southeast, and the frictional resistance of the primary coastal creek outlet was increased. The calibration improved the match between measured and simulated total flows to Florida Bay and coastal salinities. Agreement also was improved at most of the water-level sites throughout the model domain.

1 - Introduction

The Comprehensive Everglades Restoration Plan (CERP), authorized by the Water Resources Development Act of 2000, provides a framework and guide to restore, protect, and preserve the water resources of central and southern Florida, including the Everglades (U.S. Army Corps of Engineers and South Florida Water Management District, 2003). One goal of CERP is to determine the physical modifications and operational changes to the Central and Southern Florida Project necessary to restore the Everglades ecosystem of southern Florida. This requires a thorough evaluation of Florida Bay within the context of the numerous regional water-resource issues in southern Florida. To meet this need, the U.S. Army Corps of Engineers (USACE) and the South Florida Water Management District (SFWMD) initiated the Florida Bay Florida Keys Feasibility Study (FBFKFS) in 2001 (Worth and others, 2002) to (1) evaluate Florida Bay and its connections to the Everglades, Gulf of Mexico, and the Florida Keys marine ecosystems; and (2) determine the modifications that are needed to restore water-quality and ecological conditions of Florida Bay successfully, while maintaining or improving conditions in the marine ecosystem of the Florida Keys.

The need to accurately represent the Everglades flows and their respective flow alterations caused by restoration changes led the U.S. Geological Survey (USGS) to (1) develop a coupled surface-water/ground-water numerical code known as the Flow and Transport in a Linked Overland/Aquifer Density-Dependent System (FTLOADDS), and (2) apply the code to inland and coastal regions of the Everglades. The FTLOADDS code combines the two-dimensional hydrodynamic surface-water model SWIFT2D and the three-dimensional ground-water model SEAWAT, and accounts for leakage and salt flux between the surface water and ground water (Langevin and others, 2005). The code was initially applied to the Southern Inland and Coastal Systems (SICS) model domain (Swain and others, 2004; Wolfert and others, 2004). In the current effort, initiated in 2002, FTLOADDS is applied to the larger Tides and Inflows in the Mangroves of the Everglades (TIME) model domain. This ongoing effort is conducted as part of the USGS Greater Everglades Priority Ecosystem Sciences Initiative in cooperation with the SFWMD.

In order to achieve the objectives of the FBFKFS study, the TIME application is linked to a Florida Bay hydrodynamic model developed for the FBFKFS study to simulate water movement and water quality in the bay (Hamrick and Mustafa, 2003). The TIME application supplies the Florida Bay model with freshwater flow and nutrient inputs entering Florida Bay from the Everglades, and water levels and salinity on the Atlantic Ocean and Gulf of Mexico boundaries. As with the SICS application, TIME is modified to accept inland boundary conditions from the regional South Florida Water Management Model (SFWMM). This will allow the representation of proposed restoration scenarios to be input to TIME from the SFWMM, and the effects on coastal flows to be transferred from TIME to the Florida Bay model.

1.1 - Purpose and Scope

This report documents the application of the FTLOADDS code to the TIME domain to generate information for restoration objectives. Specific code enhancements to FTLOADDS and its application to the TIME domain are described in detail. The linkage of the domains to the regional southern Florida model also is described, as well as the results of scenarios using boundaries developed from the regional model. FTLOADDS is a coupled surface-water/ground-water model, but because the surface-water regime primarily controls the hydrology and is of primary interest to water managers, most of the discussion herein concerns the surface-water part of the simulation.

Parameters used as input for the TIME application are described, including topography, frictional resistance, aquifer characteristics, natural and anthropogenic barriers, rainfall and evapotranspiration, wind, water-level and salinity boundaries, and initial conditions. The application is calibrated using water levels, flows, and salinities at known stations in the model domain. Sensitivity studies of the TIME application are conducted by comparing output statistics between the calibrated application and a simulation with (1) the model-code version used for SICS, (2) local adjustment of frictional resistance, (3) no leakage, (4) a road barrier removed, and (5) lowered land surface. The sensitivity of the model to these changes is used to establish error bounds for simulation results and to identify critical factors controlling model flow and transport.

Results are presented in appendix 1 for different scenario runs conducted for the FTLOADDS application to the SICS area using boundaries generated from SFWMM runs. The TIME scenario testing is an ongoing effort, with results documented as they are produced.

1.2 - Description of Study Area

The TIME application domain consists of about 5,250 km^2 of pine uplands, cypress swamps, hardwood hammocks, wetland marsh, wet prairies, lakes, sloughs, and rivers contained within the Everglades National Park/Big Cypress National Preserve areas. The TIME domain contains the SICS domain and is bounded to the north by Tamiami Trail (U.S. Highway 41); to the west by U.S. Highway 29 and the Gulf of Mexico; to the south by Florida Bay; and to the east by Levee 31N, Levee 31W, and U.S. Highway 1 (fig. 1).

Several major drainage features, including sloughs and topographic depressions, intersect the approximately 85- × 75-km TIME domain. The largest feature is Shark River Slough, which extends southwest from the northeastern corner of the domain to the west coast shoreline. Taylor Slough is a smaller drainage feature in the southeastern corner of the domain and, together with several coastal creeks, is the main source of runoff to northeastern Florida Bay. The northwestern part of the domain has several additional sloughs

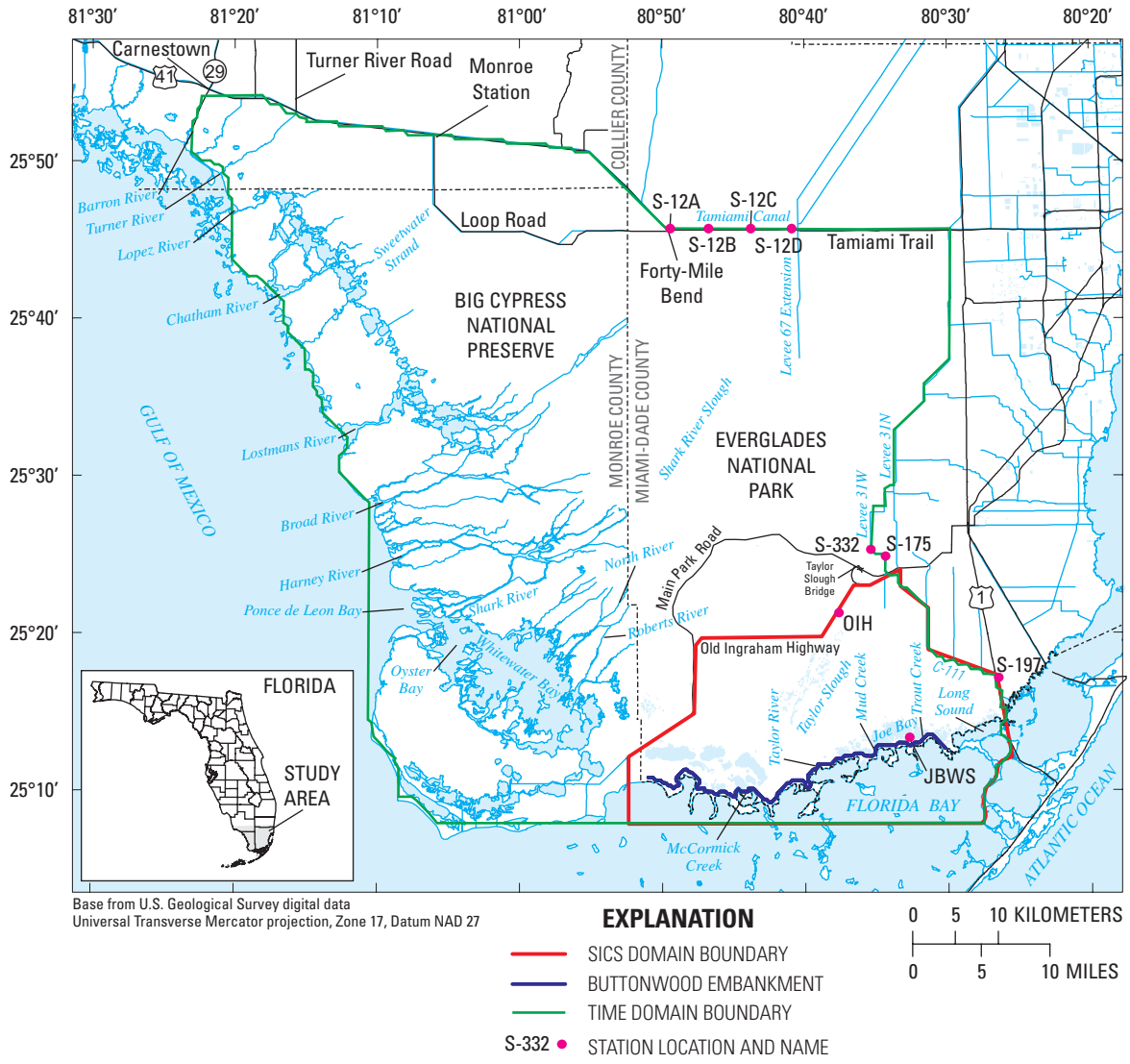

Figure 1. Location of the TIME and SICS domains, geographic features, and water-management features.

and rivers that are connected by the Wilderness Waterway and discharge to the coast. The major west coast rivers from north to the south include Barron River, Turner River, Lopez River, Chatham River, Lostmans River, Broad River, and Harney River (fig. 1). Other major west coast rivers include the Shark River, which flows into Oyster Bay, and the North and Roberts Rivers, which flow into Whitewater Bay. A higher elevation feature along the southeastern coast, the Buttonwood Embankment (fig. 1), is estimated to be about 15 cm higher than the surrounding marsh (Holmes and others, 2000).

The climate of southern Florida is characterized by a wet season from May to September and a dry season from October to April. Sixty percent of the total rainfall occurs during this wet season. Daily rainfall patterns during the wet season and dry season are characterized by local, small-scale afternoon showers and frontal patterns, respectively.

The highly permeable surficial aquifer system extends over most of the Everglades National Park/Big Cypress National Preserve area and underlies a thin peat layer in some areas. The surficial aquifer system generally thins toward the west in the study area.

1.3 - Acknowledgments

The majority of support for this model development comes from the USGS Greater Everglades Priority Ecosystem Studies Initiative. Dewey Worth of the SFWMD provided support of TIME application development with the FKFBFS. Appreciation also is extended to the Interagency Modeling Center for their consultation, advice, and reviews.

2 - Development of the FTLOADDS Model Code

The USGS developed the FTLOADDS model code by combining the SWIFT2D and SEAWAT models to provide insight into the Everglades system and supply freshwater flow information to the Florida Bay model. The FTLOADDS code integrates surface- and ground-water flow and transport (Langevin and others, 2004) and is designed to simulate two-dimensional variable-density overland flow (Schaffranek, 2004; Swain, 2005), as well as three-dimensional, fully-saturated variable-density ground-water flow (Guo and Langevin, 2002). The original FTLOADDS application (code versions 1.0 and 1.1) used only the SWIFT2D surface-water code. In subsequent applications (code versions 2.1 and 2.2), SWIFT2D was coupled to the SEAWAT ground-water model code and additional enhancements were made.

The original SICS application utilizes the SWIFT2D surface-water code only (Swain and others, 2004), and later, the coupled surface-water/ground-water FTLOADDS version 2.1 (Langevin and others, 2005). The larger TIME domain (fig. 1) utilizes the enhanced version 2.2 code.

2.1 - Version 2.1 of the FTLOADDS Code

The SWIFT2D model algorithms in version 2.1 of FTLOADDS are described by Swain and others (2004) and Swain (2005), and the SEAWAT algorithms in version 2.1 of FTLOADDS are described by Langevin and others (2004). The version of the SWIFT2D surface-water code that existed prior to the Everglades application is described by Schaffranek (2004). The primary features that distinguish the surface-water component of version 2.1 from this pre-Everglades SWIFT2D code are: (1) incorporation of rainfall and evapotranspiration effects; (2) a depth-varying Manning's friction coefficient for wetlands; (3) a wind-sheltering coefficient to represent emergent vegetation; and (4) the coupling to the ground-water model to represent leakage (transfer between surface water and ground water) with included salinity flux.

2.2 - Version 2.2

Version 2.2 of FTLOADDS has several enhancements not available in version 2.1. These enhancements can be classified as either generic code modifications or specific application modifications. The classifications do not include model input differences between applications.The generic SWIFT2D code modifications include the following:

- The wetting and drying algorithm has been modified to allow for rewetting directly from rainfall recharge.
- Frictional resistance terms are defined at cell faces in version 2.2 rather than at cell centers as in version 2.1.
- Evapotranspiration is computed using the modified Penman method (Eagleson, 1970), rather than cell-by-cell according to the best-fit equation discussed by Swain and others (2004).

Specific application modifications include the following:

- In version 2.1, rainfall is specified at 15-minute intervals and is spatially interpolated for each model cell. In version 2.2, rainfall is spatially uniform over defined zones and specified as 6-hour averages.
- In version 2.1, obstructions to surface-water flow, such as the coastal Buttonwood Embankment (fig. 1) is defined by the barriers formulation originally designed to represent weirs, and the coastal rivers are defined as low barriers with a representative flow coefficient. In version 2.2, the coastal embankment is defined by modified cell-face frictional-resistance terms, and coastal creeks are represented as gaps with specified friction terms.

A discussion of the generic code modifications follows, including those associated with drying and flooding, friction coefficients, and evapotranspiration. Specific application modifications for the study area are discussed later as part of the version 2.2 application to the TIME domain. Background information on the SWIFT2D model structure is available in Schaffranek (2004) and Swain (2005).

2.2.1 - Drying and Flooding

The SWIFT2D model requires the representation of surface-water cells in wet and dry states, as well as transitions between states. This must be represented empirically, because the hydrodynamic flow equations do not support a transition to zero flow depth. The SWIFT2D code used in version 2.1 of FTLOADDS represented drying and flooding of surface-water grid cells by a method found to be slow, prone to instabilities, and not entirely consistent between subroutines. One technique used to increase model performance in version 2.1 involved increasing the user-prescribed water depth limit at which the wet and dry transition is assumed to occur. This caused substantial water retention, however, in cells assumed to be dry. Additionally, the multiple use of the Chezy parameter, used also as a flag to denote a dry cell in the model, introduced unnecessary complexity in the code and is no longer beneficial because of the increased memory available on current computer platforms.

These issues have been resolved in version 2.2, which computes the land-surface altitude used to indicate the dry/wet state differently than version 2.1. To determine the dry/wet state for a grid cell (centered on a water-level point), version 2.2 represents the effective land-surface altitude by the maximum corner elevation of a cell plus a threshold depth where the element is considered to have no surface water. This threshold depth is typically set to 0.001 m instead of 0 m to

avoid dividing by zero in the flow equations. This land-surface definition is not used in the flow calculations; the actual grid-cell corner altitudes are used to estimate flow cross sections along a cell side. Thus, for computing the dry/wet state, land surface in a cell is represented as horizontal, which eliminates the problem of partially wet cells and associated inconsistencies in mass balance. In the constituent solution, an average of the corner land altitudes is used to calculate cell volume. This introduces the concept of captured volume, defined as the volume between the average land surface (for a specified area) and the water surface at the effective land-surface altitude defined above. Captured volume is always present in the cell and affects constituent concentrations even though the volume is hydrodynamically inactive. This volume can be visualized as water confined in depressions and ponds.

To differentiate between wet and dry states, the user defines a "marginal depth" (Schaffranek, 2004, p. 79). When the water-surface elevation is greater than the effective land-surface altitude plus one-half the marginal depth for at least three time steps, the cell is wet and the full Chezy friction coefficient is used.

When the water-surface elevation is between the effective land-surface altitude and one-half the marginal depth above this, the cell is considered semidry. Volume and mass exchange still occur in the semidry condition, with wet cells using simplified transfer rules instead of the full equations of motion. This allows cells to either continue draining until completely dry or to fill up and become wet again, depending on the water elevation of the neighboring wet cell. No transfer occurs between cells that are both semidry. Leakage and rainfall accumulation occur regardless of cell status, whereas evaporation/evapotranspiration is removed only when adequate surface water is available. Totally dry cells (when the water-surface elevation drops to the effective land-surface altitude) have the same flux calculations as semidry cells.

The wet to semidry transition is checked in subroutines SEPU, SEPV, and CVAL (Schaffranek, 2004). The semidry to wet transition is checked in subroutine FLO and occurs (once per time step) after the first sweep of the Alternating Direction Implicit (ADI) solution. The marginal depth is set to 0.01 m for applications described herein.

2.2.2 - Friction Coefficient

A change was made in the SWIFT2D simulation grid location where the frictional resistance term, Manning's *n*, is defined. In the FTLOADDS version 2.1 code, friction coefficients are assigned to cell centers, but flows are calculated at the sides of each grid cell. The friction coefficient used in the flow calculation is the mean of the friction coefficients for the two cells adjacent to the side. The version 2.1 formulation does not lend itself to anisotropic situations, such as a flow barrier along a cell side. To make the friction at the side sufficiently large to simulate a barrier, the cell friction must be set to a large value, which affects flow calculations across all sides of that cell. To alleviate this problem, version 2.2 uses an alternate formulation in which each cell face has an independently prescribed friction coefficient. For cases with a barrier such as an elevated road or other flow control, the cell-face friction coefficients in version 2.2 can be prescribed directly at the appropriate cell side to block flow until the barrier or road crown is inundated.

For backward compatibility, a frictional scheme in version 2.1 can be duplicated in version 2.2 by setting the cell-face friction coefficients to the mean of the adjacent cell friction coefficients. Other possible uses for side friction coefficients exist; for example, to represent subgrid-scale flow features such as poorly resolved channels.

2.2.3 - Evapotranspiration

Evaporation and transpiration, collectively referred to as evapotranspiration (ET) herein, are major components of the water budget in southern Florida. In FTLOADDS version 2.1, ET rates are calculated in the SWIFT2D code by a best-fit equation based on solar radiation and water depth (Swain and others, 2004). The empirical nature of this formulation is of concern, and the importance of ET must be considered in developing the FTLOADDS version 2.2 formulation. The total water budget for the domain is derived largely from the difference between ET and precipitation. ET can represent a large part of the overall water budget, so caution is necessary when estimating ET; relatively small errors in ET estimates can cause substantial water-budget changes. Because this study primarily concerns a water-budget temporal scale on the order of days or weeks, ET estimates must be as accurate as possible at those time scales. Furthermore, the ET formulation must be sufficiently robust to be used both under historically measured conditions and also under possible climatic and hydrologic scenarios proposed by CERP. These scenarios are expected to involve substantial changes to flows, stages, and hydroperiods. Therefore, the ET formulation in the FTLOADDS version 2.2 code needs to be more physically based than the formulation in version 2.1.

The regression technique in FTLOADDS version 2.1 (Swain and others, 2004) uses the Priestly-Taylor (PT) equation (Linsley and others, 1982, p. 162-163) as a "guide" for the relation between parameters. A coefficient was regressed against solar radiation and water depth to develop a best-fit equation. This coefficient then was considered regionally valid and used as an independent variable, along with solar radiation, in another least-squares best fit to measured ET values. This best-fit equation matched measured values with a multiple correlation coefficient of 0.8. The inherent assumptions were that: (1) the regressed coefficient is a representative variable that roughly corresponds to a coefficient in the PT equation, (2) solar radiation is an acceptable surrogate for net radiation, and (3) the variability of other terms in the PT equation has negligible effects. Because the PT equation is not implicitly used, this can be considered as more of an empirical equation than a physically based equation.

Although reasonable results were obtained for the range of field conditions represented in the application of FTLOADDS version 2.1 to the SICS domain, concerns about applying the formulation outside the range of field conditions in the calibration period (as well as concerns stated earlier) led to the approach presented here.

Several investigators (Abtew, 1996; German, 2000; Abtew and others, 2003) have found that measured ET rates can be reproduced with models that vary in complexity. The simpler models require adjustment coefficients but, when properly calibrated, they can provide ET hindcasts with accuracy comparable to hindcasts from models that incorporate more complete model physics. For prediction of ET, which includes the calculation of ET when conditions are different from those of the calibration period, the simplified methods may become less accurate and their use more difficult to defend. Therefore, using the empirical ET formulation in FTLOADDS version 2.1 could be problematic at other locations with different water depths and under restoration scenarios in which water depths are expected to vary substantially from historical records.

A more generally valid ET formulation was developed for the FTLOADDS version 2.2. The approach uses the Penman-Monteith (PM) formulation for vegetated sites to calculate potential evapotranspiration (PET) and to derive actual ET by modifying PET according to a measure of available water (Eagleson, 1970). The following analysis describes the calibration of the PM formula and the derivation of an available water function using available data.

The basis of the analysis presented here is provided by the data collected and reported by German (2000) and more recent data also collected by E.R. German (U.S. Geological Survey, written commun., 2005). In these studies, two open-water and seven vegetated sites were instrumented to determine ET rates (table 1) using the Bowen ratio and energy-balance method (Oke, 1978). Data collection at the stations began in January 1996 and ended between 1997 and 2002. This report discusses analyses of ET only at the vegetated sites. The collected data represent the best available information for determining actual ET at sites in the Everglades; however, additional wind-velocity profile data, such as aerodynamic roughness and boundary layer displacement, were not collected. These data would be required to apply a theoretical formulation such as the PM equation.

All observations with negative net radiation (resulting in a computed latent heat gain to the system) were assumed to be associated with zero PET. Negative net radiation was relatively small and may have resulted from soil and water heat storage rather than condensation. It was difficult to ascertain whether condensation events actually occurred because humidity sensors typically do not function well at 100 percent relative humidity—the assumed indicator for condensation. Condensation amounts probably were small; therefore, this process was ignored in version 2.2 of the FTLOADDS model.

The modified Penman formulation (alternatively, the combined or combination method) is a widely used energy balance method to estimate evaporation over open water and originally was proposed by Eagleson (1970). The basic equation of the formulation is:

$$\frac{Q_e}{A_s} = \rho_e L_e E = \frac{\Delta(Q_a / A_s) + (\rho C_p / r_a)(e_{s2} - e_2)}{\Delta + \gamma}, \quad (1)$$

where:

Q_e/A_s is evaporative heat flux per unit horizontal area;
ρ_e is density of evaporated liquid water;
L_e is latent heat of evaporation;
E is evaporation;
Δ is slope of the saturation vapor-pressure curve;
Q_a/A_s is available energy per unit horizontal area;
ρ is air density;
C_p is specific heat of air;
r_a is the aerodynamic resistance term;
e_{s2} is saturation vapor pressure at level 2;
e_2 is vapor pressure at level 2, located slightly above boundary layer displacement; and
γ is the psychometric constant.

The aerodynamic resistance term, r_a, is given by the following:

$$r_a = \frac{K_m}{K_h} \frac{1}{\kappa^2 u_z} \frac{z_e - D}{z_u - D} \ln^2 \frac{(z_u - D)}{z_o}, \quad (2)$$

where:

K_m is moisture eddy diffusivity;
K_h is heat eddy diffusivity;
κ is von Karman constant;
u_z is wind speed;
z_e is height of vapor pressure sensor;
D is boundary layer displacement height;
z_u is height of wind sensor; and
z_o is aerodynamic roughness.

For vegetated sites, this formulation was modified to estimate PET by including a resistance term that represents the resistance to flow through plant stomata. This PM formula is (Eagleson, 1970; Jacobs and Sudheer, 2001):

$$\frac{Q_e}{A_s} = \rho_e L_e PET = \frac{\Delta(Q_n / A_s) + (\rho C_p / r_a)(e_{s2} - e_2)}{\Delta + \gamma(1 + r_s / r_a)}, \quad (3)$$

where PET is potential evapotranspiration, and r_s is the average resistance of evaporative surfaces.

More sophisticated formulations exist that explicitly account for the multiple sources of evaporation in cases involving ET at vegetated sites with standing water or sites

Table 1. Evapotranspiration monitoring site characteristics.

[Site locations are shown in German (2000, fig. 1). THP, air temperature and humidity sensor]

Site number	Latitude/ longitude	Plant community	Vegetation	Lower THP	Wind sensor	Comments
			Height above land surface (meters)			
1	263910/0802432	Cattails	3.0	4.3	0.3	Considerab1e flow regulation, nutrient-rich water, abundant duckweed
2	263740/0802612	Open water	.0	1.5	None	
3	263120/0801011	Open water	.0	1.4	2.4	Some lily pads at times
4	261855/0801257	Dense sawgrass	19.8	3.0	5.8	
5	261530/0804417	Medium sawgrass	1.8	2.5	5.5	Dry part of some years
6	254443/0803011	Medium sawgrass	1.8	2.7	4.0	
7	253659/0804208	Sparse sawgrass	1.5	22.3	4.3	
8	252111/0803802	Sparse rushes	.9	1.2	3.7	Dry part of each year
9	252135/0803146	Sparse sawgrass	10.7	1.6	3.7	Dry part of each year

with humid soil. The simpler PM formula was tested for the current study, however, using a resistance value that represents an average of all evaporative surfaces; this is occasionally referred to as the "big-leaf" approximation. This simpler approach was used primarily because more advanced methodologies require additional data that were not available.

A somewhat different expression for the aerodynamic resistance term than that given in equation 2 has been proposed by others (for example, Abtew and Obeysekera, 1995). In evaluating r_a, equation 3 assumes the eddy diffusivity ratio (K_m/K_h) is 1. Equation 3 further assumes that wind frictional effects are spatially homogeneous and that heat storage in soil, water, and plants is minimal.

To prescribe the heat-flux and net-radiation variables in these formulas, it is usually also necessary to know air temperature and water-surface temperature. These data were collected by German (2000) and, therefore, are not only readily available but can be assumed to be reasonably constant in space.

A conceptual difficulty arises when selecting the temperature to use for the saturated vapor pressure/temperature slope Δ in equations 1 and 3. The slope should be estimated at the location where vapor pressure is saturated. For open water, it is appropriate to use the temperature at the water surface. For vegetated sites, however, it may be more appropriate to use the air temperature at the surface where evaporation takes place. Such a location is not uniquely determined, because evaporation can occur from both water and vegetation surfaces. Some combination of water-surface temperature and leaf-surface temperature, may therefore, be appropriate. In the PM formulation used in version 2.2 of the model, this location is assumed to be the same level where the log velocity profile indicates zero velocity, for example, at the top of the aerodynamic roughness height z_o.

A few of the input variables for equations 1, 2, and 3 (D, r_s, and z_o) are not measured and must be estimated from the measured ET data set. As guidance for determining these parameters, D is about equal to an average canopy height; r_s is on the order of 100 s/m, and z_o ranges from one to tens of centimeters over vegetation (Oke, 1978; Perrier and Tuzet, 1991; and Stannard, 1993). Actual ET can be derived from PM/PET estimates based on available water, which is formulated herein as a function of water level. The second term in the numerator on the right-hand side of equation 1, $(\rho C_p / r_a)(e_{s2} - e_2)$, is referred to as the aerodynamic term. This term is zero when the air is assumed to be saturated.

Version 2.2 of the FTLOADDS code uses the formulation in equation 3 with the assumptions described in this section to compute ET rates. Section 3.3.7 contains further discussion of the development of parameters for the TIME application.

3 - Application of FTLOADDS to Tides and Inflows in the Mangroves of the Everglades (TIME)

The application of the FTLOADDS version 2.2 code to the TIME domain is the first successful representation of this area's hydrology by such a complex model. Primary among the purposes of TIME is to represent the coastal area of Everglades National Park and link the inland regional management model to the offshore hydrodynamic model. Figure 2 shows the linkage between the models used to simulate various restoration scenarios and their effects on Florida Bay. The SFWMM, which is the primary regional tool used to assess CERP scenarios and also known as the "2 × 2 model" because of its 2- × 2-mi grid cells, provides stage and flow inputs to the SICS and TIME applications for restoration model scenarios (Wolfert and others, 2004). Additionally, the TIME domain extends south of the Florida Bay coastline (fig. 2), and provides flow and salinity inputs to the Florida Bay hydrodynamic model along its northern boundary and receives stages and salinities from the Florida Bay model in subsequent model simulations.

After the FTLOADDS code was implemented successfully for the SICS application (Swain and others, 2004; Langevin and others, 2005), and applied to restoration scenarios as shown in appendix 1, the model area was expanded to encompass the TIME domain (fig. 1). This expanded application utilizes 500-m grid spacing, and allows FTLOADDS to represent the complete coastline as well as the coastal flows used in the Florida Bay hydrodynamic model. Additionally, the water-management controls along Tamiami Canal and Levee 31N Canal (fig. 1) can be represented directly as boundary conditions in the TIME domain. The objective of the TIME application, given the limited time and effort that can be put into the calibration in order to be responsive to the restoration effort, is not to obtain the best possible fit, but rather to make timely and necessary adjustments to bring model physics in accordance with the physics illustrated in the data.

The TIME input is derived from multiple sources and makes use of the large amount of field information that has been collected in the area. A total of 157 simulations were made for model calibration and sensitivity analysis. Simulation number 142 was used as a base to compare with subsequent sensitivity simulations, and the information derived from these comparisons was used to develop simulation 157.

The calibration of the TIME application described is appropriate for use as a tool to represent system changes caused by restoration scenarios. Further refinements beyond this level of calibration were not necessary because they are not needed to make decisions on restoration management. Because the emphasis of the restoration effort is the relation of coastal flows and water deliveries, the salinity transport representation is not as refined as the flow representation.

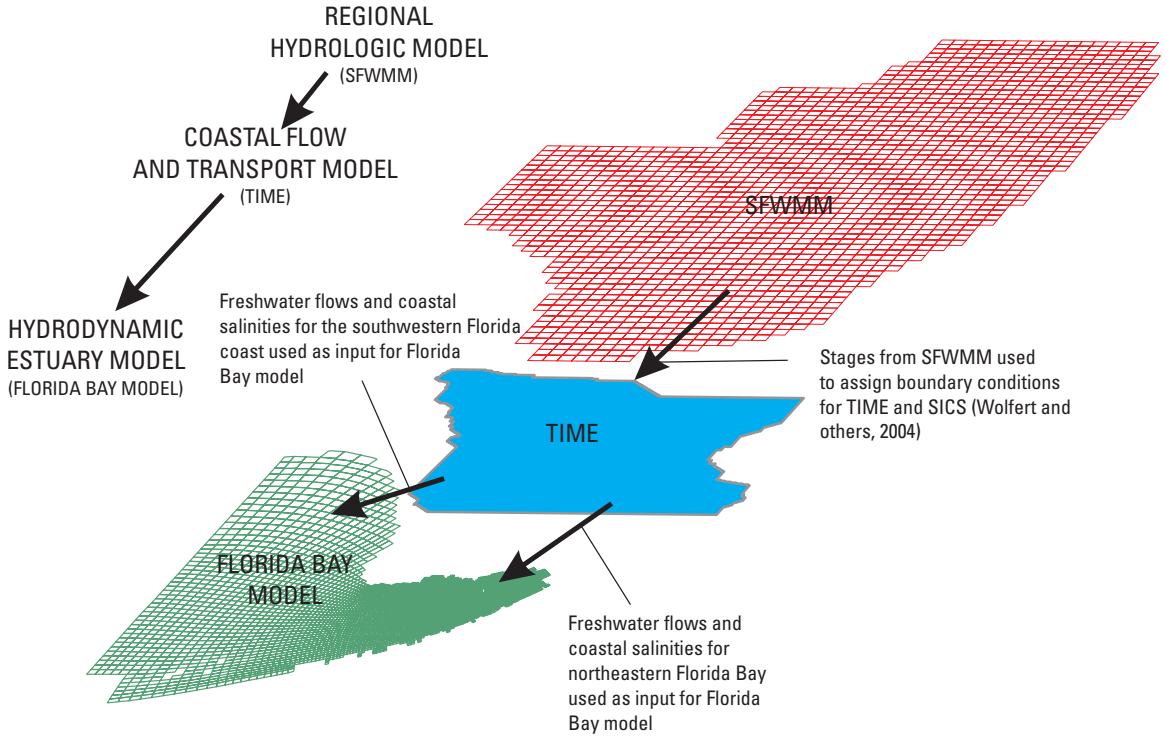

Figure 2. Linkage between models used to simulate various restoration scenarios. SFWMM is South Florida Water Management Model.

3.1 - Simulation Period

Field-measured stage, flow, and salinity data from January 1, 1996, to December 31, 2002, were used to calibrate and verify the TIME application. This 7-year Standard Data Period (SDP) was selected because it provides a more comprehensive and more complete field data set than had existed previously.

When used for CERP scenario simulations, the TIME application is driven by boundary inputs from the numerical regional water-management model (SFWMM). The CERP scenarios are designed to use the measured hydrologic conditions for the period ending in 2000. The SFWMD presently has no plans to extend SFWMM runs beyond the year 2000. Originally, the plan was to run TIME scenario simulations for the same 7-year SDP used for model calibration. In discussions between the USGS and FBFKFS Modeling Subteam, however, the following points were noted about different simulation periods:

- The 1996-2002 period may be too short to adequately assess biological performance measures under different hydrologic conditions. This period would be reduced to 5 years if the simulation is required to end at 2000.
- The 1996-2000 period may not contain representative years of dry or wet conditions.
- Given a time period of at least 10 years to encompass a variety of conditions using data from the SFWMM ending in the year 2000, choosing the 1990-2000 period represents a general compromise, considering the extra effort required to assemble input data and the need for higher model run times to represent the desired longer duration of simulation runs.

The flows and stages in the TIME domain respond to direct input such as rainfall and evapotranspiration, but also to lateral boundary input through culverts, bridge openings, structures, and ground-water flows. These model lateral-boundary input variables are available for the SDP as continuously monitored data or are modeled using rating curves and appropriate stages. Ground-water flows are determined through leakage interactions with the ground-water model. Stage data, creek/river flow data, and salinity data are used for calibration.

3.2 - Model Grid

Square grid cells centered on the water-level points are used in the FTLOADDS model for computational efficiency because the solution method for the surface-water equations assumes equal cell dimensions in both directions. Flow is defined at the center of each vertical cell face. This configuration facilitates easy formulation of mass conservation and head-gradient driven flows.

The grid for the TIME application consists of 174 rows and 194 columns of cells (fig. 3). The 500-m resolution noted earlier was chosen as a compromise between accurately representing available topographic data and obtaining reasonable run times. Of particular concern was the need to make hundreds of multiyear runs. The east-west and north-south alignment of rows and columns was not a requirement, but was chosen in this case because of the road and levee features. Grid rows are numbered from 1 to 174 (south-north) in the SWIFT2D surface-water module and from 1 to 174 (north-south) in the SEAWAT ground-water module. The reversed numbering schemes were necessary to preserve the numbering conventions used by SWIFT2D and SEAWAT in their original forms. Columns in both modules are numbered from west to east. The surface-water cell indexing used in this report is consistent with a normal right-handed Cartesian coordinate system.

The TIME model grid was referenced to Universal Transverse Mercator (UTM) coordinates for input and post processing, with the center of cell (1,1) located at the NAD 83 and UTM zone 17 coordinates listed below:

Longitude (degrees, minutes, seconds west)	Latitude (degrees, minutes seconds north)	Longitude (decimal degree west)	Latitude (decimal degree north)	UTM easting (meters)	UTM northing (meters)
81:23:12.76427	25:07:35.04428	81.38687896	25.12640119	461000	2779000

The surface-water model represents two-dimensional horizontal flow and consists of a single layer of variable water depth consistent with the vertically averaged equations of motion, whereas the ground-water model represents three-dimensional flow using 10 vertically stacked layers. Although the layers in the ground-water model can be varied in height, all layers except the surface layer (layer 1) are 7 m thick. Layer 1 is variable in thickness because the bottom of the layer is at a constant altitude of 7 m below NAVD 88, and the top represents model land surface. The numbers of layers and thickness of each were dictated by the need to accurately represent local stratigraphy and minimize model run times.

Each module requires input that specifies whether a cell is active or inactive. The governing equations are solved only for active cells to minimize computational effort. Active SWIFT2D cells correspond to those within the TIME domain boundary shown in figure 3. The active layer 1 cells in SEAWAT have the same areal extent as corresponding cells in SWIFT2D. The extent of active SEAWAT cells in lower layers is reduced as dictated by stratigraphy.

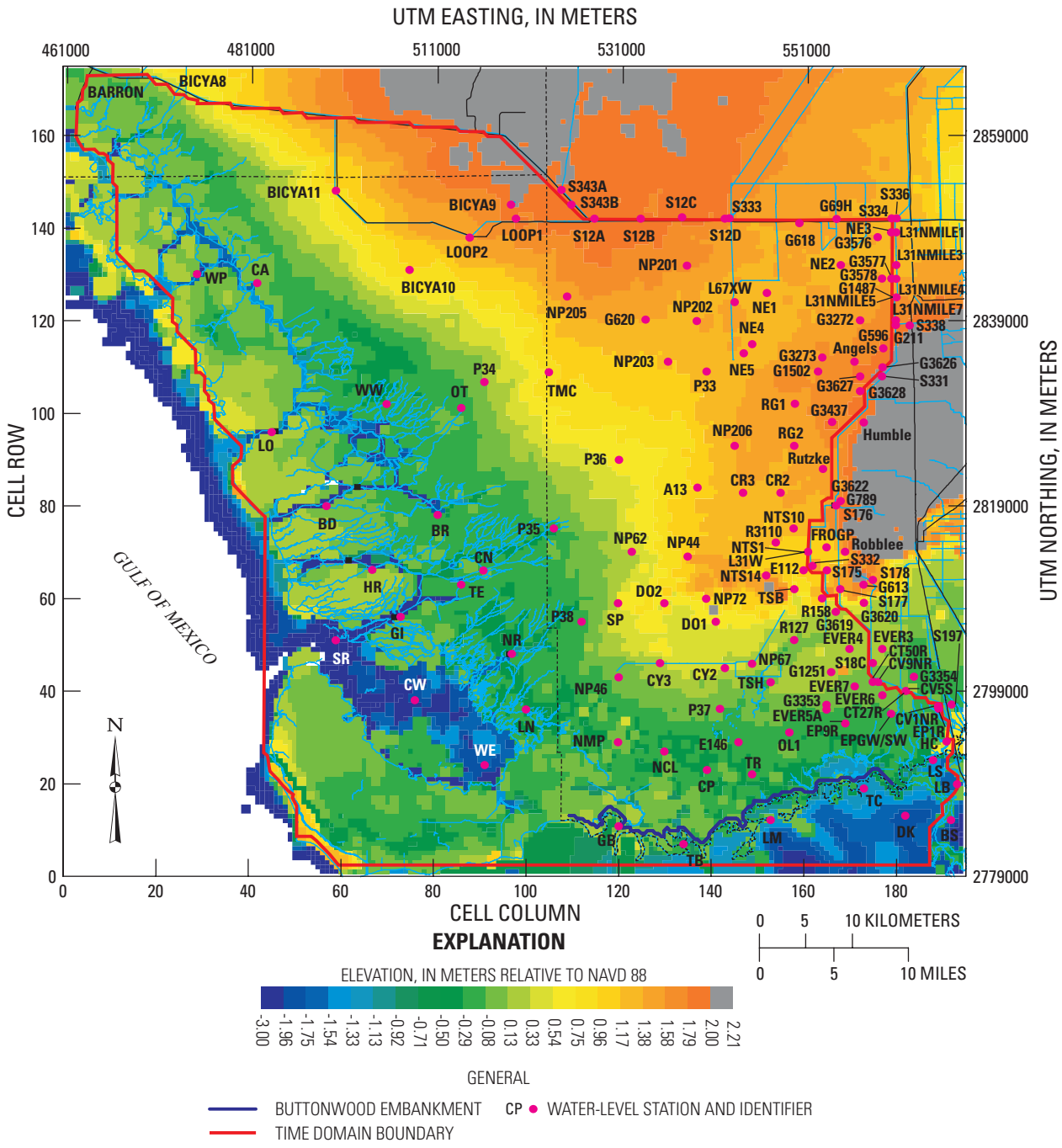

Figure 3. Extent of active cells and land-surface altitudes in the TIME area.

3.3 - Model Input

The subsequent sections describe the parameters used as input for the TIME application. These parameters include topography; Manning's *n*; soil stratigraphy; hydraulic conductivities; thin layer characteristics; roads, bridges, culverts, and structure flows; stage; rainfall; potential evapotranspiration (PET); wind; coastal water levels and salinities; and ground-water boundary conditions.

3.3.1 - Topography and Bathymetry

Topography for the TIME application, including submerged and unsubmerged inland areas plus offshore bathymetry, is derived from data collected by Desmond (2003), National Oceanographic and Atmospheric Administration (NOAA) topographic data (Hansen and Dewitt, 1999), and the National Hydrographic Database Regional Drainage coverage. The model topography is shown in figure 3, with all altitudes referenced to NAVD 88. Although the original topography for this model was obtained from the modeling effort of R.W. Schaffranek and others (U.S. Geological Survey, written commun., 2003), substantial changes have been made to the model topography to better reflect altitude data in the TIME domain. The present model topography can be reconstructed most nearly by using all altitude data points in a kriging scheme to obtain model land-surface altitudes and then modifying this topography to account for major lakes and rivers. These data also define the top of layer 1 in the ground-water input data. The files containing the topography for the surface-water model and the ground-water model are listed in appendix 2.

3.3.2 - Defining Manning's *n* at Cell Faces

A description of the frictional resistance to flow for surface water must be provided as input to SWIFT2D in the form of Manning's *n*. The Manning formulation was derived for fully developed turbulent rough flow. The TIME application uses Manning's *n* in a conventional manner; however, the meaning of *n* as a measure of roughness is compromised. In this case, *n* represents an equivalent roughness that describes the skin friction and form drag against the land surface and any vegetation within the water column. Additionally, the value of *n* is modified by subgrid-scale topography. Thus, Manning's *n* values for cells in the TIME application can differ substantially from the 0.03 *n* value typical for natural channels.

The SICS application used remotely sensed vegetation type and density to estimate Manning's *n*. For the TIME application, remote-sensed maps were obtained from John Jones (U.S. Geological Survey, written commun., 2003) at 500-m grid resolution and *n* values were derived based on previously established relations (Lee and Carter, 1999). Cells that are completely under water and have little vegetation were assigned Manning's *n* values closer to the 0.03 value as part of the calibration procedure. The calibration indicated that flow conveyance was globally too high; consequently, all *n* values were increased by 20 percent. The distribution of Manning's *n* values used in the TIME application is shown in figure 4.

The Buttonwood Embankment (fig. 1) is implemented as an obstruction to flow by setting the cell-side Chezy coefficient to 0.0001 to yield negligible flow. This coefficient cannot be set to zero because it appears in an equation denominator.

Where the Florida Bay creeks cut through the Buttonwood Embankment, the cell-side Chezy coefficient is adjusted to match calculated flows with measured flows. Using the equation Chezy coefficient = Depth$^{1/6}$/Manning's *n*, the equivalent Manning's *n* values for the individual creeks are 0.4 for Alligator Creek, 0.7 for McCormick Creek, 1.0 for Taylor River, 0.7 for Mud Creek, 0.08 for Trout Creek. The files that define the Manning's *n* for the wetland, Buttonwood Embankment, and coastal rivers are listed in appendix 2.

The low-gradient hydrologic system in the TIME domain does not respond markedly to subtle changes in Manning's *n*. When implementing sensitivity analyses and to quantify the effect of large-scale frictional changes, Manning's *n* was adjusted in the three rectangular areas shown in figure 5. The effects of this empirical test are discussed subsequently in section 3.7.2.

3.3.3 - Soil Stratigraphy, Hydraulic Conductivities, and Thin Layer Characteristics

The aquifer properties used in the ground-water module of the TIME application are based on those presented by Reese and Cunningham (2000) and Fish and Stewart (1991). Underlying the Biscayne aquifer is a semiconfining unit that becomes less confining near the east coast. Below this semiconfining layer lies the gray limestone aquifer, which becomes the surficial aquifer toward the west. As described earlier, the TIME application discretizes this stratigraphy using 10 horizontal layers, each of which (except for the top layer) is 7 m thick. Horizontal hydraulic conductivities are estimated to range between 50 and 5,000 m/d, and vertical conductivities are about 10 m/d. As examples, the hydraulic conductivity in layer 1 and the transmissivity in layer 5 are shown in figures 6 and 7, respectively. The input file for aquifer conductivities is named in appendix 2.

A thin-layer conceptual model was designed to account for a layer of peat at the soil surface. Although some observations of peat thickness exist (Cohen and Spackman, 1984; Scheidt and others, 2000), the areal coverage is sparse and maps were not available. Thus, an idealized thin layer (0.5 m thick) was implemented throughout the domain with an initially assumed vertical conductivity of 0.004 m/d. Tests indicated that decreasing the vertical conductivity of the topmost aquifer layer: (1) substantially reduced leakage and generally increased surface flows to Florida Bay, (2) substantially increased flows in Shark River and North River (fig. 1), and (3) changed flow slightly at other west coast rivers. Modeled flows with and without ground-water/surface-water leakage are presented in table 2.

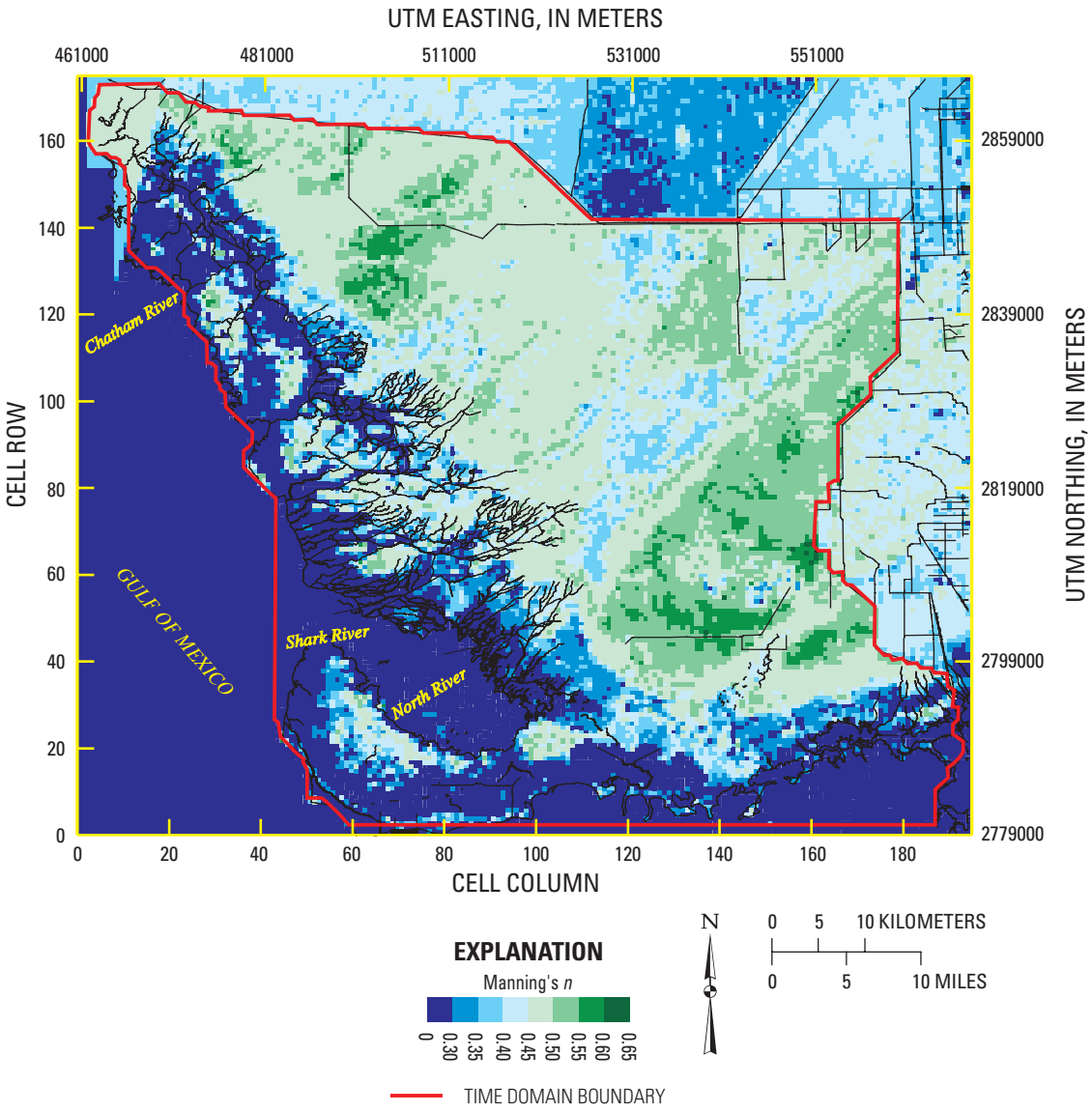

Figure 4. Distribution of Manning's *n* values in the TIME area.

Increasing vertical conductivity causes ground-water head to rise more quickly, but has little effect on total leakage unless the soil is unsaturated. An investigation was not conducted to determine the possible effects of increased vertical conductivity in areas where the soil is unsaturated.

3.3.4 - Incorporation of Roads, Bridges, Culverts, and Structure Flows

Main Park Road and Old Ingraham Highway have the potential to impede flow within Everglades National Park, even though both have numerous culverts (fig. 1). Main Park Road is an elevated paved road, whereas Old Ingraham Highway is unpaved, slightly elevated, and has been removed in some areas. A study of flows through the culverts along Main Park Road indicated that, on an event-based temporal scale of 1 day to a few days, water is impounded on the upstream side of the road, causing substantial flow through the culverts in many places (Stewart and others, 2002). Flow through the culverts seems sufficient to minimize substantial backwater effects on long time scales, allowing surface-water flow to continue coastward. The main influence of the road is hypothesized, therefore, to affect mainly the local flow pattern, and possibly a small delayed reaction in coastal flows. This study also found that flow through culverts along the southern part of Main Park Road is almost exclusively to the west.

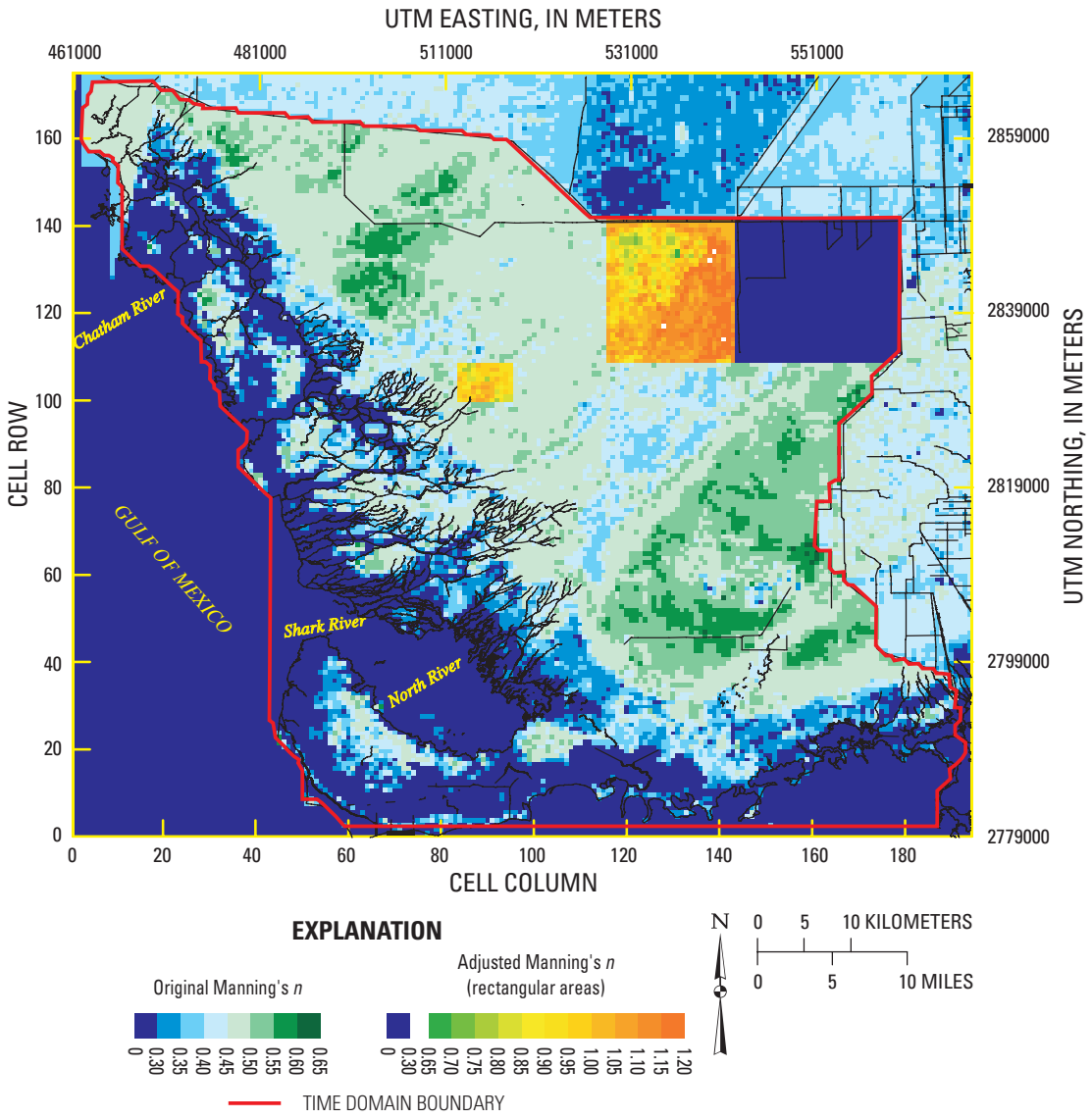

Figure 5. Adjustments to Manning's *n* values in the TIME area.

Stewart and others (2002) suggested that actual flow near Main Park Road with its culverts is expected to resemble the base case in which the road is neglected; that is, its effect is considered to be minimal. An upper bound on the possible effect of the barrier was established by simulating the case in which the road is treated as a complete flow obstruction.

Another potential barrier is Loop Road in the northwestern part of the TIME domain (fig. 1). The road is paralleled by a borrow canal that is connected directly to Tamiami Canal beneath the bridge at U.S. Highway 41. Robert Sobczak (Big Cypress National Preserve, oral commun., 2004) indicated that:

- The borrow canal (fig. 1) supplies water to Sweetwater Strand, which drains into Chatham River; this flow is large enough to drain the prairies near Monroe Station (fig. 1).
- The culverts under Loop Road are numerous, and some are in questionable condition.
- Most of the surface-water flow from Monroe Station to Forty-Mile Bend probably moves toward Sweetwater Strand and Chatham River.
- Numerous box culverts and regular culverts along the southern part of Loop Road probably drain through Dayhoff Slough into Lostmans River.

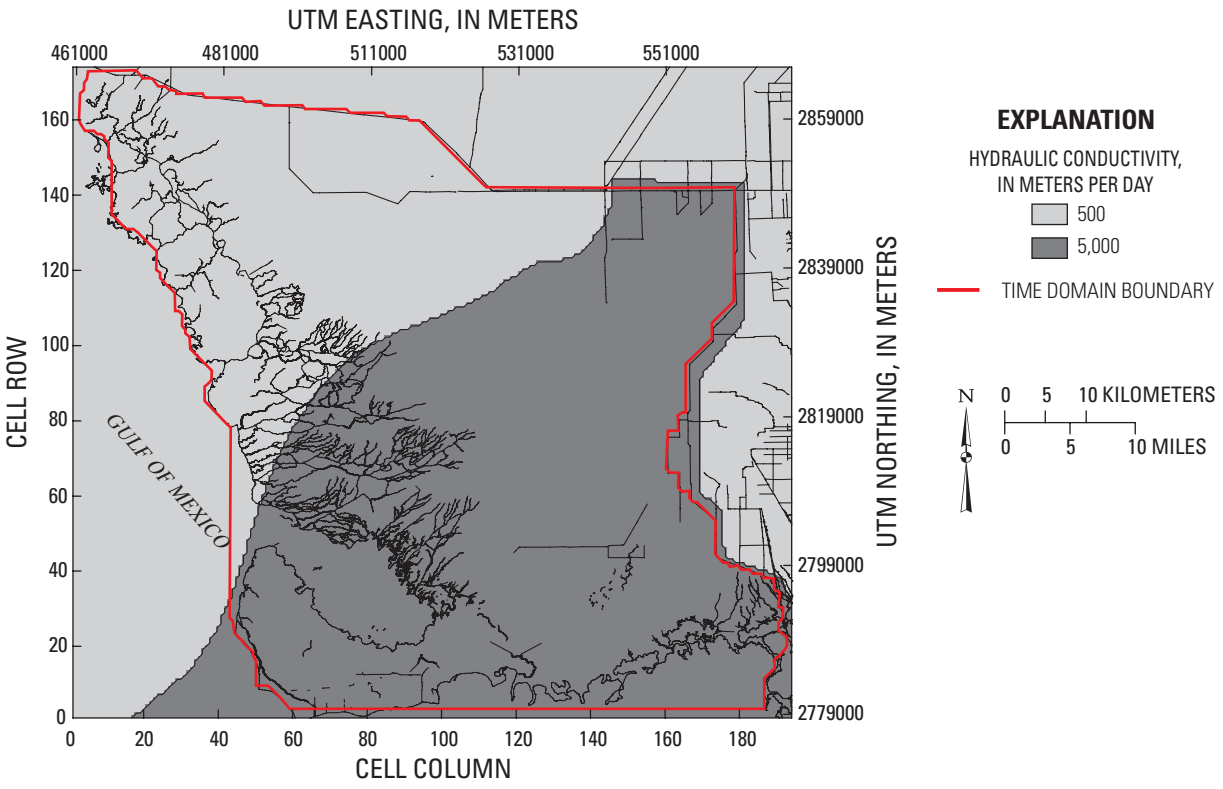

Figure 6. Hydraulic conductivities in layer 1 in the TIME area.

Based on this information, it seems justified to consider Loop Road's obstruction to be negligible.

Flows under Tamiami Trail into Everglades National Park are monitored and recorded by the USGS. The SFWMD data from the DBHYDRO database and the USGS data from the SOFIA database were used to force the model. Because stage was a primary calibration variable, it was not specified along the model boundaries except at the coastal interface. Culvert flows were grouped into three segments along the Tamiami Trail: Carnestown to Monroe Station, Monroe Station to Forty-Mile Bend, and Levee 67 extension to Levee 31N (fig. 1). Recorded inflows then were applied along each of these segments in a nearly uniform manner. Between Forty-Mile Bend and the Levee 67 extension, four major structures (S-12A to S-12D) release water into the Everglades through bridged openings (fig. 1). In this case, flows were applied across the entire side of the cell nearest to each structure.

Inflows were prescribed along the Levee 31W Canal at the S-332 pump structures and S-175 structure, and along the C-111 Canal (fig. 1). Flow from the C-111 Canal was assumed to equal the difference in flows through structures S-18C and S-197. The S-175 discharge was distributed as source flow along the length of the canal. The S-332 pump flows were treated in the same manner as flows through the S-12 structures. The input files for surface-water inflows are listed in appendix 2.

The flow quantities and relative magnitude of cumulative flows from the different structures are depicted in figure 8; structures S-12A to S-12D contribute the most flow. Collective flow beneath the Tamiami Trail west of Forty-Mile Bend nearly equals the S-12 flows, and collective flow east of S-12D equals about half of the S-12 flows.

3.3.5 - Stage Data for Boundaries

Numerous (105) water-level monitoring stations were identified, with more than 2 years of data recorded within the Everglades National Park/Big Cypress National Preserve area. These stations are distributed throughout the TIME domain, but most are located in the eastern part of the domain (fig. 9). These stations include ground-water sites (noted by the G prefix), surface-water sites, and a combination of both.

Because some areas periodically flood and dry, it was often difficult to differentiate between surface-water and ground-water measurement sites. Precise descriptions were not found regarding the type of water-level data collected at each site, which depends on exactly how each well was installed. For example, well casings are cemented in the ground at some sites and not at others—this determines whether the surface water or underlying ground water is being measured.

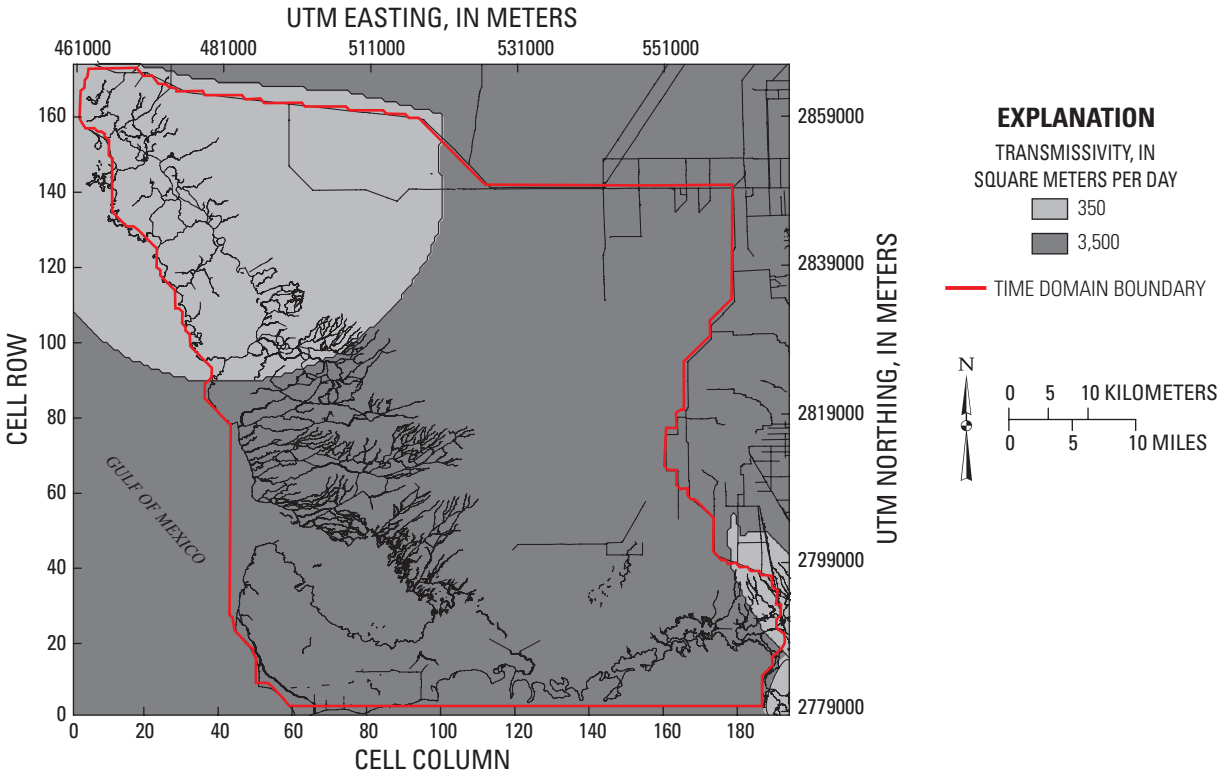

Figure 7. Transmissivity in layer 5 in the TIME area.

Table 2. Net average total flow (Q) and freshwater flow (Q_f) toward the coast for the standard data period.

[Site locations are shown in figure 1, ALAYC, vertical hydraulic conductivity; m/d, meter per day; m^3/s, cubic meter per second; Q, runoff volume; Q_f, net freshwater runoff with salt diffusion accounted for]

Location	Flow with leakage ALAYC = 0.004 m/d		Flow without leakage ALAYC = 0 m/d	
	Q (m^3/s)	Q_f (m^3/s)	Q (m^3/s)	Q_f (m^3/s)
Taylor Slough Bridge	4.57	4.57	5.97	5.96
Trout Creek	11.16	9.67	13.06	10.95
Mud Creek	1.08	.75	1.27	.87
Taylor River	1.16	.77	1.39	.91
McCormick Creek	1.15	.87	1.34	.98
Long Sound	1.39	.82	1.38	.80
Chatham River	18.29	5.26	18.46	5.16
Lostmans River	38.31	30.40	39.29	30.44
Broad River	10.65	6.24	10.97	6.29
Shark River	18.06	11.99	19.06	12.64
North River	7.11	6.12	7.56	6.80

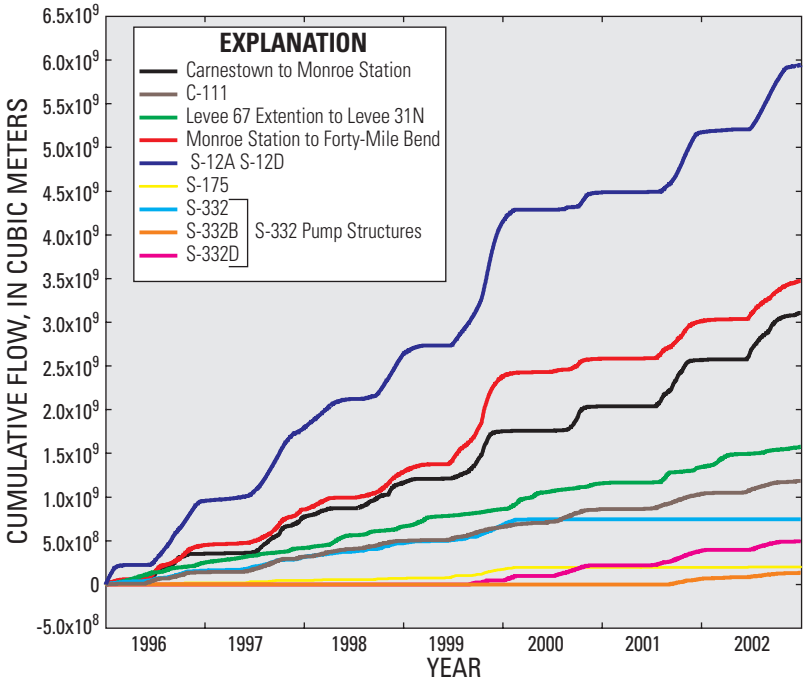

Figure 8. Cumulative flows at selected control structures in the TIME area.

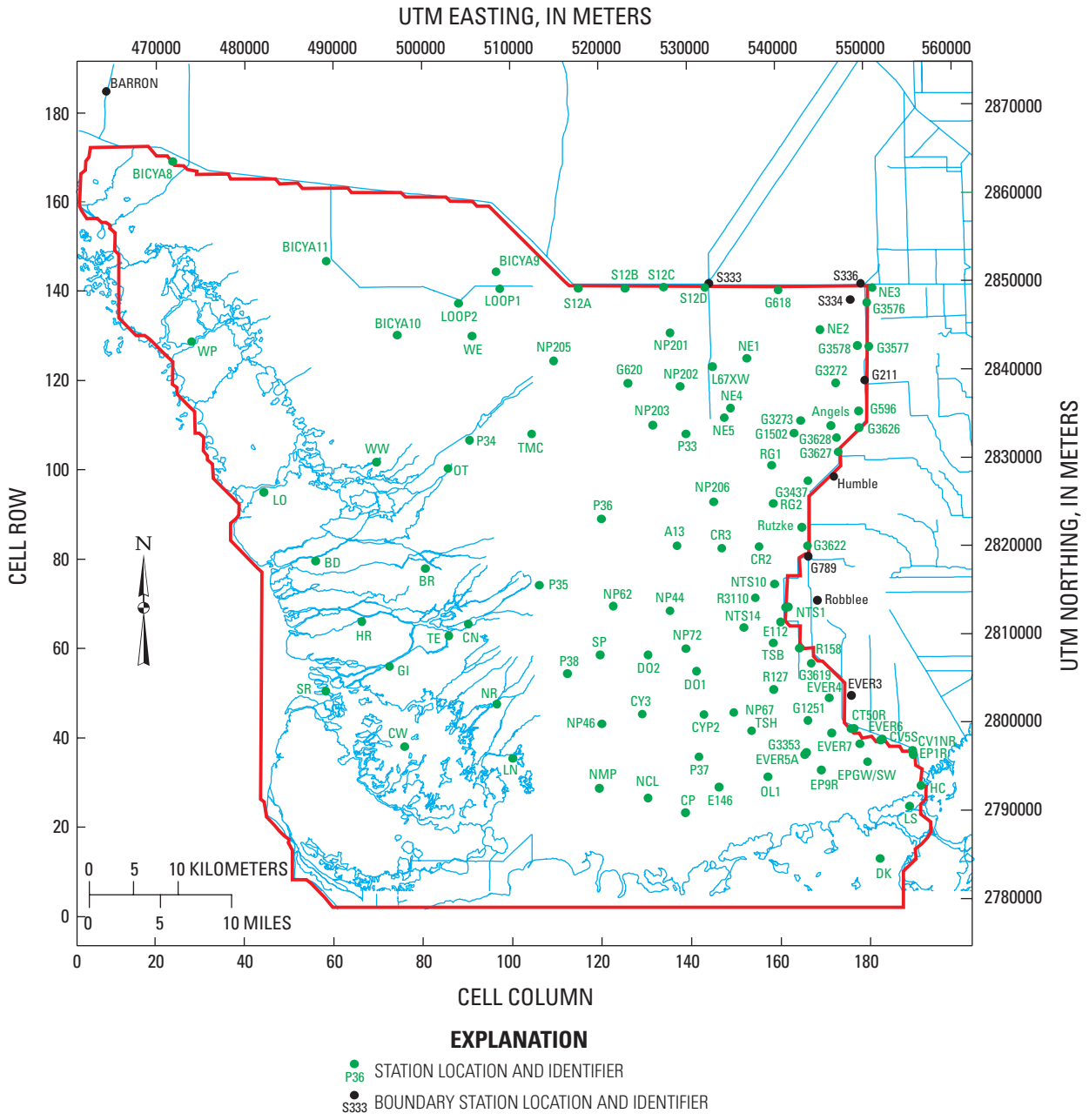

Figure 9. Location of stage recording stations in the TIME area.

For comparison with the model, gage measurements were assumed to represent surface-water stage or, when surface water was absent, ground-water head.

Most elevation records were referenced to NGVD 29, and therefore, were converted to NAVD 88 using the CorpsCon geodetic program (U.S. Army Corps of Engineers, 1999). Comparison with model results was difficult when the land-surface altitude adjacent to the gage and the corresponding model cell differed substantially. In such instances, the wetting, drying, and general water-level behavior were not directly comparable when surface-water depths were small.

Because the stage recordings are well distributed throughout the domain and records are available at most locations for a substantial portion of the SDP, stage is the primary variable used for model calibration. For this reason, stage values were not specified as boundary conditions in the model, except at the marine interface where tidal- and wind-induced water-level fluctuations must be prescribed. Several factors are responsible for the incomplete record at some of the sites. For example, Hurricane Irene damaged water-level gages as it moved up the Shark River Slough (fig. 1) in October 1999, resulting in the loss of several months of data.

3.3.6 - Rainfall Data

All available rainfall data for the period from 1996 to 2002 were compiled and used as input for TIME. Stations with more than 3 years of nearly complete record (70 of 72 stations) were used to derive an annually averaged daily rainfall rate in meters (fig. 10). The distribution of annual average rainfall reveals that relatively less rainfall occurs near the southern boundary of Everglades National Park and relatively more rainfall occurs near its eastern boundary.

To account for these variations without attempting to achieve more spatial resolution than provided by the available data, six zones were defined and assumed to have spatially uniform rainfall (fig. 11). These zones were defined on the basis of annual average daily rates (fig. 10). The rainfall rate in each zone was computed as the simple arithmetic mean of all stations in the zone with existing data. The arithmetic mean may provide less than an optimal estimate, if the rainfall gage locations are clustered. Because of the small variation in average annual rates (fig. 10), clustering of gages was considered to be of little importance. The arithmetic mean is easy to apply, even when data with substantial gaps are used, and it does not require any area-weighting assumptions. A higher resolution spatial distribution of rainfall could not be derived due to the limited number of rainfall stations. A covariance-based kriging method was not suitable because of the lack of stations in western Everglades National Park. The average rates were calculated for 6-hourly periods using hourly data, when available, and uniformly parsed daily data otherwise.

An independent review by the Interagency Modeling Center of the model rainfall procedure led to another interpolation scheme using a dynamic Thiessen polygon method (DTPM). The SFWMD performed the interpolation and provided daily rainfall amounts in each cell. The following factors are relevant for comparing the techniques: (1) the previously mentioned sparseness of rainfall gages in the western part of the domain, (2) the limited accuracy of individual rainfall observations, (3) consistency with rainfall prescribed in the SFWMM, (4) the lack of any physical basis for preferring either interpolation technique, and (5) the small variations in the average rates (fig. 10). Based on these factors, there is no justification for preferring one interpolation technique over the other. A comparison of the cumulative rainfall for each of the six zones with the average rainfall computed from the cell-by-cell DTPM interpolated values is shown in figure 12. A close agreement was found in zones 1 to 4, with the DTPM giving somewhat more rainfall in zones 5 and 6.

The zonal approach applied in the SICS model domain area yielded results similar to those obtained using the DTPM cell-by-cell spatial interpolation. Results obtained with the TIME application do not indicate any problems that could be improved using the DTPM, and thus, the zonal rainfall scheme in TIME continues to be used. The average annual zonal rainfall ranges from 1.21 to 1.53 m; other techniques yield similar rainfall totals. The input file for zonal rainfall is named in appendix 2.

3.3.7 - Potential Evapotranspiration Parameters

Evapotranspiration (ET) rates were computed for the TIME simulation at 6 hour intervals based on the formulation described in section 2.3. The input file for evapotranspiration values is named in appendix 2. ET is a primary component of the water budget; therefore, a considerable effort was made to develop the Penman (eq. 1) and Penman-Monteith (PM) (eqs. 1 and 3, respectively) formulations to adequately describe ET in the TIME domain under historical conditions and under hypothetical conditions, such as those posed in CERP scenarios (U.S. Army Corps of Engineers and South Florida Water Management District, 2003). Because the average resistance of evaporative surfaces, r_s, and the aerodynamic roughness, z_o, cannot be determined from the set of measurements collected for vegetated sites, these variables are inferred indirectly. Tests indicated that when the aerodynamic roughness term z_o is small, the aerodynamic term in equation 2 becomes insignificant regardless of the value of r_s used. In all cases, this causes a substantial underestimation of actual evapotranspiration compared with the Bowen ratio method estimates (German, 2000). For larger values of z_o, the variables r_s and z_o were adjusted to produce a "best-fit," producing ET rates with the same mean as observations as well as the largest explained variance. When aerodynamic roughness z_o was increased, the r_s value corresponding to the best-fit formulation results increased and was no longer within the 100 to 300 s/m range of reasonable values (Eagleson, 1970; Oke 1978). This problem was resolved by noting that the ranges for z_o yielding reasonable values of corresponding r_s were centered around 0.05 m for all vegetated sites when water-heat storage was taken into account and was somewhat smaller when water-heat storage was ignored. Therefore, a z_o value of 0.05 m was selected for all vegetated sites, and r_s was adjusted to obtain the same mean ET as indicated by the data.

As part of the model calibration and evaluation procedure, a comparison was made between the calibrated PM model and a Priestly-Taylor (PT) formulation previously calibrated to the same measured data set (German, 2000). The data obtained from German (2000) were filtered to remove any bad data points caused by equipment errors or downtime. In the original regression analysis by German (2000) using the PT equation, all values other than those originally screened out were used. This included nighttime ET values, which were negligible. The obtained squared correlation coefficients were about 0.7, but improved to about 0.9 when transient soil and water-heat storage were accounted for in the net radiation term.

To compare the calculated and actual ET values, the mean of the values used in the model was adjusted to 1.12 m/yr. Therefore, the value of r_s was varied until the mean calculated and actual ET rates were identical. Tables 3 and 4 display (for each data filtering technique) corresponding r_s values and the percentage of explained variance (PEV) for z_o values of 1 and 5 cm at each site; PEV is defined as 1 - (residual variance)/(data variance) and is expressed as a percentage. Other values

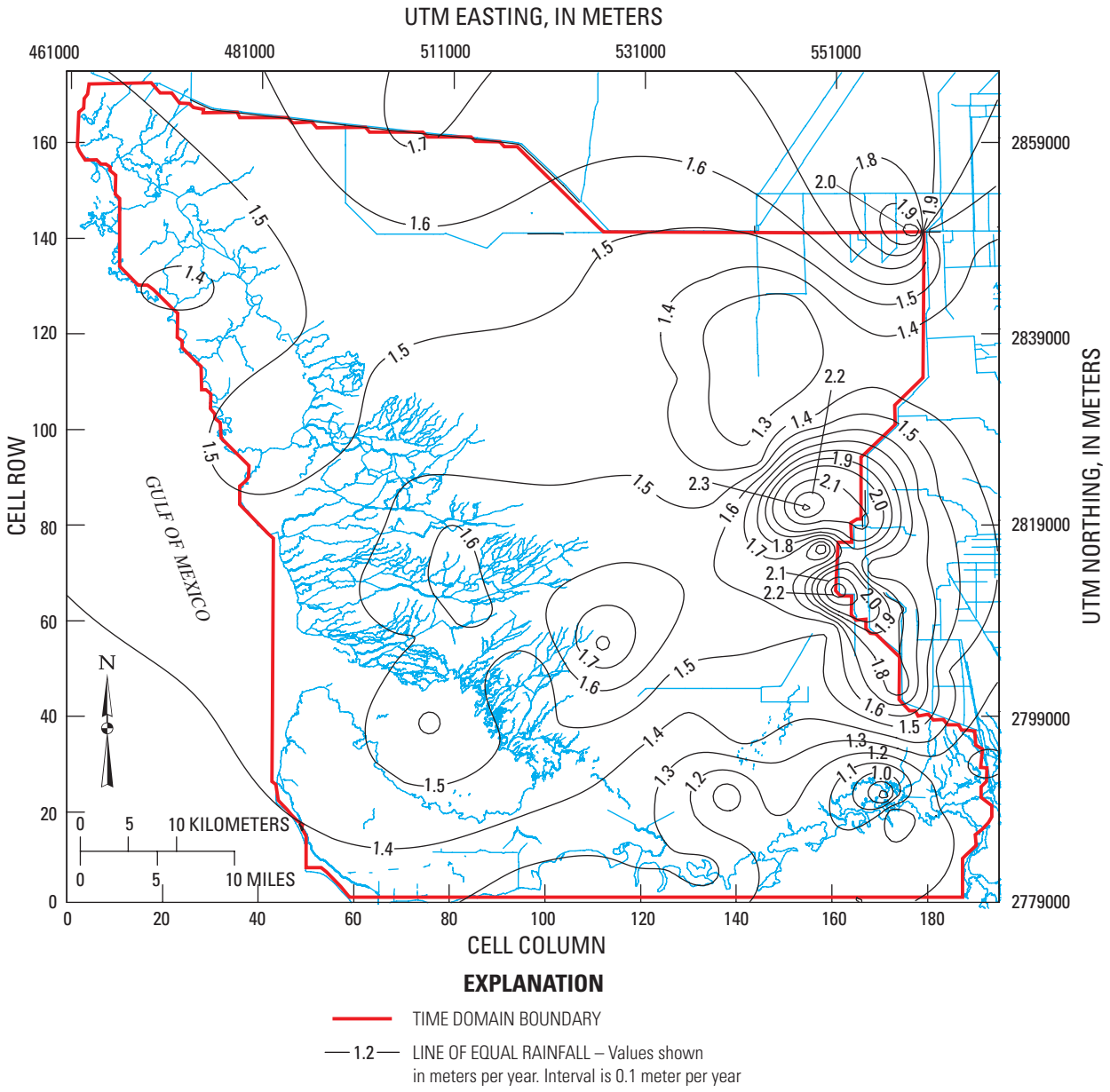

Figure 10. Distribution of annual average rainfall in the TIME area.

of z_o were tested, but produced r_s values that were outside the accepted range of values. Table 3 indicates that a z_o value of 1 cm generally results in a slightly higher PEV when water-heat storage is accounted for in the energy budget.

The just described calibration makes use of measured heat storage in the ponded water surrounding the vegetation. Specific measurements were made by German (2000) to estimate this component of the total energy budget. It is unlikely, however, that water-heat storage can be modeled in a predictive sense for this study. Ongoing advancements in utilizing air temperature for the prediction of water-heat storage (Shoemaker and others, 2005) may prove useful for future ET representation. Thus, the ability of the PM formulation to estimate ET was investigated when water-heat storage is not accounted for explicitly by adjusting net radiation. This is essentially a new PM formulation calibration that ignores water heat storage.

Table 4 shows ET values with full data filtration and without the adjustment to net radiation due to water-heat storage. This aerodynamic roughness comparison indicates

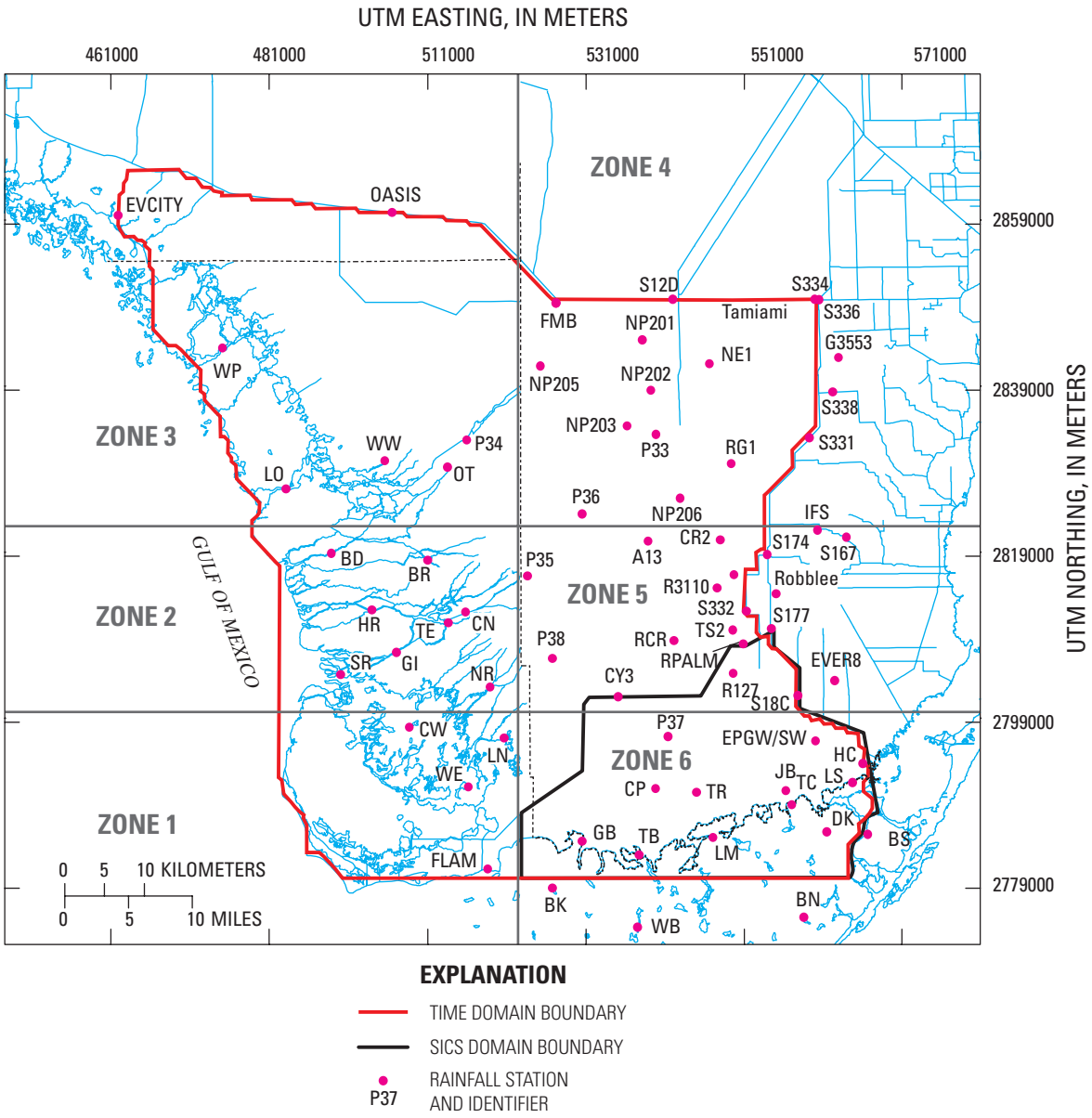

Figure 11. Location of rainfall stations within the rainfall zones of the TIME area.

that setting z_o to 5 cm yields the best results. Even though PEV typically decreased by about 20 percent, the PM method still explained a substantial part of the variance. As evidenced in table 4, the PT method yielded substantially poorer results in terms of total PEV. Water-heat storage data cannot be obtained for other time periods and hydrologic conditions. To preserve the mean ET rate, the calibration that ignores water-heat storage was used for ET modeling. The working assumption was that the calibrated model equation includes the average effect of heat storage in ponded water. The optimum r_s values obtained range between 128 and 165 s/m. The lower and upper values correspond to sites with sparse and dense vegetation, respectively. If the average r_s value for all vegetated sites was applied, however, PEV at individual sites decreased by only a few percent. It was not possible to distinguish individual site models from the average site model within the error bounds of the chosen ET formulation. Considering the other approximations and data uncertainty, a single r_s value, therefore, was applied across the entire vegetated modeling area.

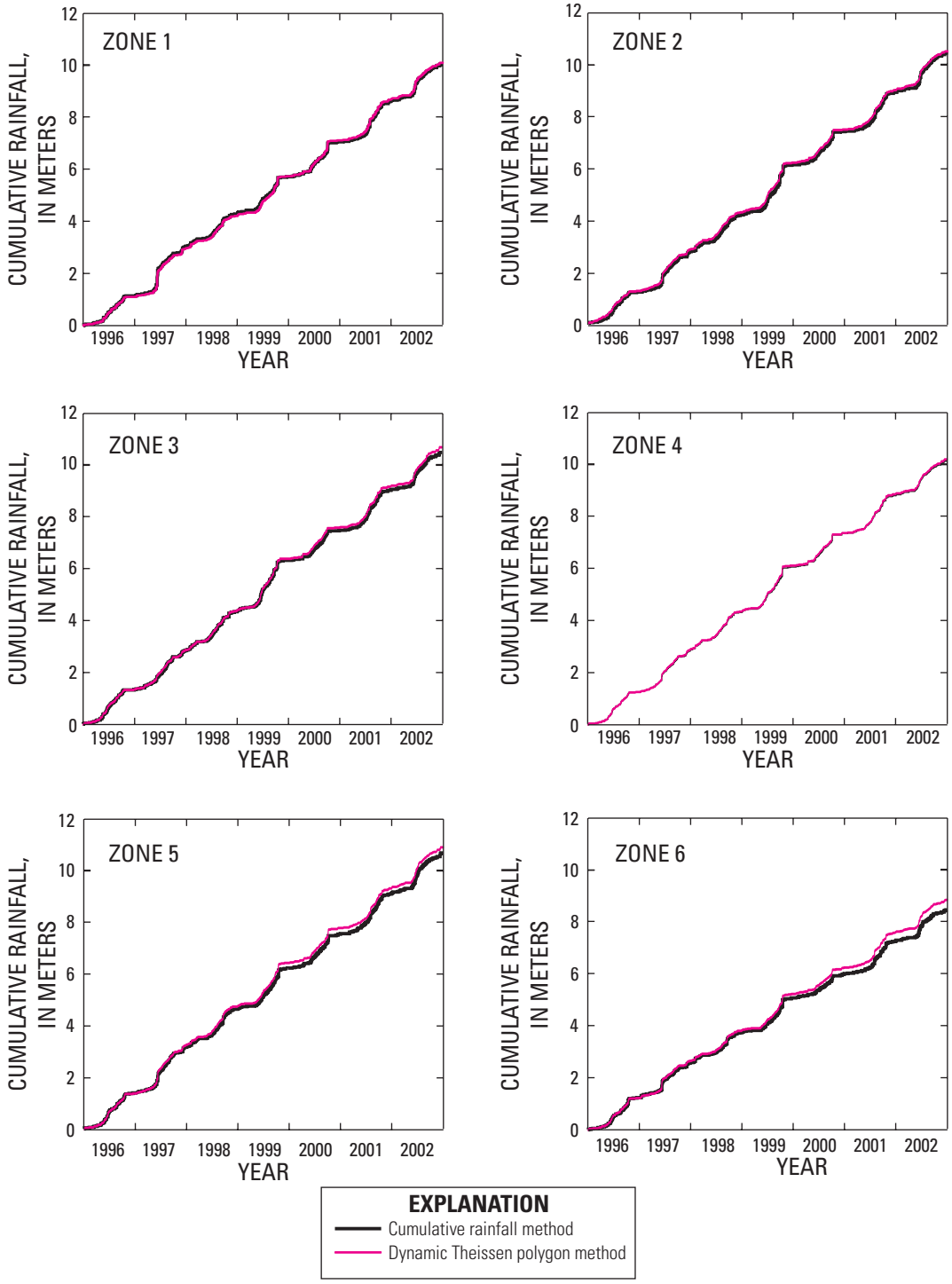

Figure 12. Comparison between cumulative rainfall for the six zones and average rainfall computed by the dynamic Thiessen polygon method. Zones are shown in figure 11.

Table 3. Calculated evapotranspiration values as a function of aerodynamic roughness (z_o) at vegetated sites in southern Florida.

[Site locations are shown in German (2000, fig. 1). r_s, average resistance of evaporative surfaces; PMPEV, Penman-Monteith method percentage of explained variance; PTPEV, Priestley-Taylor method percentage of explained variance]

Site	All data			Daytime data			Daytime data adjusted for water availability		
	r_s	PMPEV (percent)	PTPEV (percent)	r_s	PMPEV (percent)	PTPEV (percent)	r_s	PMPEV (percent)	PTPEV (percent)
z_o = 1 centimeter									
1	165	71.7	64.6	165	39.0	33.2	165	39.0	33.2
4	138	83.5	84.1	136	68.5	71.6	136	68.0	71.6
5	122	79.8	76.5	125	71.7	75.5	125	71.7	75.5
6	168	64.4	46.1	170	32.1	8.23	170	32.1	8.23
7	140	58.3	61.5	167	58.8	64.5	167	58.8	64.5
8	138	79.5	87.7	133	60.2	77.6	121	68.3	77.6
9	146	88.2	94.4	138	74.9	88.8	138	74.9	88.8
z_o = 5 centimeters									
1	146	71.3	64.6	143	38.4	33.2	143	38.4	33.2
4	132	81.6	84.1	127	64.8	71.6	127	64.4	71.6
5	120	77.6	76.5	120	65.6	75.5	120	65.6	75.5
6	150	65.3	46.1	147	33.3	8.23	147	33.3	8.23
7	138	52.1	61.5	157	51.2	64.5	157	51.2	64.5
8	132	75.0	87.7	126	52.1	77.6	116	61.0	77.6
9	133	84.7	94.4	123	68.6	88.8	123	68.6	88.8

Table 4. Calculated evapotranspiration values as a function of aerodynamic roughness (z_o) and water-heat storage.

[Site locations are shown in German (2000, fig. 1). r_s, average resistance of evaporative surfaces; PMPEV, Penman-Monteith method percentage of explained variance; PTPEV, Priestley-Taylor method percentage of explained variance]

Site	Daytime data adjusted for water availability without heat storage		
	r_s	PMPEV (percent)	PTPEV (percent)
z_o = 1 centimeter			
1	205	19.4	29
4	158	54.7	26.9
8	143	50.6	31.3
9	153	70	77.6
z_o = 5 centimeters			
1	165	23.4	29
4	140	56.4	26.9
8	128	51.1	31.3
9	131	66.1	77.6

This exercise revealed that the aerodynamic term is a significant factor. The significance of the aerodynamic term is indicated in the standard PT formula where its contribution is set to a constant that is about 26 percent of the net radiation term; however, this does not account for variability and dependence on wind speed and humidity.

To represent ET in a numerical model, the formulation must be constructed to function with only readily measurable quantities. To accomplish this, the stomatal resistance can be represented as a variable function of ponding depth and ground-water table elevation, both of which are readily measurable quantities. Aside from the difficulty in determining appropriate functional relations, this approach also requires that the PM equation be evaluated at every cell and for every time step during a model run.

Because this technique utilizes substantial computational effort, a simple depth function was derived that yields an estimate of actual evapotranspiration when factored with PM-calculated PET. Several functions were tested, including some that would decrease PET as the surface-water depth decreased to zero. The reanalysis, however, indicated that a near optimal approach (1) equated evapotranspiration to PET when the surface is wet, and (2) applied a factor equal to the greater of a calibrated value of 1.0 + depth/0.93 m or 0.0 when depth is negative. Physically, this relation corresponds to constant resistance when there is ponded water at the surface. When ponded water is absent under dry-surface conditions, water availability is limited by a calibrated root-zone depth of 0.93 m and a transpiration rate that decreases linearly with increased unsaturated zone depth. This is the approach used in the TIME application and in the final determination of r_s using the methodology described earlier. Finally, the results in tables 3 and 4 were produced using the actual ET calculation just described; therefore, the model calibration included the reduction of PET due to a lack of available water. This allows model estimates to be compared directly to measured ET rates.

An alternate test of the predictive formula ignores nighttime ET and applies the formula only during the active ET period. The PEVs in table 3 for each prediction formula are substantially smaller than those reported by German (2000). When nighttime values were included in the PM model (predicting zero ET and soil and water heat storage); however, results were obtained that are within 5 to 10 percent of those obtained using the PT approach.

The available data did not allow discrimination between the formulas for vegetated sites; therefore, the same formula was used for all of the vegetated sites. The cumulative ET is presented in figure 13, which shows a distinctive repeating annual pattern.

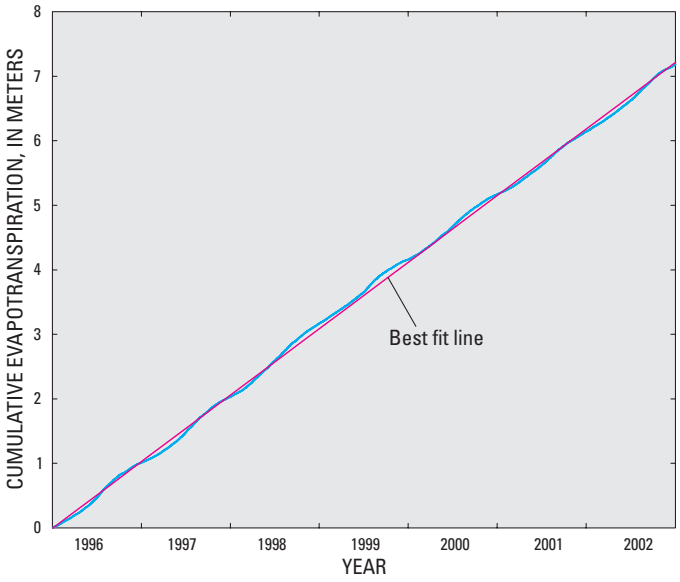

Figure 13. Cumulative evapotranspiration in the TIME area.

3.3.8 - Wind Data

Wind data obtained by German (2000) at an ET measurement site (OIH) along Old Ingraham Highway (fig. 1) are used as wind input in the TIME application. The record consists of 15-minute instantaneous data collected with a sensor 4 m above land surface. Gaps in the record were filled with data from Joe Bay Weather Station (JBWS) and Manatee Bay (MB) wind stations where necessary (fig. 1). JBWS is at the edge of Florida Bay, and thus, is more representative of winds over open water than OIH. Most wind speeds measured at OIH were about half of those measured at JBWS; therefore, it was possible to transform JBWS data by a constant multiplier and obtain reasonable estimates of OIH wind speeds using the same wind direction. The input file for wind stress is named in appendix 2.

Wind stress was calculated using a drag coefficient *WSTR* = 0.0018, and the following momentum flux formula:

$$\bar{\tau} = WSTR\ \rho_{air}\,|\bar{U}|\,\bar{U}\ , \qquad (4)$$

where ρ_{air} is the air density, and $\bar{U}$ is the wind velocity vector at 10 m above the surface. For computational efficiency, the wind stress was precomputed and input into the TIME application. The value chosen for the wind stress coefficient is more representative of stress over a vegetated land surface than over an open-water surface for relatively low (typically well below 10 m/s) wind speeds (Large and Pond, 1981).

3.3.9 - Coastal Water Levels and Salinities

Water-surface variations were prescribed along the open marine boundaries of the TIME application. The sparse measured data and the absence of a coastal hydraulic model necessitated the following approach. Harmonic constants for the three principal tidal components (*M2*, *O1*, and *K1*) were obtained from preliminary results of the Florida Bay model (J. Hamrick, TetraTech, written commun., 2005).

Seven separate boundary locations (fig. 1) were defined for the TIME simulation, corresponding to: (1) the boundary along Florida Bay; (2) the boundary encompassing Ponce De Leon Bay and the Harney and Broad Rivers; (3) Lostmans River; (4) Chatham River; (5) Lopez River; (6) Turner River; and (7) Barron River. For each of these boundaries, the Florida Bay model results were used to specify a mean level and the amplitude and phase of the *M2*, *O1*, and *K1* components. These boundaries are defined in the main input file for the surface-water simulation listed in appendix 2.

In addition to tides, low frequency sea-level variations were incorporated into the marine boundary conditions. Data from the USGS Trout Creek station were used because the record is reasonably complete for the 7-year period. A 30-day moving average was then computed, and yielded a final record with a mean of 0.518 m. The beginning and end values were made to agree by including the beginning of the dataset to compute the moving average at the end, allowing run continuation. Once the mean was subtracted, the moving average is added to the boundary levels computed by the tidal components to account for the low frequency sea-level variations. The input file for low-frequency tidal fluctuations is listed in appendix 2.

Boundary salinities are set to a constant value of 36 psu (practical salinity units) during flood flow. During the ebb flow, no value is prescribed and salinity at the boundary is computed based on values in the interior of the model grid. The return period for constituents that leave through the boundary was set to 60 minutes. These salinity boundaries are defined in the main input file for the surface-water simulation listed in appendix 2.

3.3.10 - Ground-Water Boundary Conditions

Ground-water flow is continuous across the northern and eastern domain boundaries. To simulate this flow, general-head boundaries (GHBs) are prescribed for the FTLOADDS ground-water component SEAWAT. The stages for these GHBs are interpolated from recorded stages at the Barron, S-333, S-334, S-336, G-211, Humble, G-789, Robblee, and Ever3 sites (fig. 9). An estimated conductance of 35,000 m/d was obtained by assuming local conductivity = (distance × cell width × layer thickness)/cell width, where local conductivity = 3,000 m/d (Langevin and others, 2004), distance = 300 m, cell width = 500 m, and layer thickness = 7 m. The input file for these GHB boundaries is named in appendix 2.

The marine boundaries are set as closed (no-flow) boundaries, which is justified as follows: (1) there is probably no freshwater flow through these boundaries because the salt front is located far inland (Fitterman and others, 1999); (2) some of the exchange that would occur at the lateral marine boundary instead occurs through the surface when the boundary is closed; and (3) it would be difficult to have an open boundary because of the need to specify ground-water flows or ground-water heads and salinity.

3.4 - Freshwater Flux Output at the TIME Application Boundary

One primary objective of the TIME application is to provide freshwater outflow to the coast so that the Florida Bay model (EFDC) can calculate resulting salinities. Because the EFDC model is separate from the TIME application, a method to transfer information at their interface is needed. The interface must be simplified because the models differ in structure (one being two-dimensional horizontal and the other three dimensional) and use different spatial discretizations. Fundamentally, the fluxes of water volume, momentum, and salt anywhere along the interface should be matched in the two models to satisfy continuity and conservation of salt laws in which total salt flux is the sum of advective and diffusive fluxes. Although this may be the best approach to use, a simpler method has proven to be successful in situations where the water-volume flux is small compared to offshore volume. The boundary in the bay model is represented with zero momentum and salt fluxes and with water volume flux equal to an equivalent volume of freshwater, which is applied as a zero-salinity source like rainfall.

The flow exchange between TIME and the EFDC is approximated by an equivalent freshwater flux. If the flow at a given instance from the TIME domain along the coast is q with salinity S, and q is small compared to ambient flows, then it effectively is equivalent to adding an amount of pure freshwater, q_f, equal to $q(S_0\text{-}S)/S_0$, where S_0 is a reference ocean salinity.

The salinity S is the salinity of the source water; that is, S is the salinity of the TIME domain cell just inside the boundary when flow is to the coast and S is the salinity of the boundary cell when flow is from the coast. The reference ocean salinity S_o represents an ambient open-water salinity, nominally set to 36 psu for the TIME application. Conceptually, S_o is the global reference for the fractional reduction or increase in salinity when water is added or removed from the offshore area.

The TIME application boundary freshwater flux computed by $q_f = q(S_0\text{-}S)/S_0$ is passed to the EFDC model as a volume of zero-salinity water. Figure 14 presents the four cases involved in the computation of q_f. A positive q_f represents flow to the offshore area when the inland water is less saline than the reference ocean salinity (case 1) or flow to the inland area when the offshore waters are more saline than the reference ocean salinity (case 2). A negative q_f represents flow to the inland area when the offshore is less saline than the reference ocean salinity (case 3) or flow to the offshore area when the inland waters are more saline than the reference salinity (case 4).

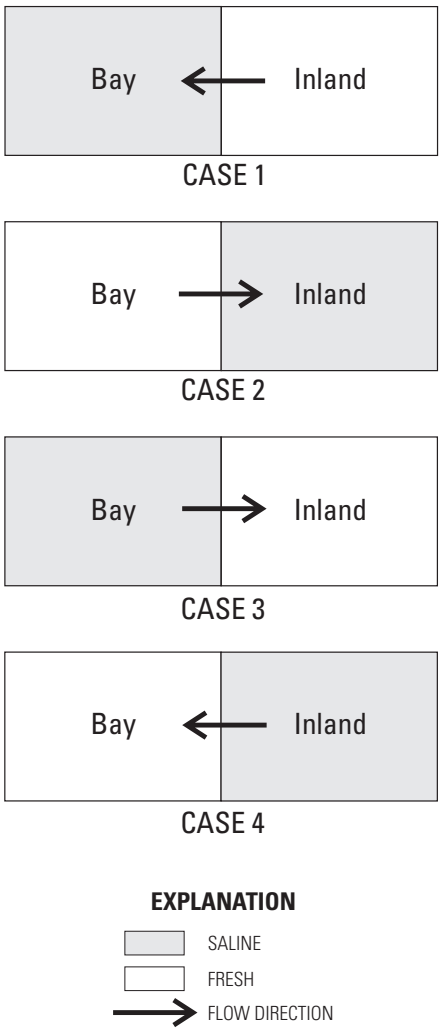

Figure 14. Freshwater flux cases.

3.5 - Model Initialization

The TIME application was initialized with water levels and salinities from a 1-year run for 1999. This year was chosen as a warm-up period because stages at the end of 1999 and the beginning of 1996 have similar water levels and flows. Surface-water flows and stages adjust relatively rapidly (within 3 to 4 months) to prescribed boundary conditions. Therefore, running the model for a full year was expected to create realistic surface-water conditions that are independent of starting conditions.

The ground-water model was initialized using ground-water heads set to 1 m below NAVD 88 and salinity values that approximate data from Fitterman and Deszcz-Pan (1998). The ground-water heads and flows reach reasonable values in about a month; however, salinities are much slower to adjust and can require decades to approach equilibrium under steady-state boundary conditions.

3.6 - Initial Model Calibration

More than 140 seven-year runs were made in the initial calibration of the TIME application. Adjustments were made to correct for errors in the initial input of boundary locations and Taylor Slough topography. Other adjustments were made to include features that were represented inadequately in the initial model input. These include river characteristics, roads, the Buttonwood Embankment, aquifer hydraulic conductivities, primary and secondary storage coefficients, conductivity of the surficial thin layer, and Manning's *n*. The parameters of the final model are contained in the FTLOADDS input files listed in appendix 2.

Additionally, the initial calibrated run (142) uses wind data from the Old Ingraham Highway (OIH) station (fig. 1) with no reduction in wind forcing due to the sheltering effect of vegetation. The thin layer over which leakage is calculated was given a conductivity of 0.004 m/d, with the underlying aquifer vertical conductivity of 1.0 m/d.

3.6.1 - Wetlands Water Levels

The model calibration uses stage values recorded at 105 different locations within the TIME domain. The following stations were chosen for graphical representation because of their extensive coverage of Shark River Slough and relatively complete data records: G-620, NE2, NP201, P33 to P38, and RG1 (figs. 9 and 15). At the beginning of 1996, simulated stages compare well with measured stages and relatively few stations show abrupt changes in stage; both characteristics support the chosen strategy of warming up the model using 1999 hydrologic conditions. The fit between measured and simulated data for each of the preceding sites is varied substantially and discussed herein.

The measured data fit simulated ground-water data better than simulated surface-water data at G-620 (fig. 15A). The ground-water head is below surface-water stage during most of the period, indicating downward leakage. Two major declines in ground-water head that occurred during the 2001 and 2002 dry seasons were simulated poorly by the model. The mean bias, correlation, and PEV are -0.004 m, 0.928, and 85.7 percent, respectively. The PEV for stage data is calculated as 1.0 – [Var(measured stage – simulated stage)/Var(measured stage)] and measures how well the model represents water-level fluctuations around a mean.

The visual fit between measured and simulated stage at NE2 (fig. 15B) is not as close as at G-620, primarily because of a bias in the mean, although all major ponding, accumulation, and depletion events are captured well. Simulated ground-water head is mostly lower than simulated surface-water stage and is in better agreement with measured head. The model land-surface altitude is apparently too high, which is confirmed by the data. The mean bias, correlation, and PEV are -0.11 m, 0.863, and 65.2 percent, respectively.

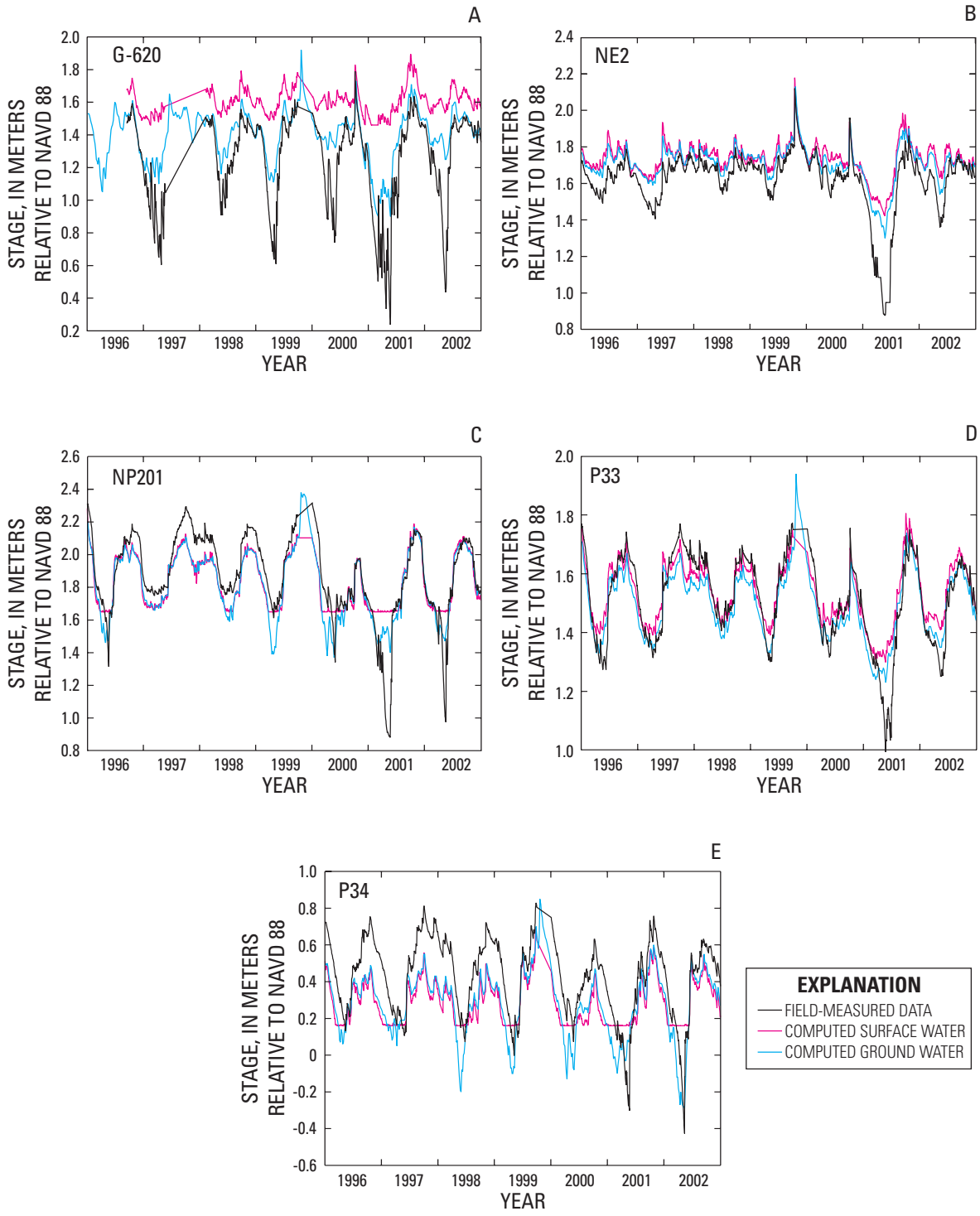

Figure 15. Comparison of water levels at selected gaging stations in the TIME area. Site locations are shown in figure 9.

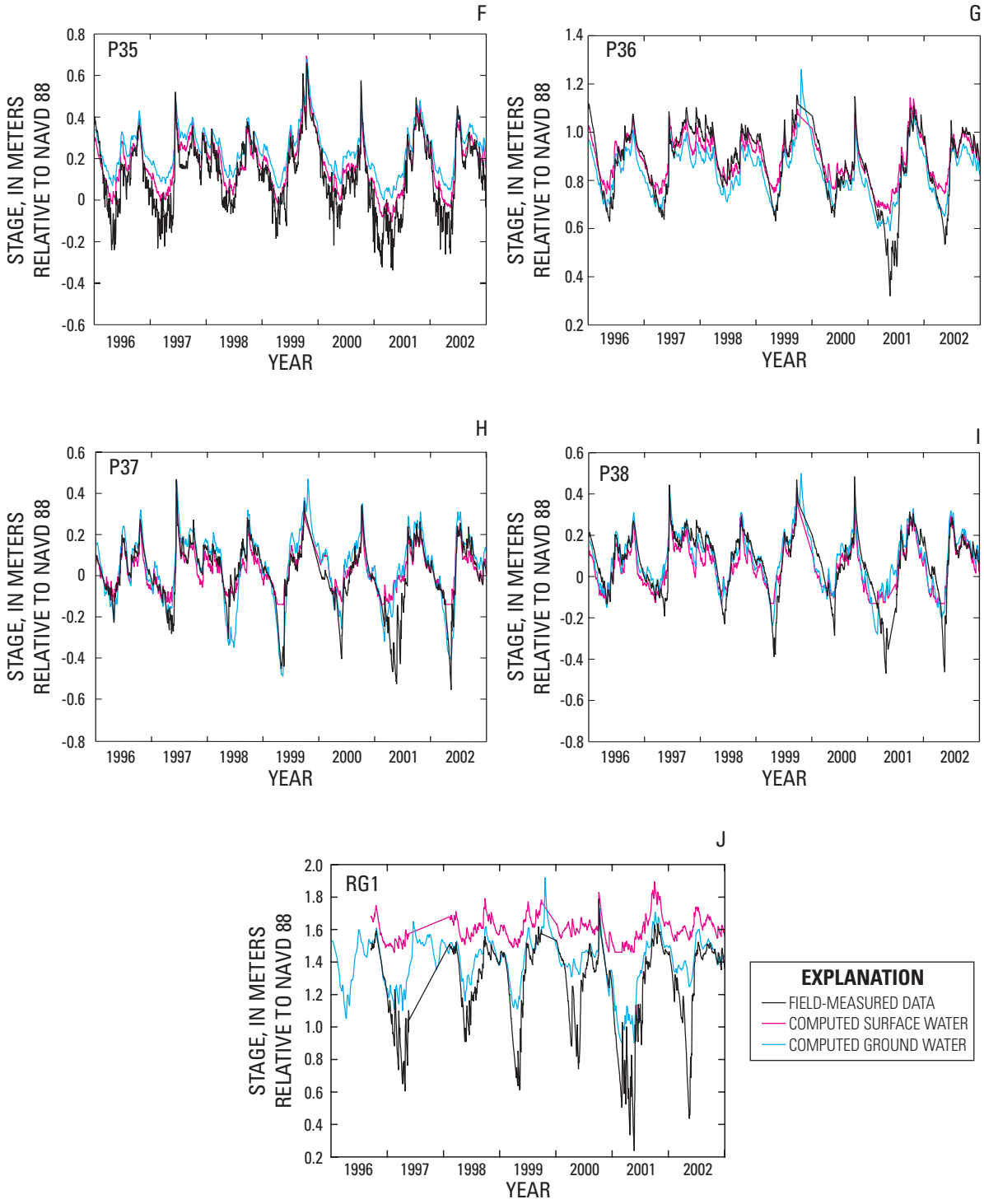

Figure 15. Comparison of water levels at selected gaging stations in the TIME area. Site locations are shown in figure 9.—Continued

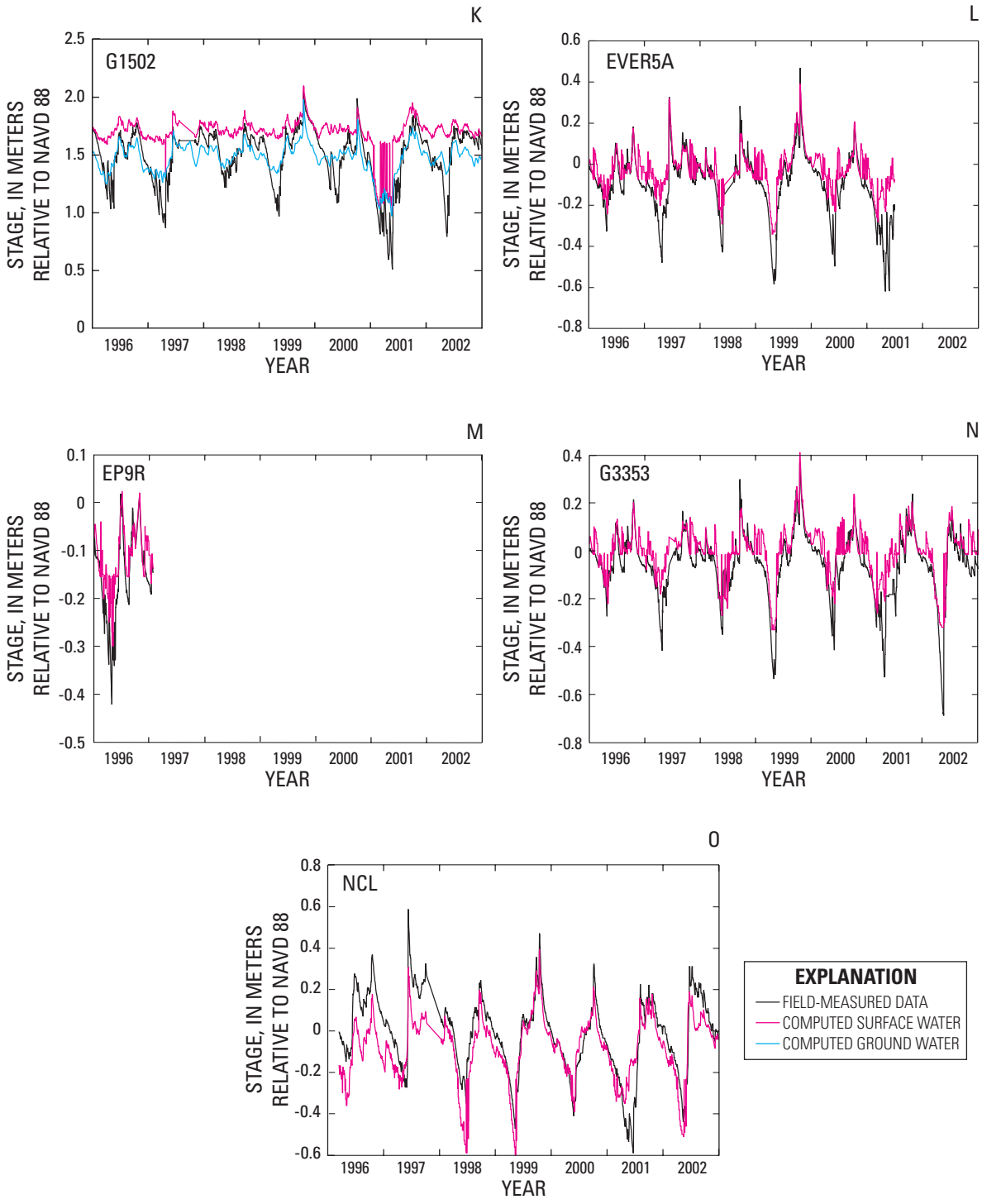

Figure 15. Comparison of water levels at selected gaging stations in the TIME area. Site locations are shown in figure 9.—Continued

Visual comparison of NP201 stages (fig. 15C) shows a mean shift during the first 4 years, followed by close agreement of measured and simulated surface-water stage. The two major declines in ground-water head are not well simulated, perhaps warranting an adjustment to the ground-water storage coefficient. The reason for mean shift is unclear, and by itself, might indicate a data problem; however, similar conditions at other stations indicate a more regional effect. At NP201 the model land-surface altitude is 0.23 m above measured land-surface altitude at the gage. The mean bias, correlation, and PEV are 0.04 m, 0.855, and 71.0 percent, respectively.

Stage at P33 (fig. 15D) shows a mean shift similar to NP201, but much smaller. The measured data fit simulated surface-water stage better at high water levels and simulated ground-water heads better at low water levels. The ground-water declines in 2001 and 2002 are much deeper at NP201, than P33, possibly indicating that they are caused by drainage to the east. The mean bias, correlation, and PEV are -0.02 m, 0.919, and 79.6 percent, respectively. The closeness of the agreement at P33 and its occurrence in the middle of Shark River Slough lend support to model performance in this part of the domain.

Measured trends at P34 (fig. 15E) are represented by the model data, but there is substantial bias in the mean. The shift during the first 4 years is evident at this site, although the ground-water level declines in 2001 and 2002 are simulated more accurately at this site than in preceding cases. Because model land-surface altitudes have no obvious errors, the bias may indicate a local frictional problem (discussed in section 3.7.2). The mean bias, correlation, and PEV are 0.16 m, 0.855, and 71.6 percent, respectively. Simulated ground-water head and surface-water stage agree closely throughout most of the wet season.

The surface-water hydrograph fit at P35 (fig. 15F) is closer than at most other sites; in this case, ground-water head is mostly above surface-water stage, indicating upward leakage. The mean bias, correlation, and PEV are -0.058 m, 0.947, and 88.2 percent, respectively. The surface-water fit at P36 (fig. 15G) is also closer that at most other sites. In this case, simulated ground-water head is mostly below simulated surface-water stage, and the fit to measured water-level data is best during low-stage conditions. The mean bias, correlation, and PEV are -0.02 m, 0.908, and 79.7 percent, respectively.

Measured and simulated stage closely correspond at P37 and P38 (fig. 15H, I), with ground-water head mostly above surface-water stage at both sites. The mean bias, correlation, and PEV are -0.01 m, 0.866, and 73.6 percent, respectively at P37; these same parameters are 0.02 m, 0.849, and 71.5 percent, respectively, at P38.

At RG1 (fig. 15J, Rocky Glades), simulated ground-water head agrees closely with measured stage. The 0.4-m discrepancy between the land-surface altitude measured at the gage and that measured by the topographic survey indicates the gage is located in a shallow depression, and that its measurement is more representative of ground-water head. The mean bias, correlation, and PEV statistics are -0.347 m, 0.673, and 40.4 percent, respectively. These statistics would improve substantially if simulated ground-water head is compared to measured stage instead of surface-water stage.

Although other stage records were not examined in the same detail, all were included in the calculation of model performance statistics. The model performance statistics consist of: (1) overall measured data mean; (2) measured data standard deviation; (3) overall model mean; (4) model standard deviation; (5) correlation between measured data and model output; (6) difference in means (DIFMEAN) (1) – (3); (7) difference in standard deviations; (8) PEV; (9) number of points used for calculations; (10) land-surface altitude defined for model cells; and (11) land-surface altitude as measured adjacent to the water-level gage.

The correlation between measured and simulated data is calculated with the mean removed from the series. The difference in means is a measure of the bias between the data and the model. Only quality-approved measured data values and their corresponding simulated values are used; missing data points are ignored in data and model statistics. Simulated ground-water head is used when model surface-water stage drops below the criteria for a semidry state described in section 2.2.1. The land-surface altitudes (items 10 and 11 noted earlier) are included to indicate, when elevations differ, whether extra care is needed to interpret the results (for example, RG1, fig 15J).

Surveying water-level gages to datum is difficult in the terrain of the TIME domain. The quality of the leveling at some stations has been found to be poor. Many of the field gages do not have a known land-surface altitude, and the following sites have not been referenced to a vertical datum: BD, BR, CN, GI, HR, LN, LO, NR, SR, TE, WE, WP, and WW (fig. 9). The summary statistics of stage comparisons for all 105 gages are listed in table 5.

Table 5. Summary statistics of stage comparisons for station data used in the TIME application.

[TIME, Tides and Inflows in the Mangroves of the Everglades]

Simulation run	Sum of absolute mean difference (meters)	Sum of squares of mean difference (meters^2)	Sum of correlations (percent)	Sum of explained variance (percent)
139	23.880	19.211	79.283	38.716
142	23.896	19.293	77.432	31.86
143	23.947	19.256	78.297	37.043
145	28.352	22.129	69.499	-5.352
146	23.259	19.022	76.794	38.547
157	22.088	18.195	81.141	39.687
157GW	19.725	17.454	83.179	54.038

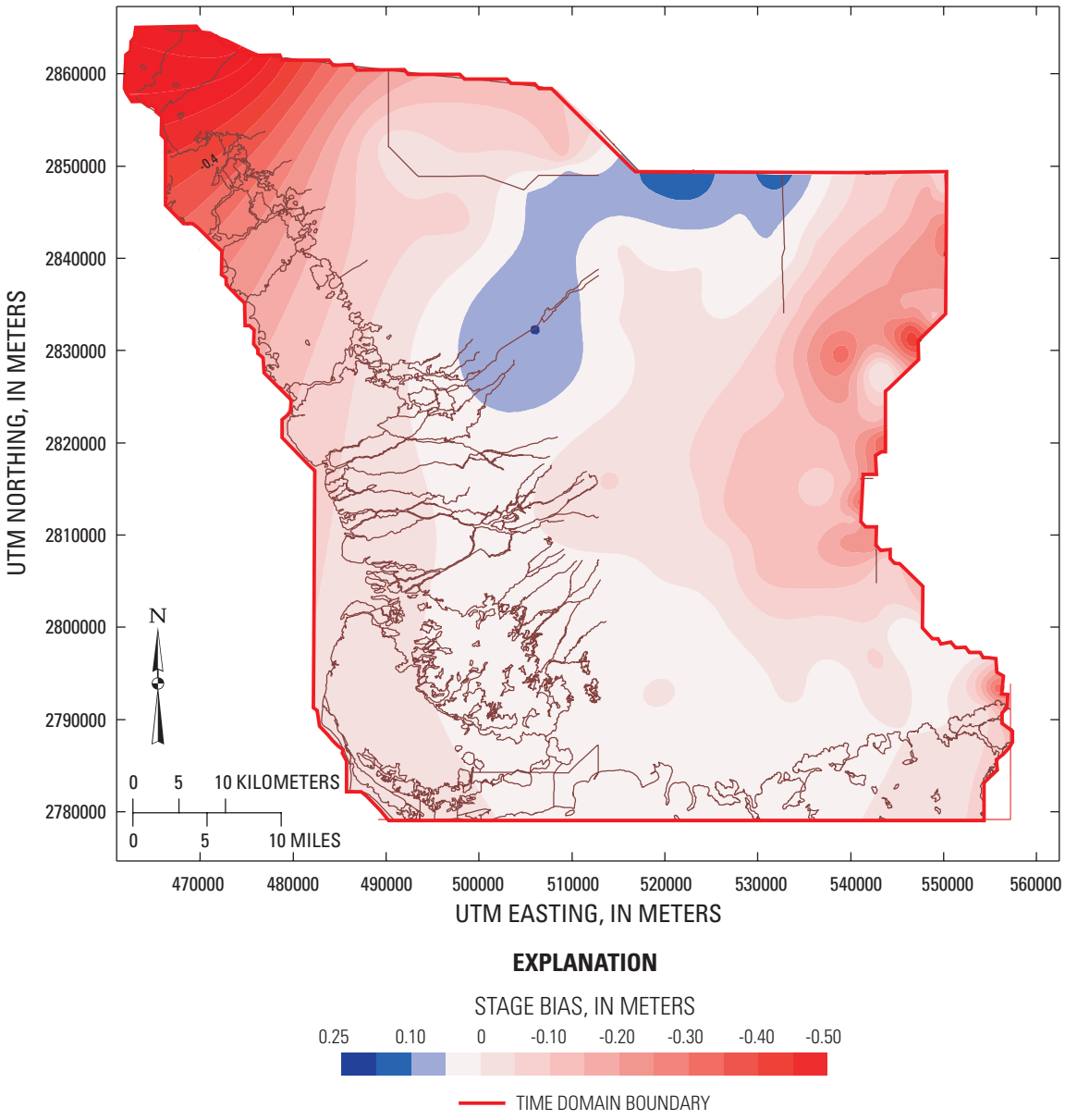

Figure 16. Spatial distribution of model mean stage bias in the TIME area for run 142.

Figure 16 shows the spatial distribution of the mean measured water level minus simulated water level (DIFMEAN); illustrating the spatial distribution of mean bias. Only stations referenced to a vertical datum were used to construct this map. The large negative bias in the north-western corner of the model is due to one gage (BICYA8) that is close to the model boundary (fig. 9). Unfortunately, there is no measured land-surface altitude for this gage to allow comparison with model topography. It is possible that a small river drains the area but is not accounted for in the model topography. Further investigation is needed to resolve this problem, which is confined to a small region of the domain.

The mean stage south of the S-12A, B, C, and D structures, and near P34, are somewhat lower than predicted, whereas stages near Levee-31 are somewhat higher than predicted (locations in fig. 9 and values in figs. 15E, J). This could indicate that the actual frictional resistance within the intervening area is less than that represented in the model. The bias for the ground-water stations, most of which are on the eastern side of the model domain, is generally larger than for surface-water stations and may influence contour locations in figure 16. This may be due partly to the effect of the storage coefficient, which has not been calibrated extensively in the model.

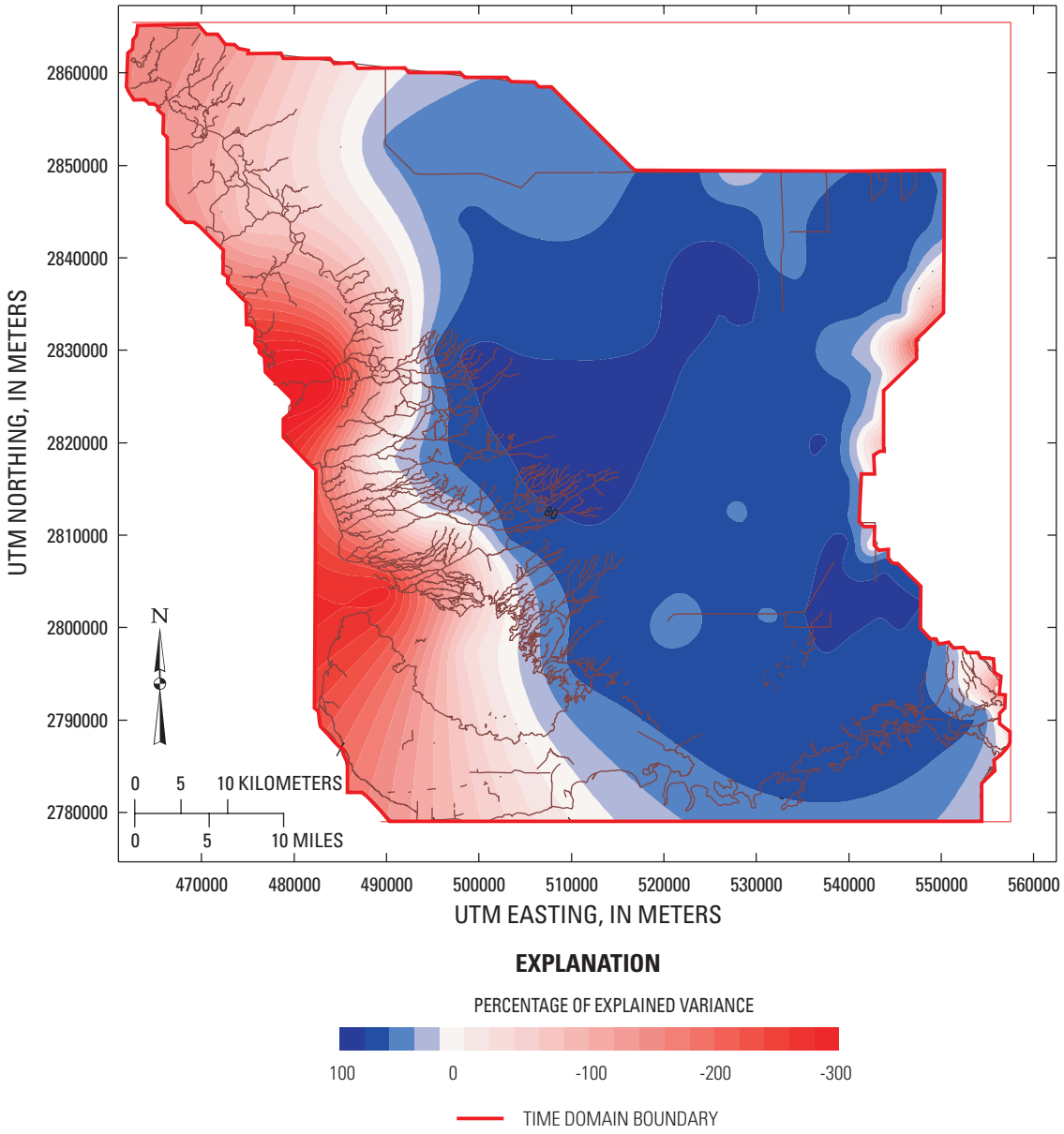

Figure 17. Spatial distribution of percentage of explained variance in the TIME area for run 142.

A contour map of the PEV for stage shows values ranging from 60 to 90 percent in most of the nontidal marshes (fig. 17). The PEV is lower in the tidal areas because relatively small errors in model tides result in large decreases in PEV. Small or negative PEV values occur near the northeastern edge of the domain where prevalent dry-surface conditions make simulations more difficult and dependent upon accurate topography. The negative PEV values in the C-111 Canal area, where the mean bias also is negative, indicate that modeled drainage may need some improvement; but tidal response is probably poor as well. The negative bias indicates mean model stage is greater than mean measured stage. The prescribed tide in northeastern Florida Bay obtained from the preliminary bay model has an *M*2 amplitude of 0.03 m, which is known to be too large.

3.6.2 - West Coast River Stages and Flows

Direct comparisons of measured and simulated stage at the USGS west coast river stations is considered problematic because of difficulties associated with leveling of field gages, lack of boundary input data from a marine model for wind-induced water slope and tides, and use of tidal harmonic characteristics derived from the Florida Bay model to create the tidal boundary conditions. The comparisons are shown in figure 18; for clarity, a 15-day period corresponding to the duration of a spring neap cycle is shown. All sites, except for the Chatham River gage, were referenced to a datum; therefore, the Chatham data cannot be used for comparisons of mean. The time-series plots show a clear decline in sea level during April 18-20, 2001, which is likely attributable to wind.

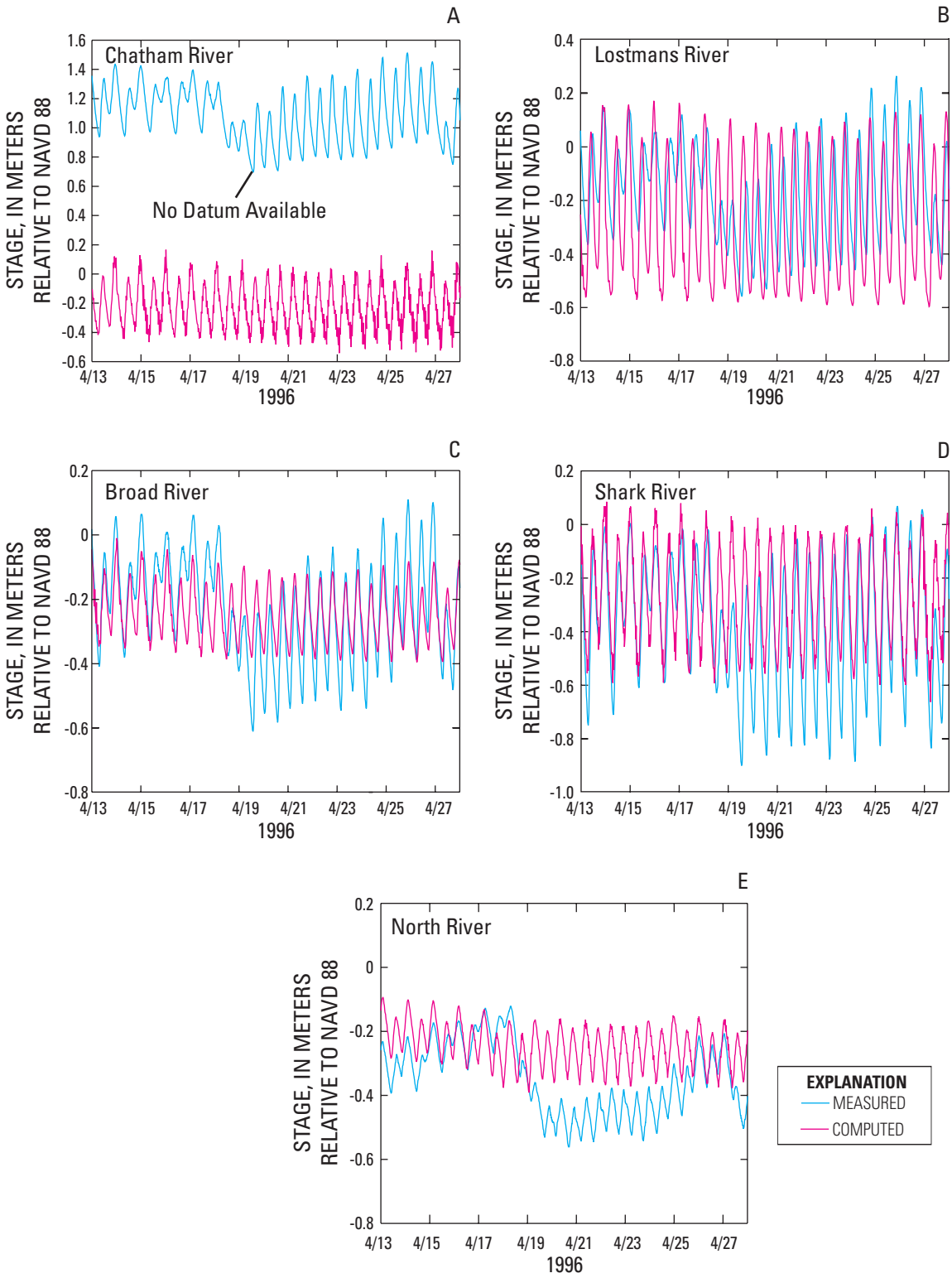

Figure 18. Measured and computed stage at selected west coast rivers over time. River locations are shown in figure 1.

Table 6. West coast river stage comparison statistics for run 142.

[Rivers are shown in figure 1]

Station	Measured stage mean (meters)	Computed stage mean (meters)	Measured stage standard deviation (meters)	Computed stage standard deviation (meters)	Percentage of explained variance	Number of points
Chatham River	1.20	-0.01	0.20	0.18	61	27,822
Lostmans River	-.02	-.06	.20	.24	40	27,554
Broad River	-.05	-.01	.18	.15	61	30,244
Shark River	-.19	-.07	.23	.19	68	29,187
North River	-.20	-.04	.12	.11	61	27,695

Wind-induced water-level slope at the boundary, however, is not prescribed in the model forcing, and the model response includes direct wind-stress effects that fail to produce a similar slope in the model. The tidal ranges and lower frequency (monthly) water-level fluctuations are captured by the model, but the spring-neap variations in diurnal tide inequalities are not as well represented. It is likely that the preliminary tidal harmonic components inadequately describe actual tides.

Base run stage comparison statistics were compiled for the five west coast river stations presented in table 6. The comparison was based on half-hourly values, and time values without valid gage data are excluded. The differences in measured means indicate further investigation is needed to resolve problems related to datum referencing at the west coast river sites. If monitoring stations are in tidal reaches of the rivers and have strong hydraulic connections with the ocean, their associated means should agree closely, and this is the case with the model means. Because preliminary boundary conditions are used, these statistics can be used to measure any improvement that results from prescribing better boundary conditions as they become available from the Florida Bay model. The PEV values at four of the five stations are greater than 0.6, however, which is satisfactory when considering the large errors that can be induced by small phase errors. The primary problem with tidal data is matching phase; a large water-level error can be caused by a small phase error. The smaller PEV at Lostmans River is most likely due to: (1) an overestimation of the standard deviation by the model, which results from representing tidal fluctuations that are too large; and (2) a model phase that leads the measured phase, particularly at low tide. These characteristics indicate that the model friction in the lower reach of Lostmans River needs to be increased to achieve a better match between measured and computed tidal water-level fluctuations.

Using the measured flows at the five west coast river stations noted earlier, an evaluation of model-predicted flows was made for the part of the Standard Data Period (SDP) for which data were available. The flow records at the different locations started at different times during 2001 and all extended beyond 2002. Owing to the constrained model resolution, it was necessary, in some instances, to approximate several rivers as one. To drain water efficiently to the coast, rivers in the model must have sufficient depths so as to not dry out at the wrong level. River cells, therefore, must have a bottom altitude representative of the river rather than the adjacent banks or an average of both. Where natural rivers lie relatively close to each other, it is difficult to implement the necessary depth along each river in the model without making the local model topography too low. For example, a number of parallel rivers are combined with the Shark and North Rivers in the model (figs. 1 and 3); all are hydraulically connected to Whitewater Bay. These approximations should yield acceptable values for runoff to the bay, even though local flow paths and flow volumes will differ somewhat from actual conditions.

Model calibration consisted of modifying model topography to assure that rivers had sufficient depth and covered enough area to allow realistic drainage as indicated by the descending phases of the stage time series. Adjustments to topography and upstream friction also were made to match model drainage to the magnitudes of net seaward flows measured at the five USGS west coast river stations. Chatham, Shark, and North Rivers were allowed to have more flow because they represented a combination of adjacent, mostly parallel rivers. Finally, the friction in the downstream sections of the rivers was adjusted to match tidal stage and flow ranges. The calibrated Manning's *n* values for the rivers are shown in figure 4.

A 15-day, neap-spring cycle period was chosen from April 23, 2001, to May 8, 2001, and flow comparisons for this period are shown in figure 19. The simulated tidal flows are in phase with the measured flows. The model overestimated the magnitude of flow at Shark and North River, and to a lesser extent, Chatham River, which is expected because all these rivers include flows of adjacent smaller rivers as previously described.

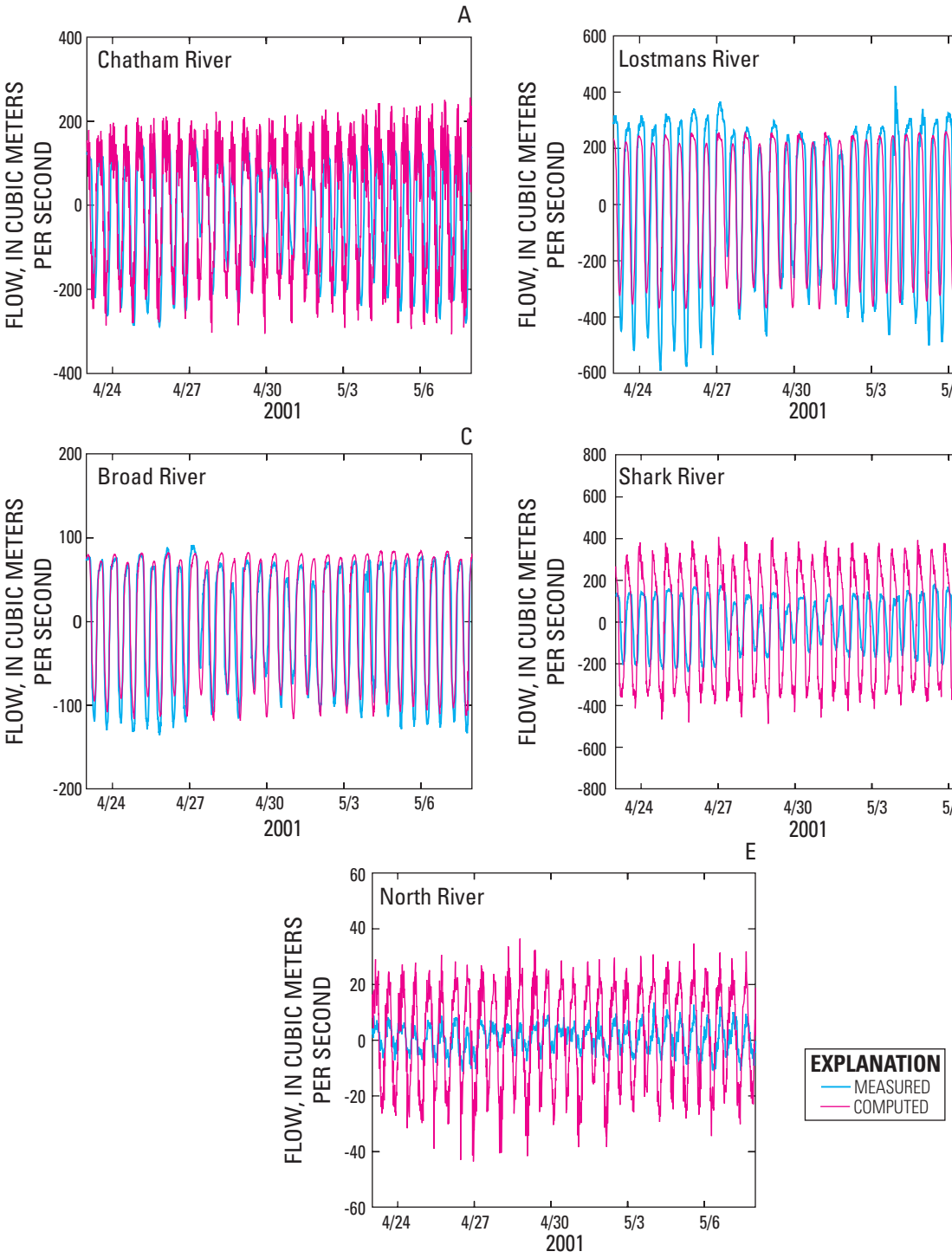

Figure 19. River flow over neap-spring cycle at selected west coast rivers. The rivers are shown in figure 1.

Flow comparison statistics were compiled for the five west coast river stations noted earlier, based on 15-minute data and ignoring missing data points (table 7). The PEV values are poor at locations corresponding to the combined rivers. The flow comparison graphs shown in figure 19 indicate, however, that PEV would improve substantially at Chatham, Shark and North Rivers if their flows were partitioned into individual rivers. The graphs of cumulative flows shown in figure 20 do not show any unusual trends; measured and computed flows show similar seasonal variations. The computed cumulative flows are consistently higher than measured cumulative flows at these three rivers because they encompass a number of smaller rivers. As noted earlier, table 2 gives the computed net average flows at gaging stations along the rivers.

Table 7. Comparison statistics for measured and computed west coast river flows.

[Rivers are shown in figure 1]

Station	Measured discharge mean (meters)	Computed discharge mean (meters)	Measured discharge standard deviation (meters)	Computed discharge standard deviation (meters)	Percentage of explained variance	Number of points
Chatham River	10.6	19.1	162.0	128.7	0.5	54,032
Lostmans River	39.2	39.1	340.4	277.6	.7	52,722
Broad River	10.3	8.3	76.7	78.6	.7	60,482
Shark River	14.1	20.3	131.2	360.7	-3.9	57,122
North River	1.9	6.8	9.2	21.5	-2.5	54,958

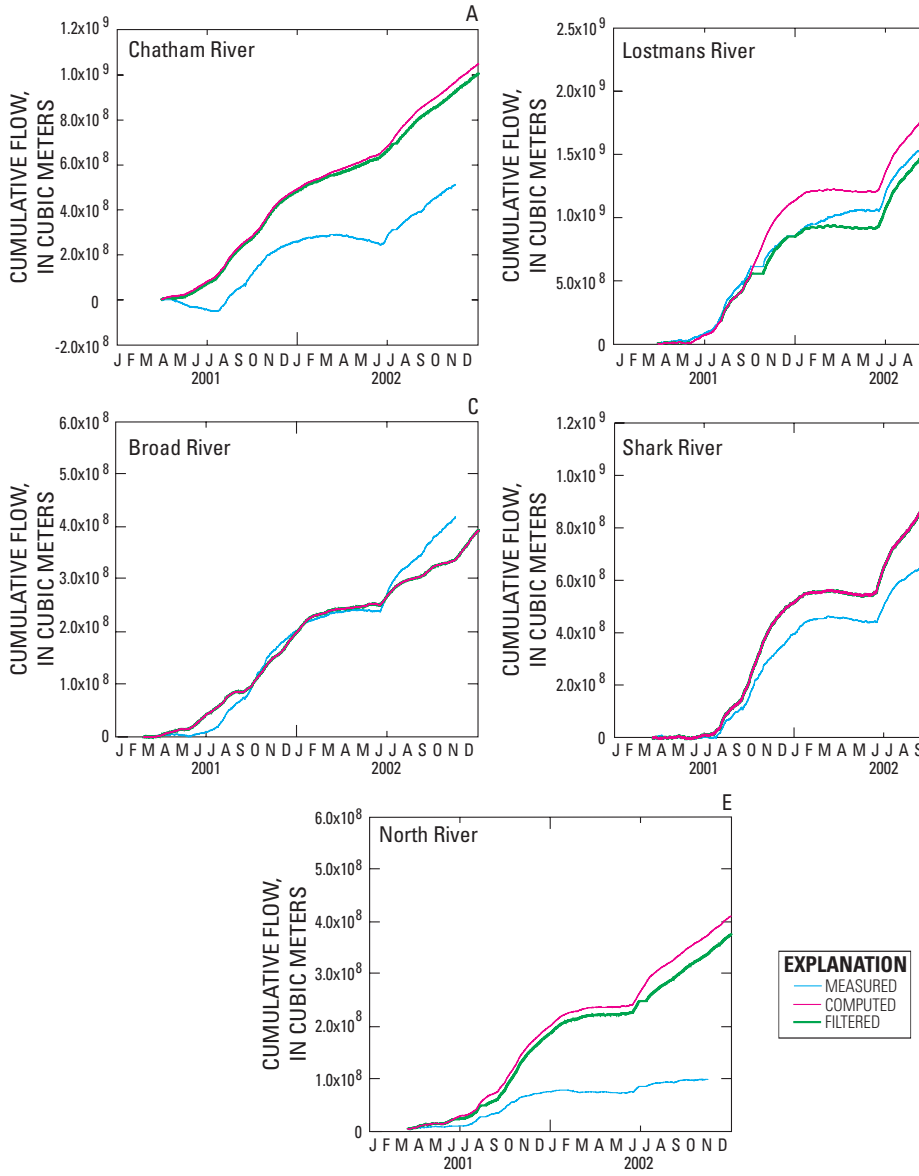

Figure 20. Cumulative flows at selected west coast rivers over time. Rivers are shown in figure 1.

3.6.3 - Stages and Flows at Taylor Slough

The recorded inflows at Taylor Slough Bridge (TSB), S-175, and C-111, together with the difference between measured rainfall and estimated evapotranspiration, indicate that flows to Florida Bay should be somewhat greater than those actually measured; the source of this discrepancy is not known, although unmeasured coastal flows are likely. Flows through TSB are overestimated by the model (2.85 m^3/s measured compared to 4.57 m^3/s for model run 142), which would further increase creekflows. The following may have contributed to this discrepancy: underestimation of measured creekflows, evapotranspiration and flow toward the west; overestimation of rainfall; or unmonitored runoff.

3.6.4 - Surface-Water Depths, Flows, and Salinities

The spatial and temporal distribution of surface-water depth provided by the model is useful for evaluating various biological/ecological performance measures. Model output is saved to allow an instantaneous depth map to be produced for each day within the simulation period. The spatial and temporal distribution of instantaneous surface-water depth and velocity at 90-day intervals is shown in figures 21A-I.

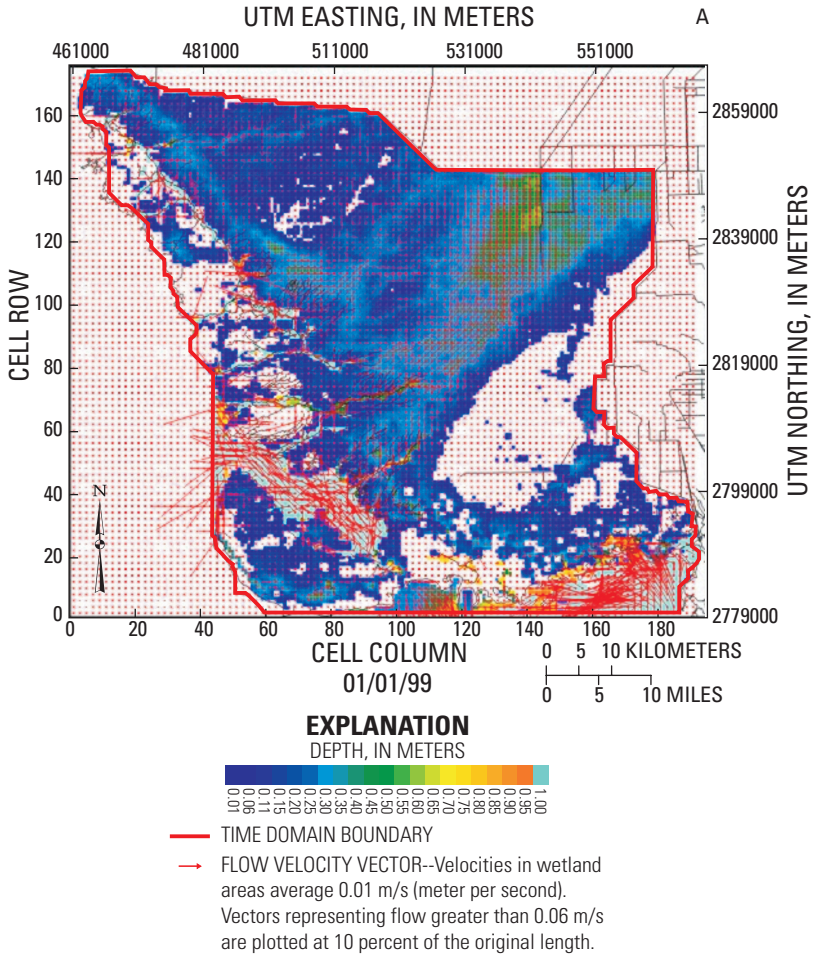

Figure 21A. Spatial and temporal distribution of surface-water depth and velocity in the TIME area.

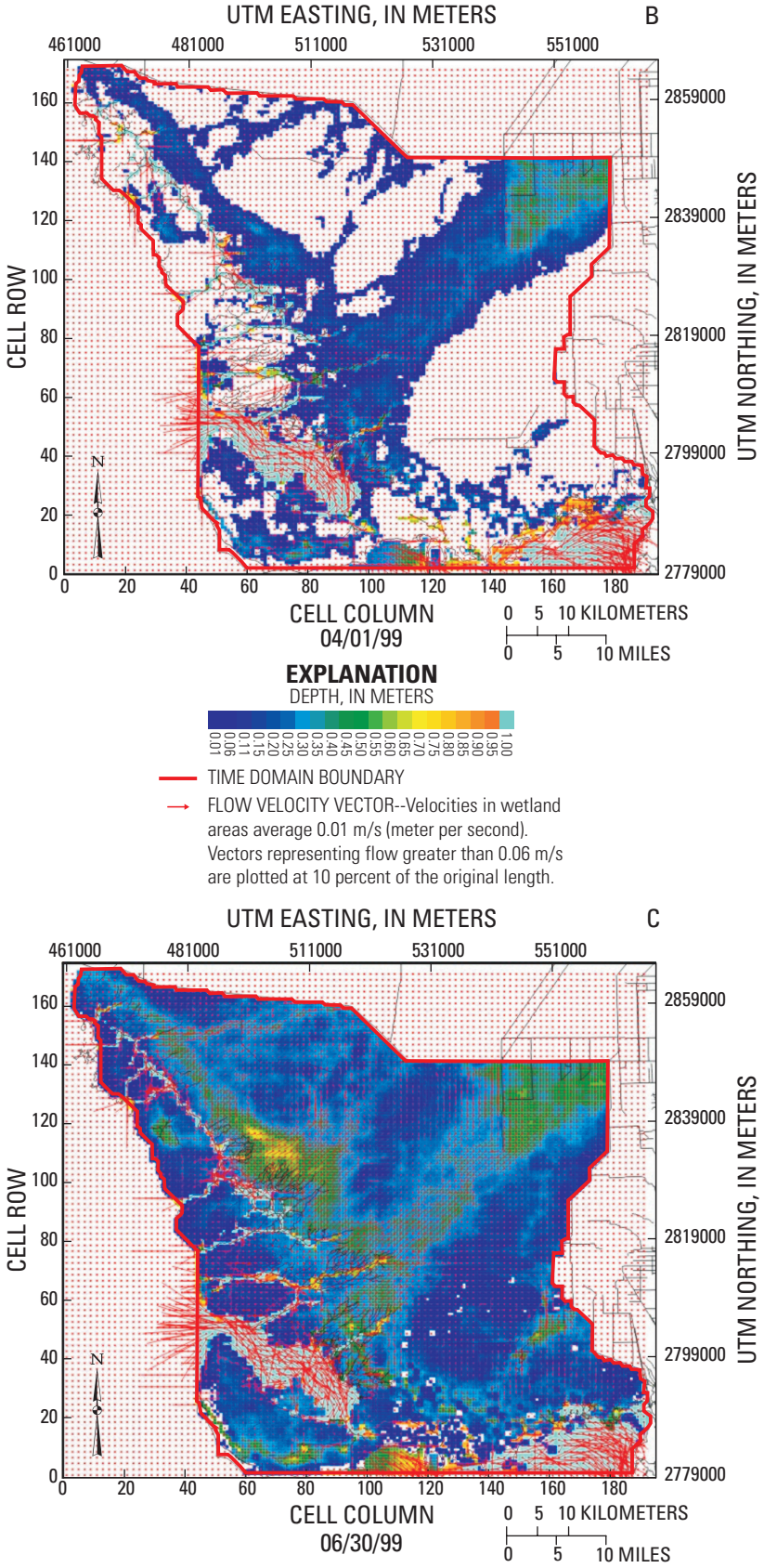

Figure 21B-C. Spatial and temporal distribution of surface-water depth and velocity in the TIME area.—Continued

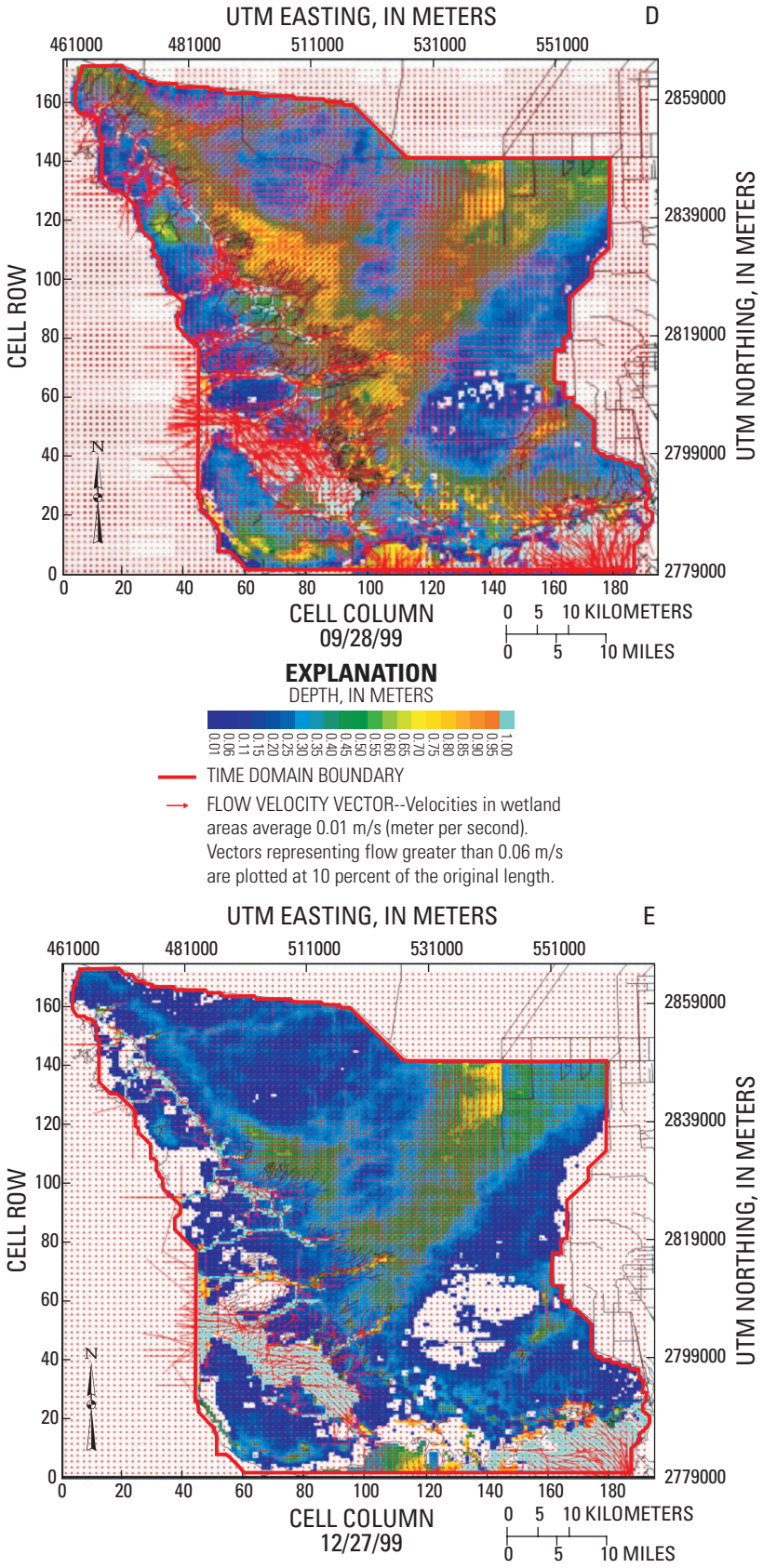

Figure 21D-E. Spatial and temporal distribution of surface-water depth and velocity in the TIME area.—Continued

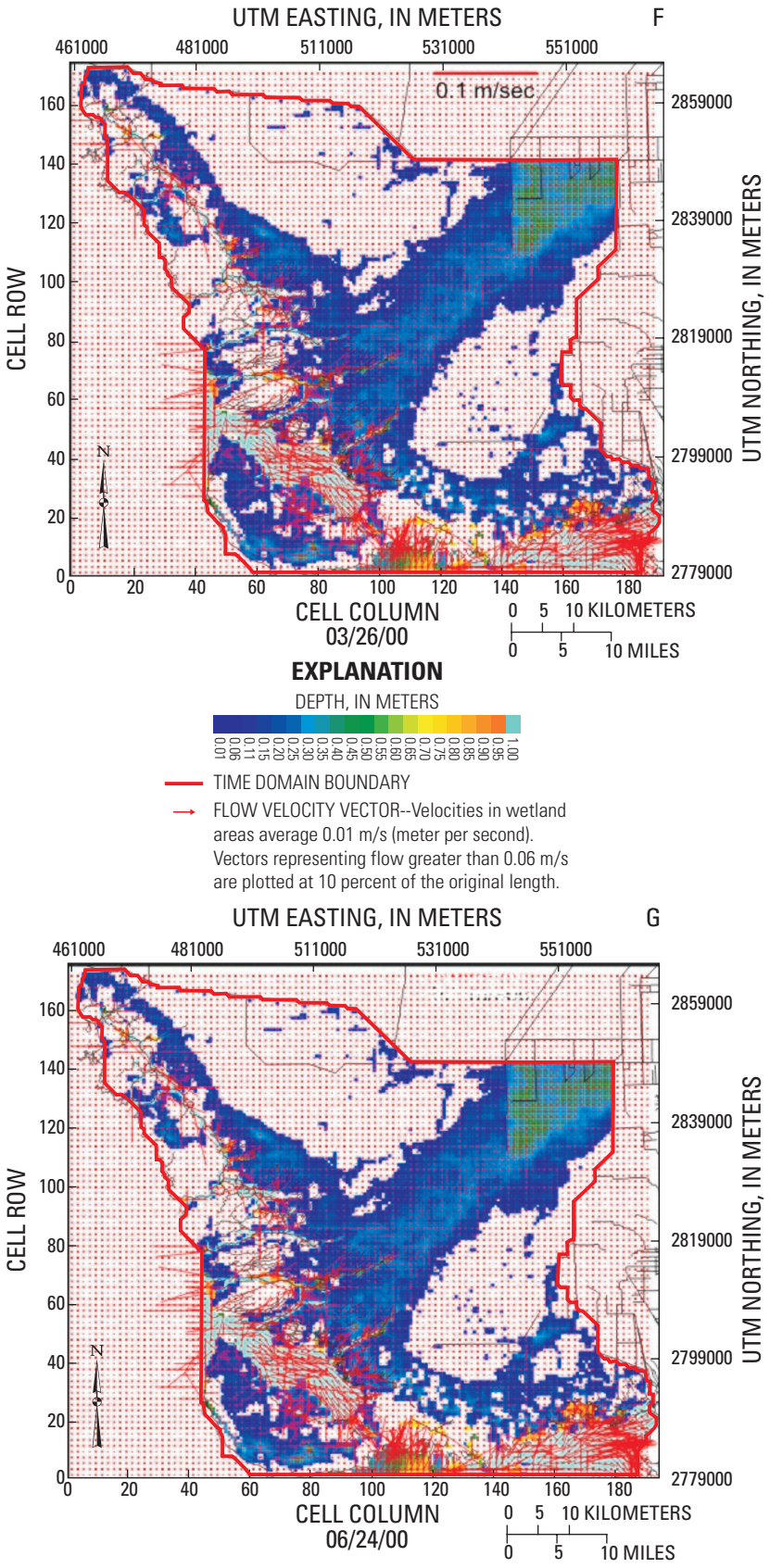

Figure 21F-G. Spatial and temporal distribution of surface-water depth and velocity in the TIME area.—Continued

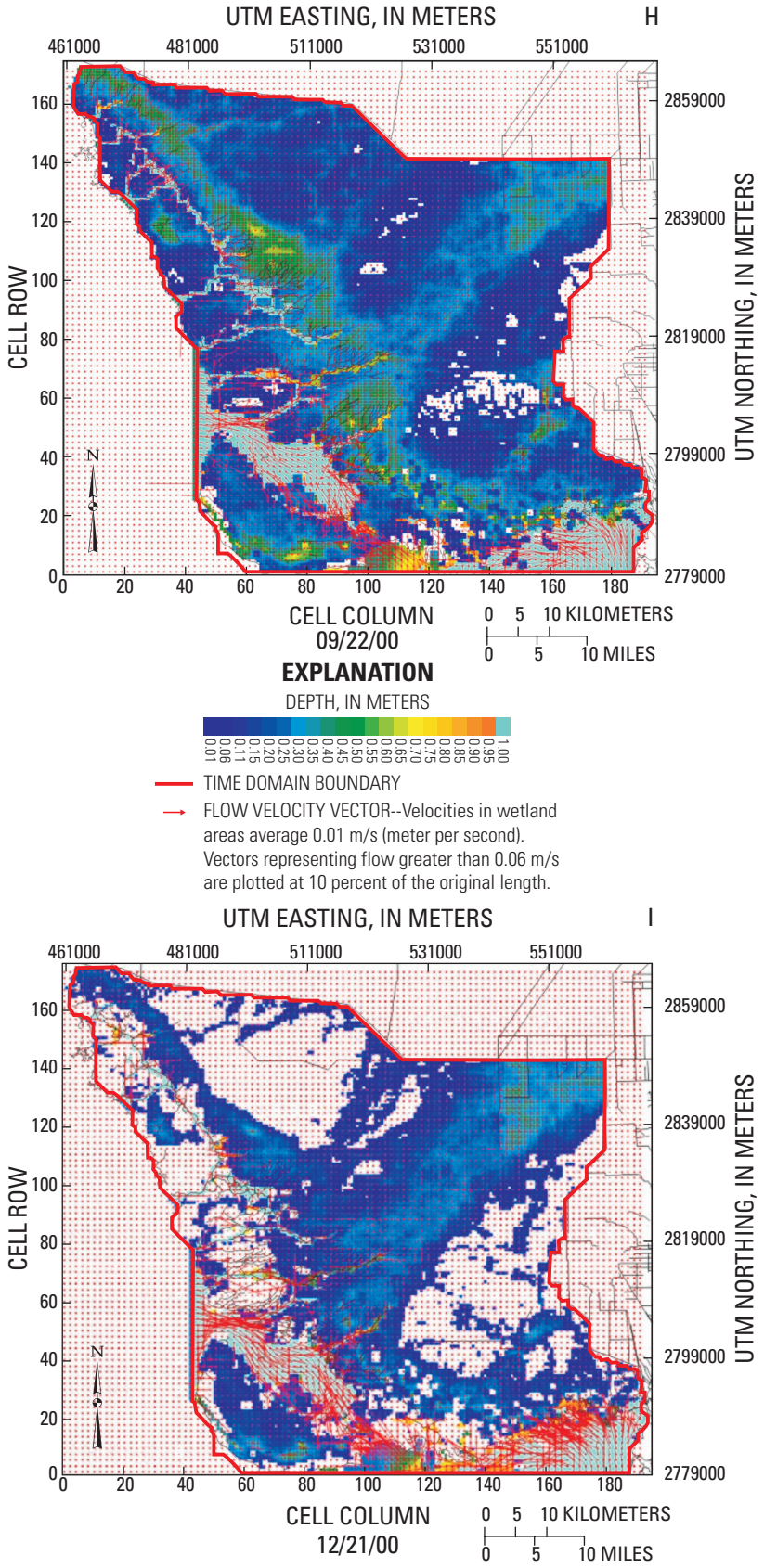

Figure 21H-I. Spatial and temporal distribution of surface-water depth and velocity in the TIME area.—Continued

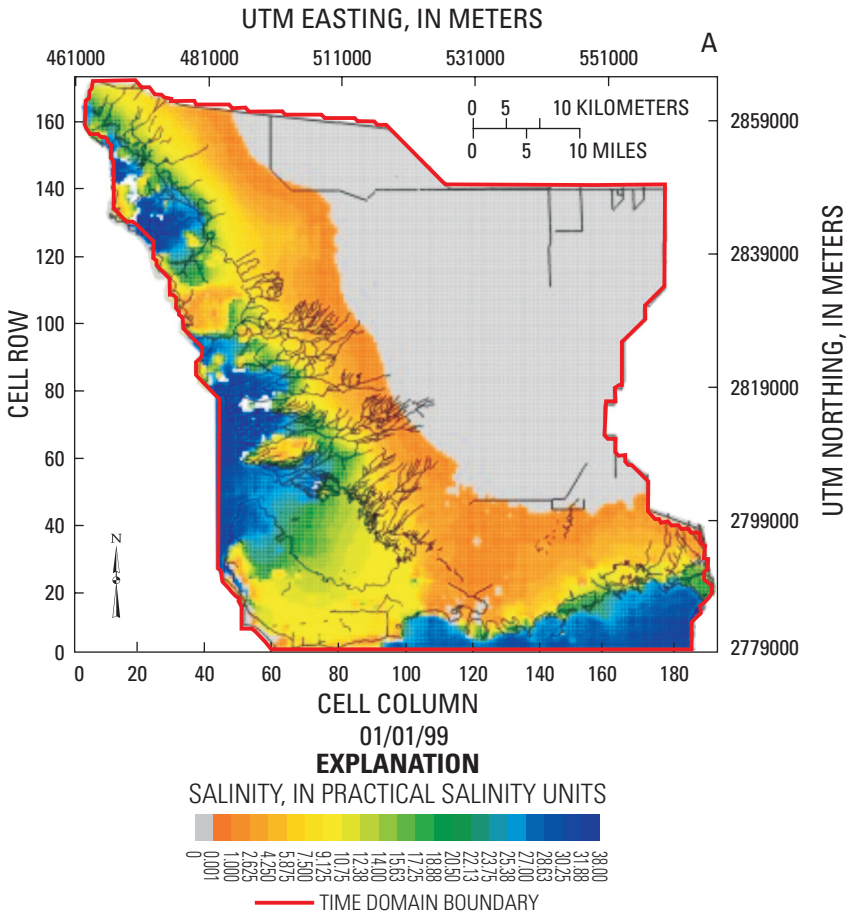

Figure 22A. Spatial and temporal distribution of surface-water salinity in the TIME area. TIME is Tides and Inflows in the Mangroves of the Everglades.

There are no known surface-water flow measurements within Everglades National Park and Big Cypress National Preserve that are suitable for model comparison during the SDP. As a result, the surface-water velocity fields shown in figure 21 are based on model results. Each velocity value is plotted as a vector from the point where the velocity applies. For clarity, only every other vector is shown, and vectors representing flows greater than 0.06 m/s are reduced to 10 percent of their original length. Velocities typically average about 0.01 m/s within the wetlands, and substantially more in tidally influenced areas near the coast.

A series of surface-water salinity maps are presented in figure 22A-I to illustrate model performance. It seems reasonable to assume that salinities during the wet season are too high because the open boundary condition is fixed at 36 psu. This may also affect dry-season salinities because salt can be trapped in isolated surface-water bodies and in the top layer of ground water. Evapotranspiration (ET) then can further concentrate the salt in the remaining water.

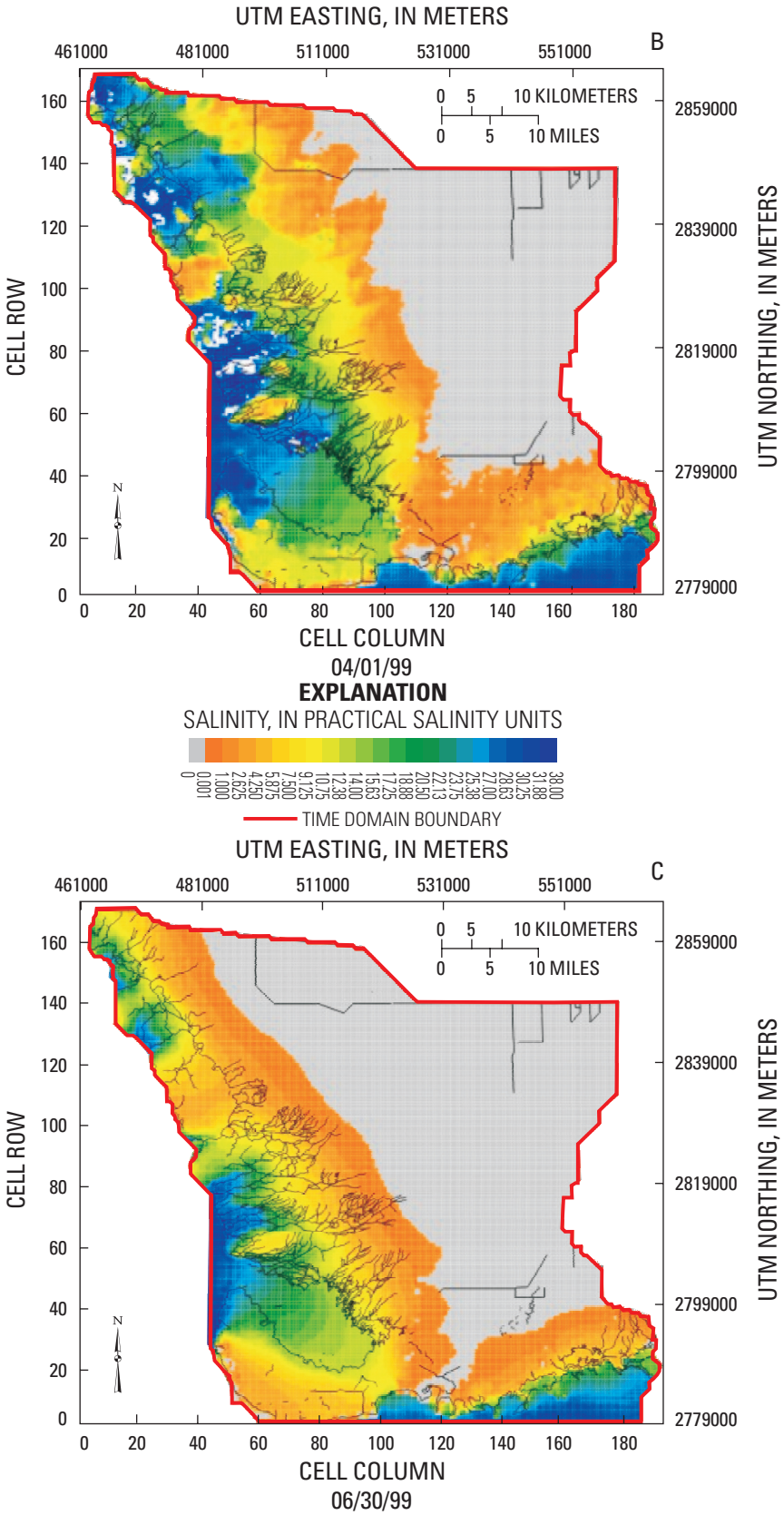

Figure 22B-C. Spatial and temporal distribution of surface-water salinity in the TIME area. TIME is Tides and Inflows in the Mangroves of the Everglades.

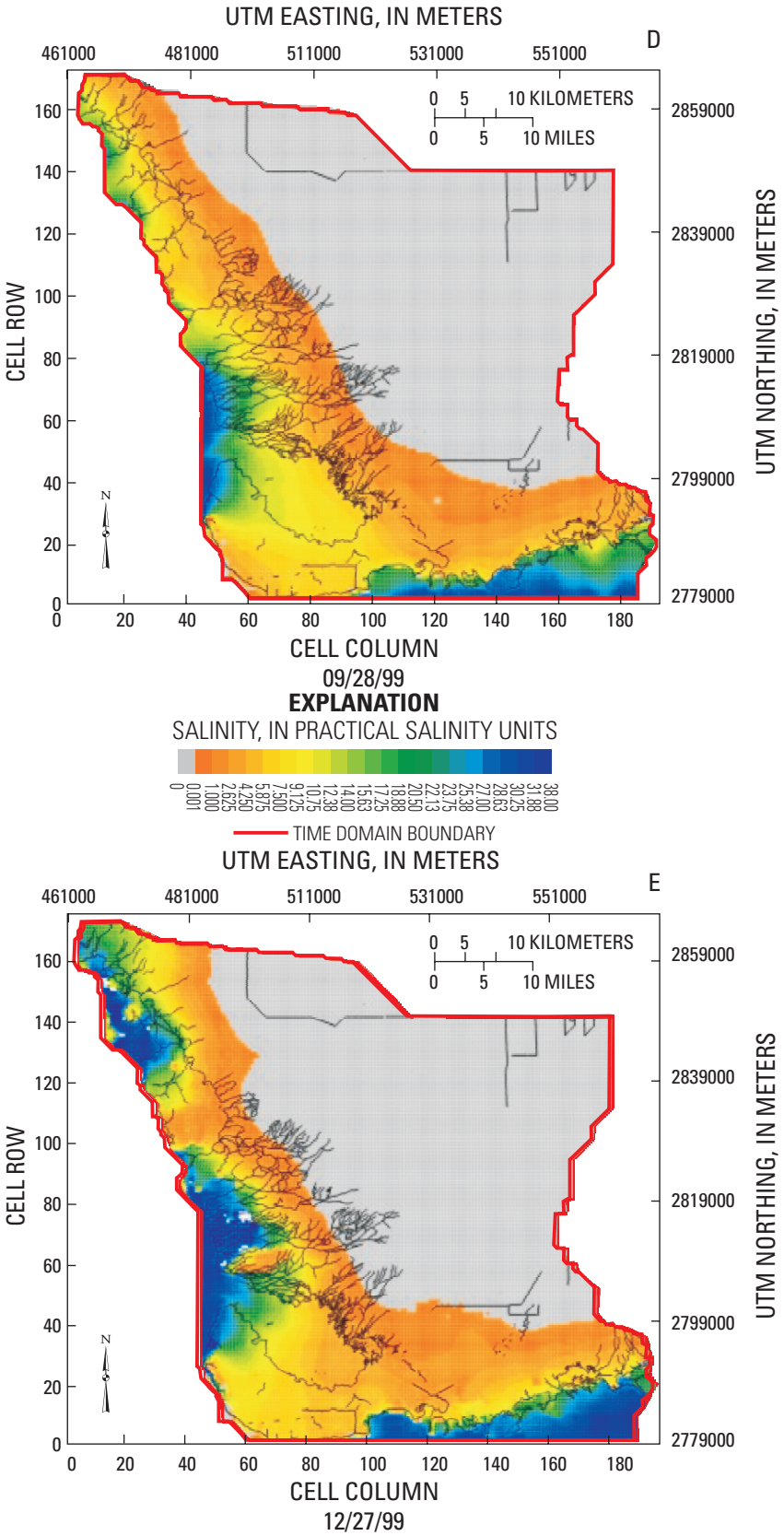

Figure 22D-E. Spatial and temporal distribution of surface-water salinity in the TIME area. TIME is Tides and Inflows in the Mangroves of the Everglades.

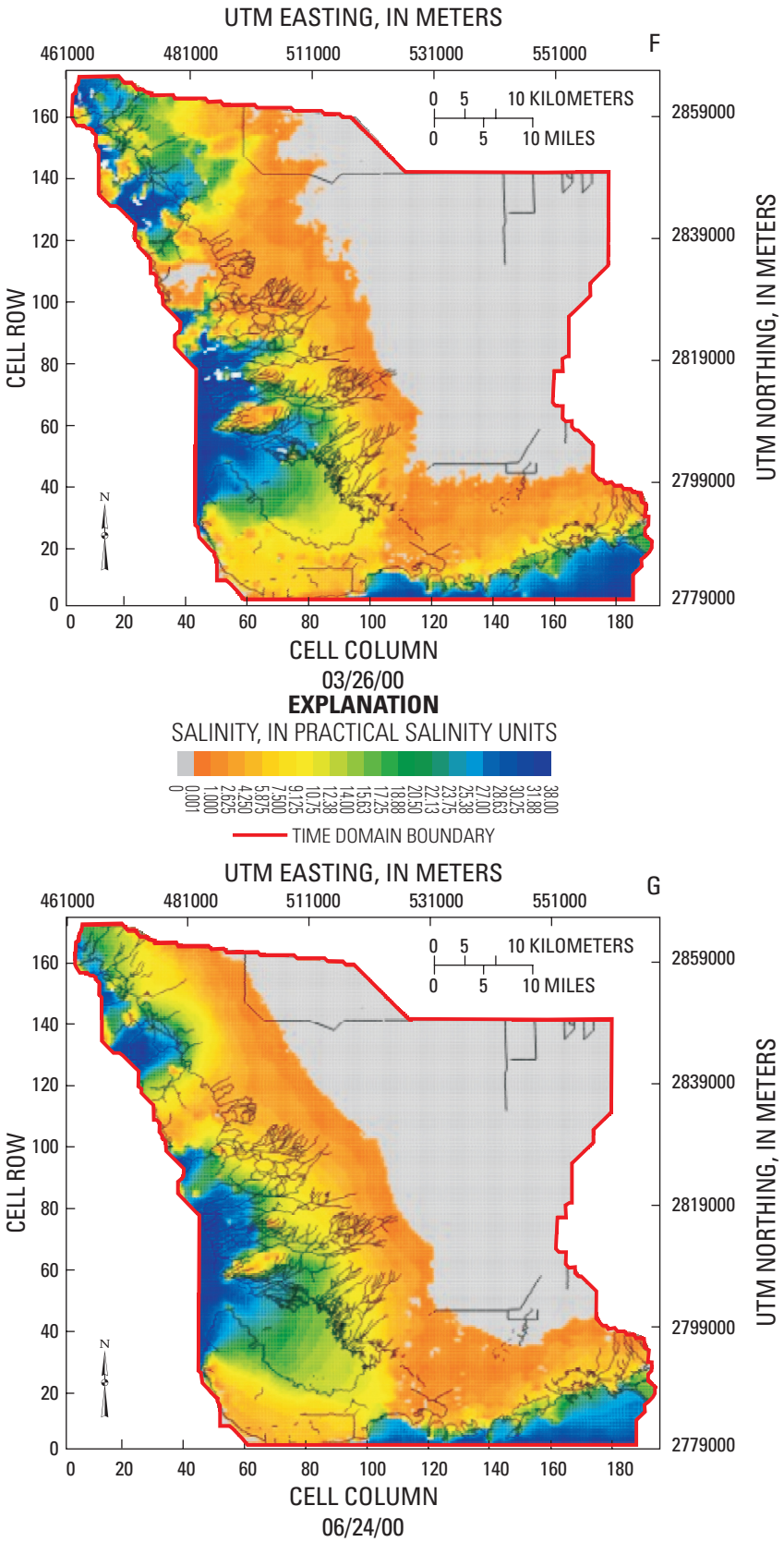

Figure 22F-G. Spatial and temporal distribution of surface-water salinity in the TIME area. TIME is Tides and Inflows in the Mangroves of the Everglades.

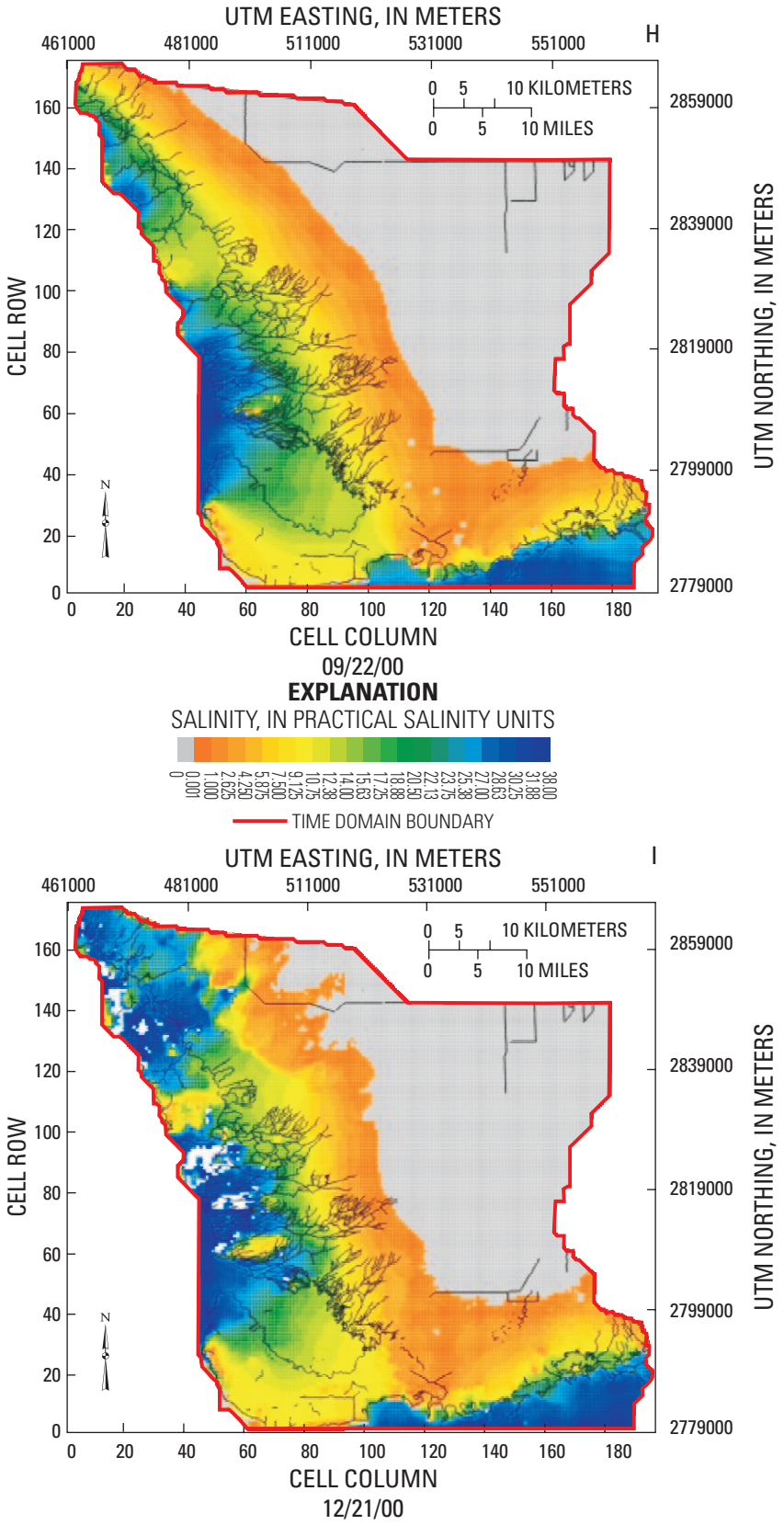

Figure 22H-I. Spatial and temporal distribution of surface-water salinity in the TIME area. TIME is Tides and Inflows in the Mangroves of the Everglades.

3.6.5 - Leakage and Evapotranspiration Rates

Maps of average calculated leakage rates for the SDP show a zone of strong upward leakage on the southern side of Tamiami Trail (figs. 1 and 23). This zone of upward leakage is created by ground water flowing beneath the trail as a result of higher ground-water heads on the northern side of the trail. Conversely, a zone of strong downward leakage and eastward ground-water flow exists along Levee 31, and results from the drained conditions in developed coastal areas east of the levee. Zones of relatively minor upward leakage occur where relatively low land-surface altitudes are present south and west of the C-111 Canal and in waterways along the coast.

Total flux, including (1) upward and downward surface- and ground-water leakage, and (2) ground-water ET during the SDP, was summed spatially and temporally (fig. 24). Consumptive ground-water use due to evapotranspiration during a period of 7 years (3.64×10^9 m^3) exceeds losses asociated with upward ground-water leakage (2.40×10^9 m^3); the sum of vertical flux and consumptive losses closely corresponds to downward vertical leakage of surface water (5.94×10^9 m^3). Head-dependent ground-water boundary flux across all GHBs should equal the net volume of vertical flow. In this instance:

5.94×10^9 m^3 (downward vertical surface-water leakage)
- 3.64×10^9 m^3 (consumptive losses by evapotranspiration)
- 2.40×10^9 m^3 (head-dependent ground-water boundary flux)

-0.10×10^9 m^3 (negative sign indicates leakage of ground water from aquifer to surface)

The model budget shows a head-dependent flow into the aquifer of 2.07×10^9 m^3 compared to an outflow of 1.9637×10^9 m^3, which is presumed to be leakage to coastal canals, resulting in a net inflow to the aquifer of about 0.10×10^9 m^3. This

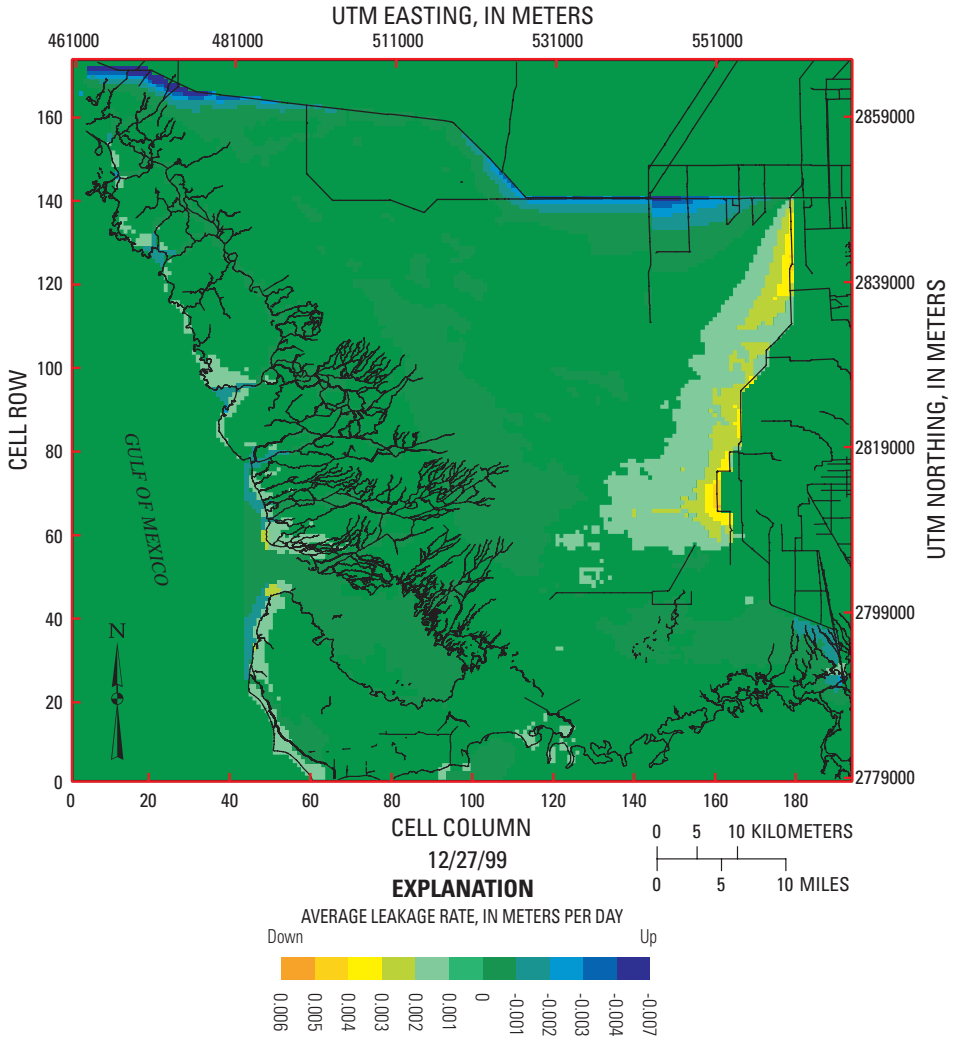

Figure 23. Average leakage rates in the TIME area.

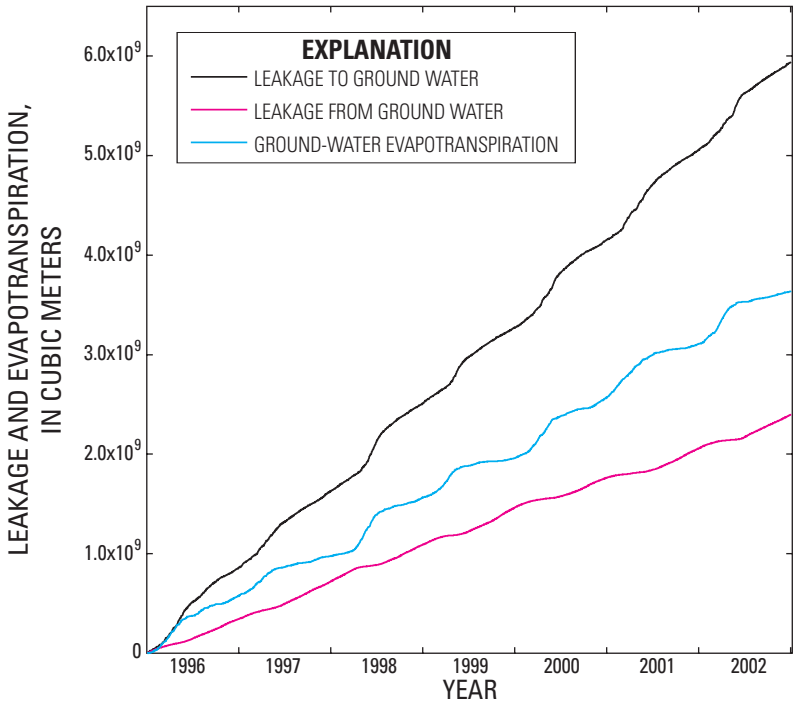

Figure 24. Cumulative leakage and evapotranspiration from ground water in the TIME area for the standard data period.

is equal and opposite to the net vertical volume flow and is relatively small compared to leakage or ET from ground water.

Nemeth and others (2000) estimated that leakage beneath Levee 31N ranges from –18.7 to +46.5 m^3/d per meter of levee. Assuming an average leakage of 30 m^3/d per meter and a levee length of 25 km yields a total leakage of 1.92 $x10^9$ m^3 for the SDP, which is in good agreement with the model result noted earlier. In contrast, the total flow from S-12D noted earlier is 2×10^9 m^3, which is an order of magnitude greater than the net head-dependent ground-water inflow. Thus, the ground acts as a surface-water sink, with total volume into ground water equal to 2.3 $x10^9$ m^3. This is a small fraction of the total flow from all culverts and structures, and therefore, perhaps of secondary importance.

3.6.6 - Ground-Water Flows and Salinities

The ground-water flows in layer 1 of the model reflect the leakage pattern, with flows directed toward the east along most of Levee 31 and toward the south along Tamiami Trail. In lower layers, flow divergence is evident along the salinity front. The flows at the beginning and end of the simulation are similar, indicating that ground-water flow adjustments occur slowly and may take several decades to reach equilibrium.

Ground-water salinities are influenced by the assumed initial conditions and additionally are affected by open-boundary conditions in the surface-water model. The simulations, however, show that the salinity front is far inland on the western side of the domain as indicated by resistivity studies (Fitterman and Deszcz-Pan, 2002). Until better boundary conditions can be prescribed and simulations can be run for longer time periods, computed ground-water salinities are not significant, and therefore, are not shown.

3.7 - Model Sensitivity Studies

To better understand model response and the robustness of calculated flows to the coast, a number of runs were conducted in which the major assumptions and parameters were varied. Several indices were used to measure model performance: (1) the sum of the absolute values of the difference in means, (2) the sum of squares of the difference in means, (3) the sum of correlations, and (4) the sum of PEV values for all 105 stage stations for which comparisons were made between model output and field data. These measures are not completely independent, but are reported in table 5 to accommodate different aspects of the analysis. Additionally, the average flows to the coast for the SDP are compared in figure 25, which shows the average flow at: (1) open-boundary

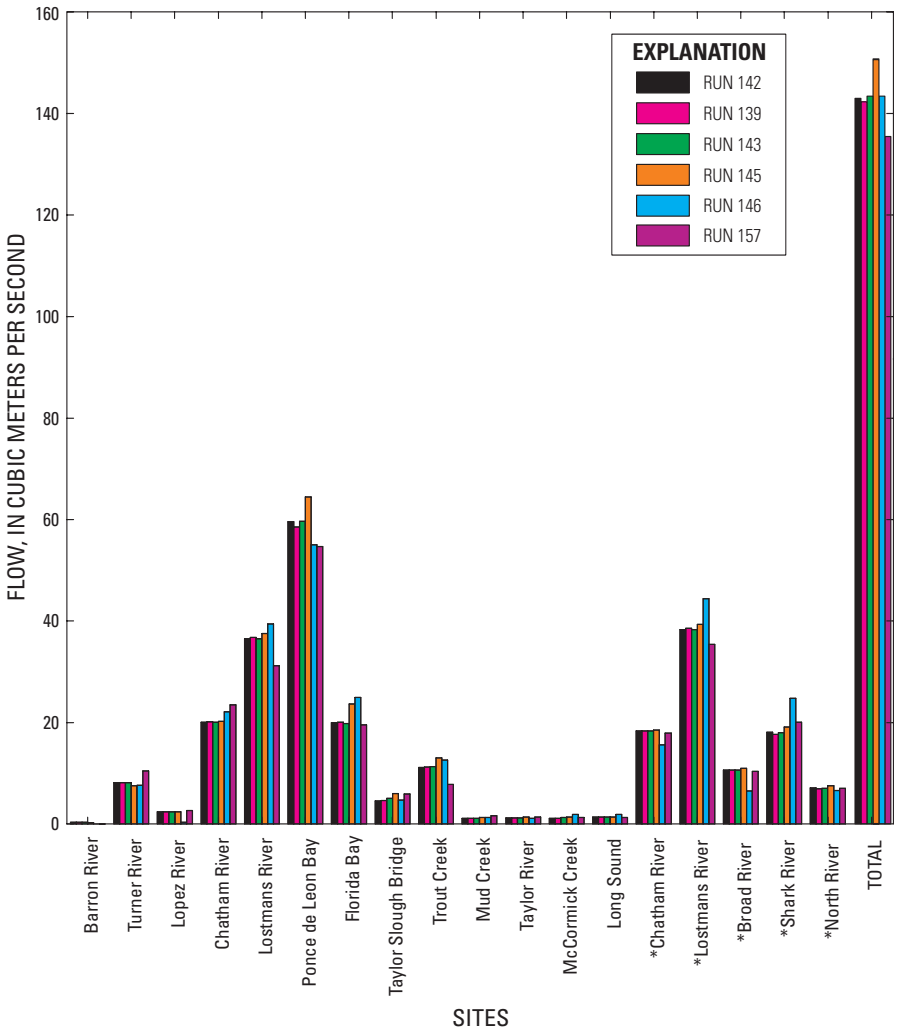

Figure 25. Average flows to the coast for the standard data period. Asterisk indicates flow at location of U.S. Geological Survey monitoring station.

locations, (2) mouths of creeks along the Florida Bay coastline, (3) USGS monitoring stations along the west coast rivers, and (4) TSB.

3.7.1 - Comparison of Versions 2.1 and 2.2 of the FTLOADDS Code

The TIME application can be further examined in the Taylor Slough area by comparison to the previous SICS application. Toward this end, a simulation was developed that isolates the SICS domain within the TIME domain. This simulation permitted direct comparison between applications using the same domain and boundary conditions, but with somewhat different model formulations, rainfall distributions, and grid resolutions.

As discussed in section 2.2, the FTLOADDS code version 2.2 in the TIME application includes several modifications not available in the version 2.1 SICS application. The TIME application also has inherent differences in grid spacing, time-step length, creek representation, and boundary conditions. It was, therefore, of interest to compare the new and old formulations and applications. To accomplish this, the area of the TIME application grid outside the domain of the original SICS application was made inactive, and boundaries around the active region were defined with the same flow and water-level conditions used in the SICS application. This modified application is referred to as the Embedded SICS (ESICS) application, the domain of which is shown in figure 26. Boundaries were modified by specifying: flow at TSB, Levee 31W Canal, and C-111 Canal, water levels along Old Ingraham Highway, and ground-water heads beneath the levee along the northern part of C-111 Canal. The

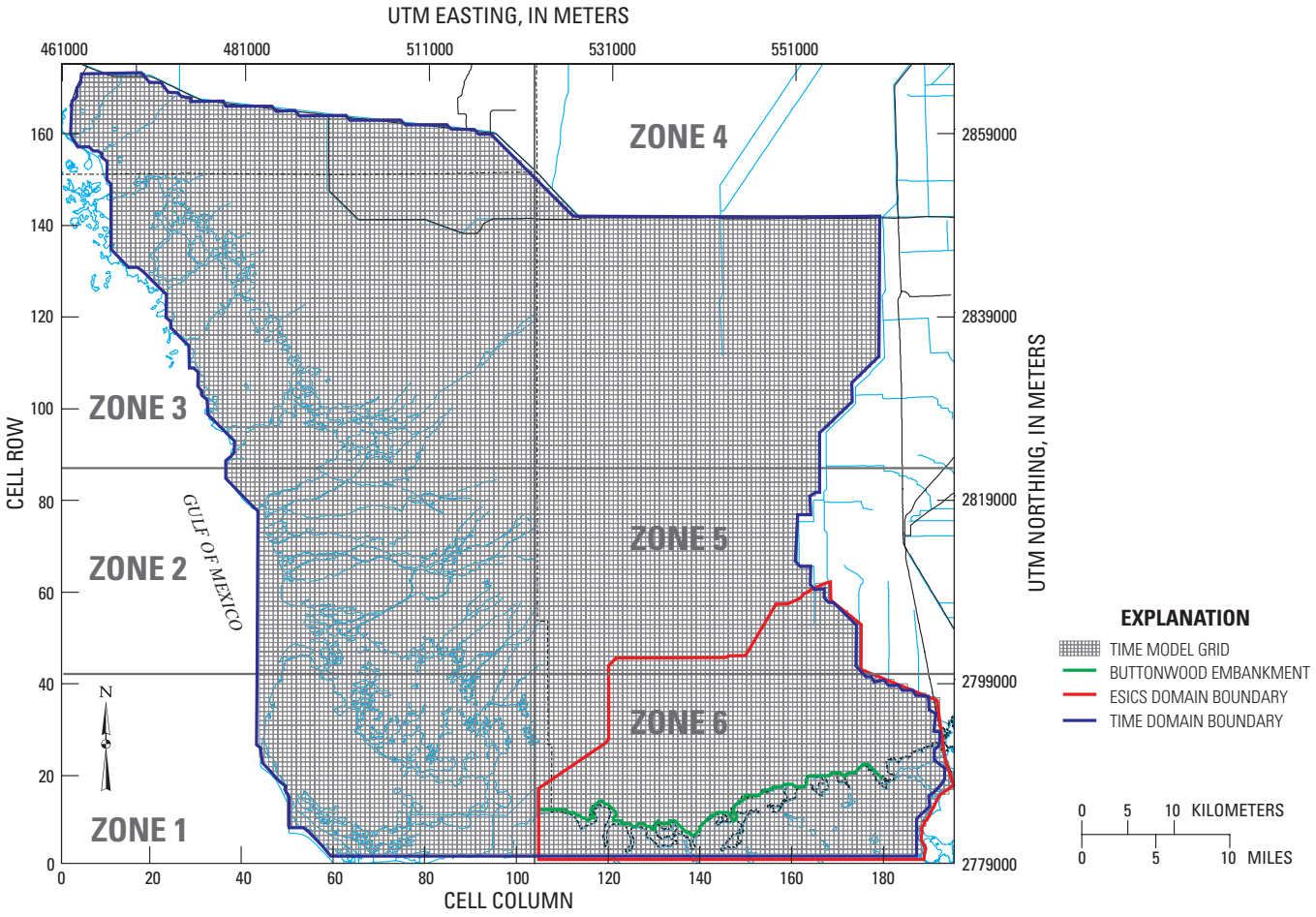

Figure 26. Area of the TIME domain used to create the ESICS domain.

Table 8. Comparison of SICS and ESICS applications.

[SICS, Southern Inland and Coastal Systems; ESICS, Embedded Southern Inland and Coastal Systems]

Model characteristic	Model	
	SICS	ESICS
Grid Spacing	305 meters	500 meters
Rainfall	Specified at 15-minute intervals and spatially interpolated for each model cell	Specified as 6-hour averages and partially uniform over zones defined for the TIME application.
Evapotranspiration	Computed cell-by-cell according to the best-fit equation discussed by Swain and others (2004)	Computed using the modified Penman method
Wetting and drying	Model cell removed from computational domain when water-level drops below user-defined depth	Algorithm modified to allow for rewetting directly from rainfall recharge and evapotranspiration from residual water
Frictional-resistance terms	Defined at cell centers	Defined at cell faces
Coastal embankment	Defined by the formulation of barriers originally designed to represent weirs; coastal rivers are defined as low barriers with a representative flow coefficient	Defined by modified cell-face frictional-resistance terms; coastal creeks are defined as gaps with specified friction terms

boundary conditions of the ESICS application were defined with the same field time-series data used for the original SICS application. The basic differences between the SICS and ESICS applications are the same as those between SICS and TIME, and versions 2.1 and 2.2 of FTLOADDS (table 8).

The ESICS and TIME applications are identical (or nearly so) in several respects:

- The TIME grid is retained in ESICS; therefore, the same 500-m grid spacing is used.
- Rainfall zonation is identical in ESICS and TIME, although only rainfall zones 5 and 6 have portions within the ESICS domain.
- Evapotranspiration is identical for equivalent cells in ESICS and TIME.
- Frictional terms used at the cell faces are identical in ESICS and TIME. The terms are varied at the coastal embankment and at the coastal creeks as part of the calibration procedure. After the terms are calibrated in the ESICS application, they are transferred to the TIME application for use in representing the embankment and creeks.

SICS and ESICS application results were compared to evaluate the implications of differences between versions 2.1 and 2.2 of the FTLOADDS code. The comparison also provides insight into the relative accuracy of the TIME and SICS applications. One of the version differences is in the representation of coastal creeks. The calibrated frictional values (Manning's n) at the cell faces representing the creeks cannot be equated directly to the properties of the actual creeks, primarily because cell cross-sectional areas are greater than the actual creeks and cell depths are generally less than the actual creeks. Additionally, a given creek may occupy only a fraction of the distance between centers of adjacent cells. In order to relate cell frictional resistance to the actual creek, it is useful to visualize the total head loss between the two cells representing the creek in three parts: head loss between the upstream cell center and the upstream end of the creek, h_1; head loss through the creek, h_2; and head loss between the end of the creek and the center of the downstream cell, h_3. Using Manning's equation, the sum of these three variables must equal the head loss depicted in the model:

$$h_1 + h_2 + h_3 = \frac{Q^2 n_{cell}^2 l_{cell}}{d_{cell}^{10/3} w_{cell}^2}, \quad (5)$$

where Q is flow rate, n_{cell} is Manning's n in the cell, l_{cell} is length dimension of the cell, d_{cell} is cell depth, and w_{cell} is cell width (the same as the cell length for a square cell). The head loss terms take the form:

$$h_1 = \frac{Q^2 n_{up}^2 \left(l_{cell} - l_{creek}/2\right)}{d_{cell}^{10/3} w_{cell}^2}, \quad (6)$$

$$h_2 = \frac{Q^2 n_{creek}^2 l_{creek}}{d_{creek}^{10/3} w_{creek}^2}, \quad (7)$$

and:

$$h_3 = \frac{Q^2 n_{dn}^2 \left(l_{cell} - l_{creek}/2\right)}{d_{cell}^{10/3} w_{cell}^2}, \quad (8)$$

where

n_{up} is Manning's n in the upstream cell area,
l_{creek} is creek length,
n_{creek} is Manning's n in the creek,
n_{dn} is Manning's n in the downstream cell area,
d_{creek} is creek depth, and
w_{creek} is cell depth.

Combining these three equations yields:

$$n_{creek} = \sqrt{\frac{n_{cell}^2 l_{rat} - \left(n_{up} + n_{dn}\right)/2 \left(l_{rat} - 1\right)}{d_{rat}^{10/3} w_{rat}^2}}, \quad (9)$$

where l_{rat} is the ratio of cell length to creek length, d_{rat} is the ratio of cell depth to creek depth, and w_{rat} is the ratio of cell width to creek width. Using a model cell width of 500 m and known creek widths from Swain and others (2004), the ratios of cell to creek widths are as follows: McCormick Creek w_{rat} is 29.76, Taylor River w_{rat} is 74.63, Mud Creek w_{rat} is 40.98, Trout Creek w_{rat} is 13.66, and West Highway Creek w_{rat} is 23.47.

The ratios of cell to creek depths vary with water level, thus a representative mean stage must be used. With an assigned stage of about 0 m relative to NAVD 88, the ratios are as follows: McCormick Creek d_{rat} is 0.658, Taylor River d_{rat} is 0.691, Mud Creek d_{rat} is 0.592, Trout Creek d_{rat} is 0.789, and West Highway Creek d_{rat} is 1.0.

Creek length was determined from digital maps of the area. For a creek longer than a cell dimension, the cell dimension was used because it is the relevant distance over which the water-level difference is represented. The following ratios of cell length to creek length were then calculated: McCormick l_{rat} = 1.0, Taylor l_{rat} = 1.0, Mud l_{rat} = 1.21, Trout l_{rat} = 3.29, and West Highway l_{rat} = 1.66. This results in the following n values: McCormick Creek n_{cell} = 0.7, n_{creek} = 0.047; Taylor River n_{cell} = 1.0, n_{creek} = 0.047; Mud Creek n_{cell} = 0.7, n_{creek} = 0.045; Trout Creek n_{cell} = 0.08, n_{creek} = 0.015; and West Highway Creek n_{cell} = 0.4, n_{creek} = 0.022.

This computation yields low Manning's n values compared to previously accepted values (Swain and others, 2004); however, this easily could be due to the different representation of the creeks. The ability of the model to represent coastal flow conditions is the best measure of the utility of each method.

The primary model output used for comparison is the discharge at the coastal creeks, primarily McCormick Creek, Taylor River, Mud Creek, Trout Creek, and West Highway Creek. It is generally more difficult to represent discharge than water levels in numerical models. Coastal discharges are of primary interest, however, to the restoration efforts as a measure of freshwater flow to the estuaries. A comparison between flows from field data, the original SICS application, and ESICS is shown in figure 27. The improvement with ESICS is apparent, especially in the representation of flow peaks. Computing the mean absolute error (MAE) between each of the applications (SICS and ESICS) and the field data yields the following results:

Creek	Mean absolute error (cubic meter per second)	
	SICS	ESICS
McCormick Creek	1.69	1.27
Taylor River	.928	.900
Mud Creek	.962	.801
Trout Creek	6.20	5.07
West Highway Creek	1.42	1.27

A consistent reduction in the MAE occurs at all flow locations with ESICS versions 2.1 and 2.2

Two different methods for representing the frictional-resistance term are used in the ESICS comparison. The constant Manning's *n* representation uses the standard representation of Manning's frictional resistance with a constant value to compute the Chezy *C* value (Swain, 2005, p. 11). The variable Manning's *n* representation uses the empirically derived variation of *n* with depth from Swain and others (2004). This variable formulation is designed to approximate the effects of emergent vegetation and microtopography on the frictional resistance. The coefficients in the formulation were varied empirically, however, to obtain the best fit with the original SICS application, and thus the method had no theoretical foundation. The comparison of these two methods is shown in figure 28. The variable Manning's *n* method provides results that are closer to field measurements, but still reduces the rapid recessions when regional drying occurs. A comparison of stages produced by SICS and ESICS at selected wetland stations is shown in figure 29. Although model performance is demonstrated more critically with comparisons of volume fluxes, the ability to represent similar stage values also indicates coherence and agreement between SICS and ESICS.

3.7.2 - Sensitivity to Manning's *n* Adjustment

In run 139, Manning's *n* is adjusted in the arbitrary rectangles shown in figure 5 to determine the effects of gross changes in friction. The locations of the rectangles were chosen to affect the mean bias at NP201, S12B, S12C, NE2, and P34 (fig. 9). As evidenced by the stage comparison statistics for runs 139 and 142 (the base run) in tables 9 and 10, respectively, the simulated mean (compared to the measured mean) changes at these sites as follows:

Site	Model mean compared to measured mean (meters)	
	Original Manning's *n*	Adjusted Manning's *n*
NP201	0.04 low	0.06 high
S-12B	.15 low	.06 high
S-12C	.06 low	.05 low
NE2	.11 high	.09 high
P34	.004 high	.106 high

There are few substantial changes in mean stage difference other than at stations NP201, S12B, S12C, NE2, and P34, and these represent mixed results. The spatial distribution of mean stage difference, defined as abs[DIFMEAN(run 142)-abs(DIFMEAN(run 139)], is shown in figure 30. The map shows improvements in stage mean differences, which are defined as being closer to the data mean, as positive values and deteriorations in stage mean differences as negative values. The local changes to Manning's *n* result in local changes to (mean) stages, such as those south of the S-12 structures (figs. 1 and 30).

The improvements achieved at some locations were not sufficient to improve substantially the overall performance indices because these improvements are cancelled effectively by deteriorations at other locations (table 9) and coastal discharges probably are not affected substantially. Any applicable change in Manning's *n* would have to be more physically based than this sensitivity test.

3.7.3 - Neglecting Ground-Water Leakage Effects

A scenario also was made with TIME to investigate the effect of neglecting surface-water and ground-water leakage (run 145). Net-average flows were reduced up to 20 percent in Barron River and 7 percent in Turner River, whereas flows into Ponce De Leon Bay and Florida Bay increased by 8 and 20 percent, respectively.

The spatial distribution of mean stage differences [mean(R142)-mean (R145)] is shown in figure 31, which indicates that neglecting leakage adversely affects all model performance indices (stage means, correlation, and PEV). This effect is due primarily to the substantial changes that occur in ground-water heads, which differ substantially when leakage is neglected. Surface-water stages change slightly at most sites, although substantial differences occur at some locations (table 11). At these sites, however, stage is influenced strongly by ground-water head. By not having any vertical leakage, surface water along the eastern domain boundary flows

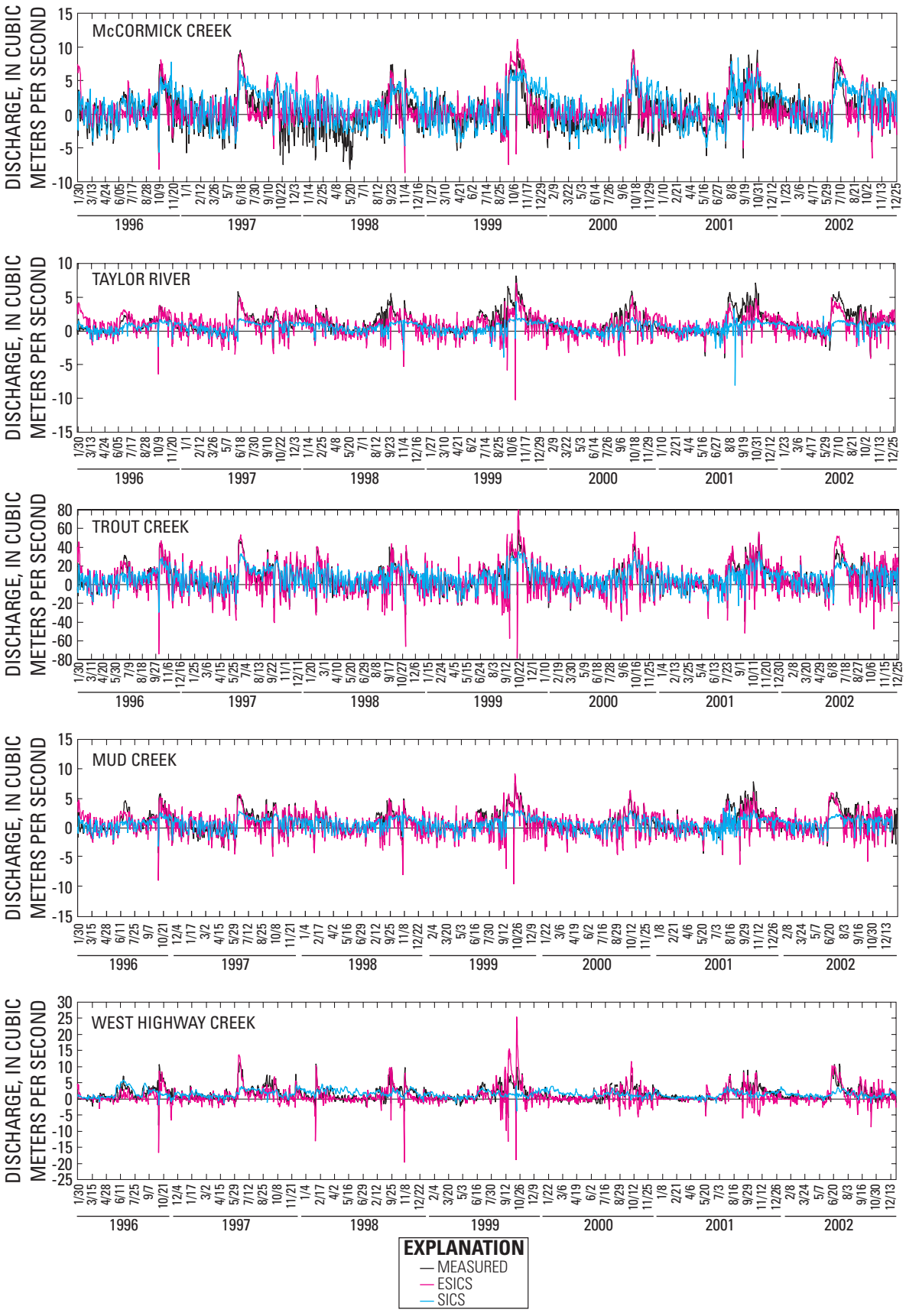

Figure 27. Comparison of flows from field data and the SICS and ESICS applications at selected coastal creeks, 1996-2002.

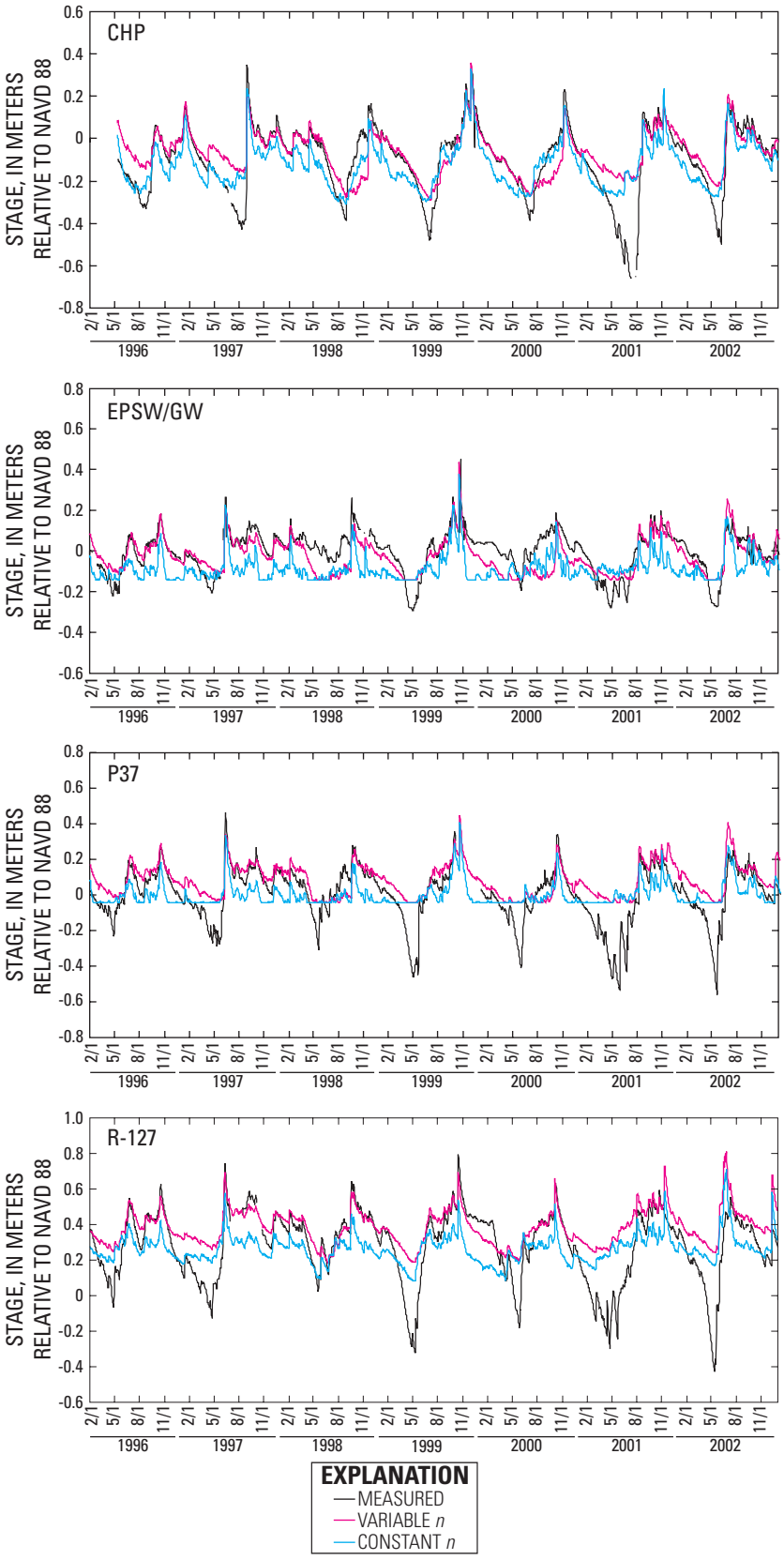

Figure 28. Comparison of wetland stages using constant and variable Manning's *n* values at selected sites.

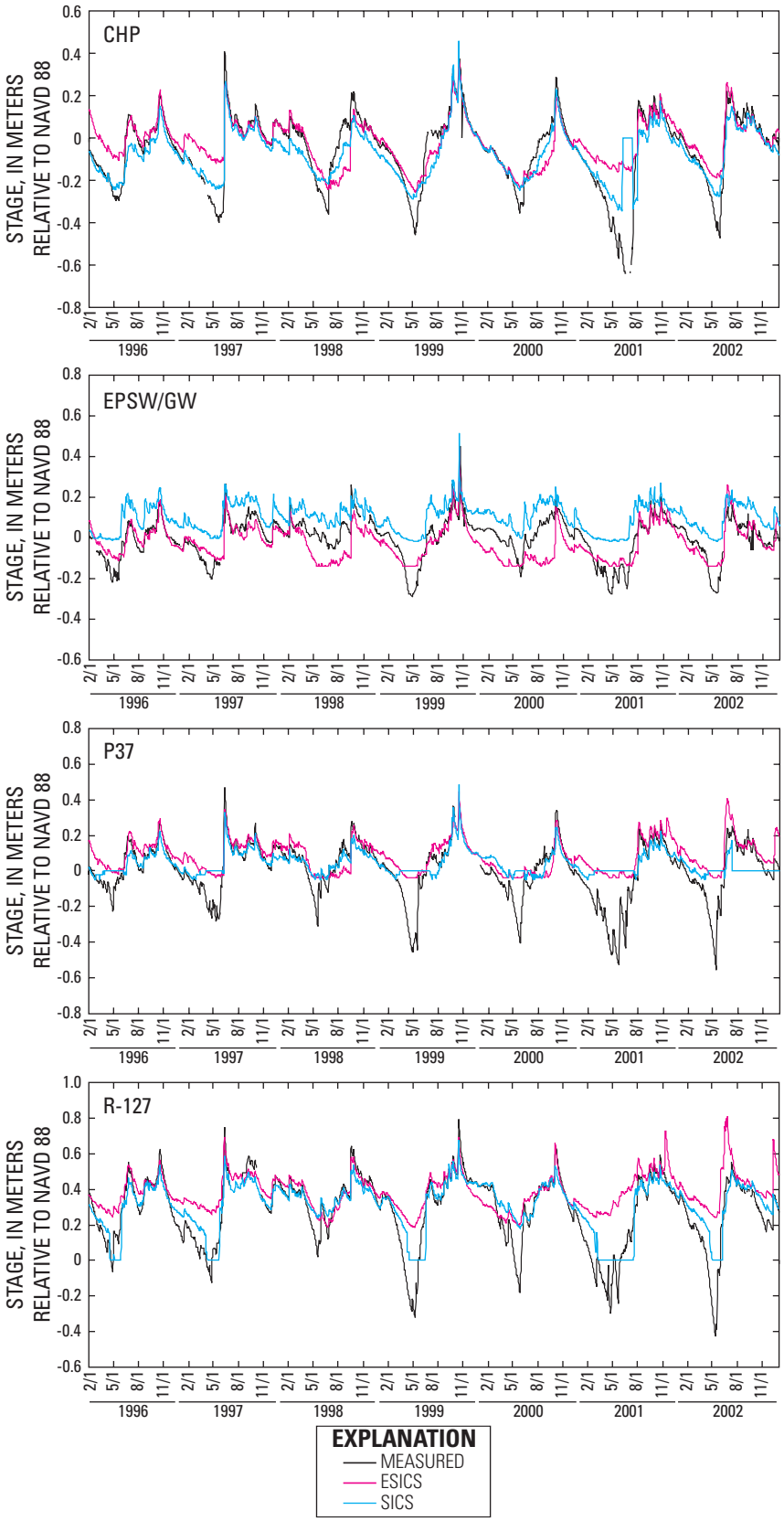

Figure 29. Comparison of stages between the SICS and ESICS applications at selected wetland stations.

Table 9. Water-level comparison statistics for run 139, local Manning's *n* adjustments.

[NAVD 88, North American Vertical Datum of 1988; n, number of points utilized from the time series]

Station	Mean stage (NAVD 88)		Stage standard deviation		Correlation coefficient	Mean difference between measured and computed values		Percentage of explained variance	n	Land surface altitude (NAVD 88)	
	Measured (meters)	Computed (meters)	Measured (meters)	Computed (meters)		Stage (meters)	Standard deviation (meters)			Model input (meters)	Measured (meters)
A13	0.968	1.091	0.259	0.144	0.867	-0.123	0.152	65.4	2197	0.980	0.969
Angels	1.329	1.500	.264	.282	.741	-.171	.197	44.3	2557	1.730	1.451
BD	.826	.062	.123	.088	.412	.764	.118	7.4	1945	.010	2.612
BICYA8	.215	.850	.328	.457	.217	-.635	.501	-133.9	1959	.270	--
BICYA9	1.726	1.853	.211	.189	.763	-.126	.139	56.3	1869	2.060	--
BICYA10	.718	.788	.303	.228	.780	-.071	.190	60.8	1854	.890	--
BICYA11	.920	.938	.380	.172	.718	-.017	.283	44.4	1883	.880	--
BR	1.074	.025	.131	.114	.837	1.049	.072	69.8	2331	-.150	1.838
CN	.713	.025	.123	.079	.860	.688	.068	69.1	2447	-.080	1.323
CP	-.056	-.081	.169	.120	.879	.025	.085	74.4	2479	-.440	-.503
CR2	1.121	1.283	.307	.289	.895	-.162	.138	79.9	2161	1.330	1.231
CR3	1.119	1.270	.298	.228	.879	-.151	.146	75.9	2212	1.310	1.234
CT27R	.143	.082	.148	.126	.570	.062	.128	24.8	1903	-.060	-.085
CT50R	.106	.100	.140	.091	.859	.005	.078	69.3	1896	.010	.088
CV1NR	.121	.080	.149	.128	.400	.041	.153	-5.3	1840	-.060	--
CV5S	.123	.115	.132	.103	.441	.008	.127	7.9	601	-.060	--
CW	-.048	-.065	.103	.126	.486	.017	.118	-31.0	2261	-1.830	--
CYP2	.235	.292	.206	.205	.787	-.057	.134	57.5	2157	.480	1.643
CY3	.202	.195	.214	.169	.785	.008	.133	61.6	2206	.280	1.518
DK	-.207	-.177	.118	.096	.712	-.030	.083	49.6	1317	-1.860	--
DO1	.349	.479	.267	.181	.845	-.130	.149	68.6	2451	.560	.567
DO2	.432	.450	.278	.199	.825	-.018	.160	67.0	2237	.700	.570
E112	.846	.979	.301	.406	.880	-.133	.201	55.7	2320	1.050	.527
E146	-.096	-.083	.147	.132	.864	-.013	.074	74.5	2435	-.210	-.369
EP1R	.044	.065	.132	.120	.415	-.021	.137	-7.1	2406	-.060	-.262
EP9R	-.159	-.117	.087	.057	.840	-.042	.050	67.2	366	-.160	-.314
EPGW/ SW	-.015	-.066	.099	.074	.696	.051	.071	48.1	2387	-.110	-.158
EVER4	.170	.327	.145	.174	.925	-.157	.068	78.2	2521	.240	.085
EVER5A	-.097	-.026	.153	.101	.829	-.071	.089	66.0	1945	-.080	-.174
EVER6	.141	.033	.126	.083	.780	.107	.080	59.4	2294	.000	-.006
EVER7	.201	.103	.120	.109	.891	.098	.054	79.3	2342	.040	.131
G1251	.185	.230	.168	.178	.901	-.045	.078	78.7	2026	.230	.390
G1502	1.485	1.697	.242	.143	.780	-.211	.158	57.3	2453	1.580	2.060
G3272	1.491	1.699	.247	.144	.821	-.208	.153	61.8	2528	1.570	1.612
G3273	1.476	1.695	.239	.147	.822	-.219	.145	63.2	2557	1.600	1.667

Table 9. Water-level comparison statistics for run 139, local Manning's *n* adjustments.—Continued

[NAVD 88, North American Vertical Datum of 1988; n, number of points utilized from the time series]

Station	Mean stage (NAVD 88)		Stage standard deviation		Correlation coefficient	Mean difference between measured and computed values		Percentage of explained variance	n	Land surface altitude (NAVD 88)	
	Measured (meters)	Computed (meters)	Measured (meters)	Computed (meters)		Stage (meters)	Standard deviation (meters)			Model input (meters)	Measured (meters)
G3353	-0.058	-0.001	0.137	0.108	0.858	-0.057	0.071	73.0	2519	-0.020	1.149
G3437	1.194	1.124	.259	.273	.682	.070	.213	32.4	2510	1.850	1.615
G3576	1.562	1.698	.207	.113	.898	-.136	.117	68.2	1965	1.370	1.353
G3577	1.426	1.703	.272	.112	.849	-.277	.186	53.0	2014	1.360	1.356
G3578	1.520	1.710	.213	.103	.887	-.190	.131	62.3	2494	1.370	1.356
G3619	.326	.391	.147	.155	.894	-.065	.070	77.5	2446	.210	.579
G3622	.879	1.231	.239	.418	.677	-.352	.311	-68.8	2306	1.390	1.347
G3626	.975	1.122	.174	.304	.409	-.147	.282	-161.8	2357	2.030	1.743
G3627	.860	1.247	.167	.264	.534	-.386	.225	-81.3	2368	1.910	1.942
G3628	1.011	1.473	.203	.396	.497	-.462	.343	-186.0	2336	1.730	1.667
G596	1.146	1.292	.197	.313	.595	-.146	.252	-62.7	2546	1.810	1.753
G618	1.696	1.714	.146	.088	.731	-.018	.101	51.9	2457	1.480	1.466
G620	1.574	1.680	.205	.192	.930	-.106	.075	86.6	2451	1.380	1.311
GI	1.363	-.081	.113	.179	.378	1.444	.172	-130.0	1616	-2.500	--
HC	-.186	.158	.111	.222	.599	-.344	.179	-159.2	1434	.560	--
HR	.931	.017	.119	.144	.624	.915	.116	5.3	1461	.120	--
L67XW	1.761	1.706	.237	.098	.832	.055	.165	51.5	1883	1.350	--
LN	1.524	-.033	.120	.100	.821	1.557	.069	67.4	1430	-.410	--
LO	.818	-.069	.119	.249	.145	.887	.260	-378.1	1335	-2.000	--
LOOP1T	1.910	1.841	.158	.172	.727	.070	.123	39.8	2024	1.860	--
LOOP2T	1.540	1.498	.220	.178	.698	.042	.159	47.4	2086	1.480	--
LS	-.190	-.174	.106	.099	.775	-.016	.069	57.5	1461	-1.520	--
NCL	-.015	-.086	.190	.161	.834	.071	.105	69.5	2390	-.240	--
NE1	1.664	1.711	.131	.093	.903	-.047	.062	77.7	2509	1.290	1.314
NE2	1.627	1.713	.156	.090	.890	-.087	.086	69.4	2503	1.340	1.241
NE3	1.695	1.721	.115	.075	.808	-.027	.070	63.0	1838	1.340	--
NE4	1.606	1.706	.158	.095	.882	-.100	.087	70.0	2416	1.260	1.213
NE5	1.601	1.700	.146	.096	.895	-.100	.074	74.5	2539	1.270	--
NMP	-.118	-.106	.151	.167	.856	-.012	.087	67.1	2113	.010	--
NP201	1.869	1.934	.257	.236	.865	-.065	.130	74.7	2439	1.650	1.420
NP202	1.679	1.752	.196	.183	.970	-.073	.048	94.0	2309	1.350	1.164
NP203	1.471	1.508	.181	.124	.938	-.038	.078	81.6	2426	1.220	.890
NP205	1.478	1.520	.264	.165	.853	-.042	.150	67.6	2447	1.440	1.332
NP206	1.282	1.425	.272	.136	.819	-.143	.179	56.8	2453	1.380	1.366
NP44	.636	.783	.351	.232	.765	-.147	.229	57.4	2342	1.270	1.073
NP46	0.018	-0.018	0.171	0.147	0.740	0.036	0.117	53.3	2429	0.050	-0.052

Table 9. Water-level comparison statistics for run 139, local Manning's *n* adjustments.—Continued

[NAVD 88, North American Vertical Datum of 1988; n, number of points utilized from the time series]

Station	Mean stage (NAVD 88)		Stage standard deviation		Correlation coefficient	Mean difference between measured and computed values		Percentage of explained variance	n	Land surface altitude (NAVD 88)	
	Measured (meters)	Computed (meters)	Measured (meters)	Computed (meters)		Stage (meters)	Standard deviation (meters)			Model input (meters)	Measured (meters)
NP62	.399	.417	.197	.120	.798	-.018	.124	60.1	2229	.310	.835
NP67	.215	.274	.179	.151	.899	-.059	.079	80.4	2406	.240	.582
NP72	.503	.613	.316	.221	.788	-.110	.197	61.3	2222	.980	.899
NR	1.181	-.049	.117	.109	.772	1.230	.077	56.9	1380	-1.200	1.682
NTS1	.841	1.171	.293	.302	.766	-.330	.204	51.7	2457	1.020	1.076
NTS10	.927	1.060	.310	.369	.889	-.133	.170	70.0	2152	1.270	1.237
NTS14	.732	.863	.386	.339	.787	-.131	.241	61.1	2395	1.380	.756
OL1	-.059	-.089	.160	.121	.898	.030	.074	78.7	2447	-.220	--
OT	.251	.152	.189	.150	.916	.099	.079	82.4	2464	-.170	--
P33	1.509	1.558	.148	.095	.930	-.049	.070	78.0	2406	1.230	1.024
P34	.419	.312	.213	.172	.890	.108	.099	78.5	2428	.160	.119
P35	.118	.174	.171	.129	.945	-.056	.065	85.6	2552	-.400	-.195
P36	.868	.886	.146	.094	.920	-.018	.070	77.0	2407	.630	.530
P37	.002	.014	.155	.116	.867	-.012	.079	73.7	2465	-.140	-.183
P38	.069	.047	.148	.110	.836	.022	.082	68.9	2360	-.130	-.192
R127	.267	.363	.197	.147	.932	-.096	.080	83.4	2384	.060	--
R158	.416	.665	.239	.380	.810	-.250	.233	5.2	2445	.980	.927
R3110	.919	1.010	.331	.346	.893	-.091	.157	77.4	2456	1.240	1.094
RG1	1.242	1.605	.284	.124	.723	-.363	.212	44.1	1941	1.460	1.061
RG2	1.138	1.401	.286	.260	.852	-.264	.151	72.2	2108	1.450	1.390
Rutzke	.940	1.089	.260	.390	.804	-.149	.238	16.2	2432	1.510	1.103
S12AT	2.182	2.091	.288	.191	.878	.091	.151	72.5	2530	1.870	--
S12BT	2.205	2.142	.317	.248	.956	.063	.108	88.4	2532	1.860	--
S12CT	2.239	2.288	.323	.250	.829	-.049	.181	68.5	2520	1.870	--
S12DT	2.209	2.140	.419	.279	.819	.069	.249	64.7	2526	1.690	--
SP	.211	.263	.217	.176	.770	-.052	.139	59.2	2188	.480	.280
SR	.886	-.097	.109	.216	.260	.983	.215	-290.9	1354	-2.800	--
TE	1.242	.016	.127	.093	.857	1.226	.067	71.9	1438	-.190	--
TMC	.902	.894	.239	.133	.892	.008	.135	68.3	2232	.770	.732
TSB	.628	.854	.278	.248	.961	-.226	.080	91.8	1327	.490	.610
TSH	.156	.178	.163	.141	.911	-.022	.068	82.7	2445	.000	-.021
WE	1.611	-.053	.114	.122	.631	1.664	.102	20.3	1461	-1.610	--
WP	1.365	-.029	.128	.171	.385	1.394	.169	-74.6	1096	-1.870	--
WW	1.435	.047	.151	.144	.853	1.388	.080	71.8	1461	-.230	--

Table 10. Water-level comparison statistics for run 142, base case simulation.

[NAVD 88, North American Vertical Datum of 1988; n, number of points utilized from the time series]

Station	Mean stage (NAVD 88)		Stage standard deviation		Correlation coefficient	Mean difference between measured and computed values		Percentage of explained variance	n	Land surface altitude (NAVD 88)	
	Measured (meters)	Computed (meters)	Measured (meters)	Computed (meters)		Stage (meters)	Standard deviation (meters)			Model input (meters)	Measured (meters)
A13	0.968	1.077	0.259	0.161	0.861	-0.109	0.145	68.5	2,197	0.980	0.969
Angels	1.329	1.534	.264	.285	.719	-.206	.207	38.9	2,557	1.730	1.451
BD	.826	.062	.123	.089	.407	.764	.119	6.1	1,945	.010	2.612
BICYA8	.215	.848	.328	.457	.223	-.633	.499	-132.6	1,959	.270	--
BICYA9	1.726	1.849	.211	.188	.761	-.123	.139	56.3	1,869	2.060	--
BICYA10	.718	.786	.303	.228	.781	-.068	.189	61.0	1,854	.890	--
BICYA11	.920	.938	.380	.171	.715	-.018	.284	44.2	1,883	.880	--
BR	1.074	.026	.131	.116	.837	1.048	.072	69.8	2,331	-.150	1.838
CN	.713	.026	.123	.082	.867	.688	.066	71.1	2,447	-.080	1.323
CP	-.056	-.081	.169	.120	.879	.025	.085	74.4	2,479	-.440	-.503
CR2	1.121	1.256	.307	.302	.896	-.136	.139	79.6	2,161	1.330	1.231
CR3	1.119	1.249	.298	.244	.868	-.130	.149	75.1	2,212	1.310	1.234
CT27R	.143	.082	.148	.126	.570	.062	.128	24.8	1,903	-.060	-.085
CT50R	.106	.100	.140	.091	.858	.006	.078	69.1	1,896	.010	.088
CV1NR	.121	.080	.149	.128	.399	.041	.153	-5.4	1,840	-.060	--
CV5S	.123	.115	.132	.103	.441	.008	.127	7.9	601	-.060	--
CW	-.048	-.065	.103	.126	.485	.017	.118	-31.3	2,261	-1.830	--
CYP2	.235	.290	.206	.206	.787	-.055	.134	57.2	2,157	.480	1.643
CY3	.202	.194	.214	.170	.783	.008	.133	61.2	2,206	.280	1.518
DK	-.207	-.177	.118	.096	.712	-.030	.083	49.7	1,317	-1.860	--
DO1	.349	.477	.267	.182	.844	-.129	.149	68.6	2,451	.560	.567
DO2	.432	.448	.278	.202	.828	-.016	.158	67.5	2,237	.700	.570
E112	.846	.976	.301	.406	.875	-.130	.204	54.3	2,320	1.050	.527
E146	-.096	-.083	.147	.133	.863	-.012	.075	74.2	2,435	-.210	-.369
EP1R	.044	.065	.132	.120	.415	-.021	.137	-7.0	2,406	-.060	-.262
EP9R	-.159	-.117	.087	.057	.838	-.042	.050	66.8	366	-.160	-.314
EPGW/ SW	-.015	-.066	.099	.074	.696	.051	.071	48.2	2,387	-.110	-.158
EVER4	.170	.326	.145	.175	.924	-.156	.069	77.7	2,521	.240	.085
EVER5A	-.097	-.027	.153	.101	.830	-.070	.089	66.1	1,945	-.080	-.174
EVER6	.141	.033	.126	.083	.777	.107	.081	59.0	2,294	.000	-.006
EVER7	.201	.103	.120	.109	.889	.099	.055	79.0	2,342	.040	.131
G1251	.185	.230	.168	.178	.899	-.044	.078	78.4	2,026	.230	.390
G1502	1.485	1.700	.242	.132	.749	-.214	.168	51.9	2,453	1.580	2.060
G3272	1.491	1.716	.247	.143	.792	-.225	.160	58.1	2,528	1.570	1.612
G3273	1.476	1.705	.239	.138	.793	-.229	.155	58.3	2,557	1.600	1.667
G3353	-0.058	-0.002	0.137	0.108	0.857	-0.056	0.071	72.9	2,519	-0.020	1.149

Table 10. Water-level comparison statistics for run 142, base case simulation.—Continued

[NAVD 88, North American Vertical Datum of 1988; n, number of points utilized from the time series]

Station	Mean stage (NAVD 88)		Stage standard deviation		Correlation coefficient	Mean difference between measured and computed values		Percentage of explained variance	n	Land surface altitude (NAVD 88)	
	Measured (meters)	Computed (meters)	Measured (meters)	Computed (meters)		Stage (meters)	Standard deviation (meters)			Model input (meters)	Measured (meters)
G3437	1.194	1.118	.259	.277	.683	.076	.214	31.6	2,510	1.850	1.615
G3576	1.562	1.725	.207	.105	.902	-.163	.121	65.8	1,965	1.370	1.353
G3577	1.426	1.728	.272	.096	.885	-.302	.193	49.8	2,014	1.360	1.356
G3578	1.520	1.733	.213	.094	.872	-.214	.139	57.4	2,494	1.370	1.356
G3619	.326	.390	.147	.154	.894	-.064	.070	77.5	2,446	.210	.579
G3622	.879	1.218	.239	.419	.670	-.339	.314	-72.5	2,306	1.390	1.347
G3626	.975	1.111	.174	.287	.423	-.136	.265	-131.9	2,357	2.030	1.743
G3627	.860	1.247	.167	.263	.558	-.387	.219	-71.8	2,368	1.910	1.942
G3628	1.011	1.466	.203	.398	.482	-.455	.349	-194.9	2,336	1.730	1.667
G596	1.146	1.330	.197	.334	.598	-.184	.268	-84.1	2,546	1.810	1.753
G618	1.696	1.740	.146	.087	.804	-.044	.092	60.4	2,457	1.480	1.466
G620	1.574	1.578	.205	.179	.928	-.004	.078	85.7	2,451	1.380	1.311
GI	1.363	-.082	.113	.179	.385	1.445	.171	-126.7	1,616	-2.500	--
HC	-.186	.158	.111	.221	.599	-.343	.178	-157.7	1,434	.560	--
HR	.931	.018	.119	.144	.626	.913	.116	5.0	1,461	.120	--
L67XW	1.761	1.720	.237	.090	.743	.040	.181	41.9	1,883	1.350	--
LN	1.524	-.033	.120	.101	.821	1.557	.069	67.3	1,430	-.410	--
LO	.818	-.070	.119	.248	.141	.888	.260	-377.9	1,335	-2.000	--
LOOP1T	1.910	1.837	.158	.170	.722	.073	.123	39.7	2,024	1.860	--
LOOP2T	1.540	1.494	.220	.181	.712	.046	.156	49.5	2,086	1.480	--
LS	-.190	-.173	.106	.098	.777	-.017	.069	58.0	1,461	-1.520	--
NCL	-.015	-.086	.190	.162	.834	.071	.105	69.5	2,390	-.240	--
NE1	1.664	1.727	.131	.088	.853	-.063	.072	69.4	2,509	1.290	1.314
NE2	1.627	1.737	.156	.087	.863	-.110	.092	65.2	2,503	1.340	1.241
NE3	1.695	1.748	.115	.069	.774	-.054	.075	56.9	1,838	1.340	--
NE4	1.606	1.705	.158	.086	.835	-.099	.098	61.4	2,416	1.260	1.213
NE5	1.601	1.687	.146	.085	.854	-.086	.086	65.6	2,539	1.270	--
NMP	-.118	-.106	.151	.167	.856	-.012	.087	66.9	2,113	.010	--
NP201	1.869	1.825	.257	.183	.855	.044	.139	71.0	2,439	1.650	1.420
NP202	1.679	1.646	.196	.156	.960	.033	.063	89.5	2,309	1.350	1.164
NP203	1.471	1.467	.181	.126	.920	.004	.082	79.7	2,426	1.220	.890
NP205	1.478	1.484	.264	.179	.828	-.006	.153	66.2	2,447	1.440	1.332
NP206	1.282	1.380	.272	.170	.851	-.098	.156	67.2	2,453	1.380	1.366
NP44	.636	.777	.351	.237	.771	-.141	.226	58.5	2,342	1.270	1.073
NP46	.018	-.017	.171	.148	.742	.035	.117	53.6	2,429	.050	-.052
NP62	0.399	0.418	0.197	0.128	0.811	-0.019	0.119	63.2	2,229	0.310	0.835
NP67	.215	.273	.179	.151	.899	-.058	.079	80.5	2,406	.240	.582

Table 10. Water-level comparison statistics for run 142, base case simulation.—Continued

[NAVD 88, North American Vertical Datum of 1988; n, number of points utilized from the time series]

Station	Mean stage (NAVD 88)		Stage standard deviation		Correlation coefficient	Mean difference between measured and computed values		Percentage of explained variance	n	Land surface altitude (NAVD 88)	
	Measured (meters)	Computed (meters)	Measured (meters)	Computed (meters)		Stage (meters)	Standard deviation (meters)			Model input (meters)	Measured (meters)
NP72	.503	.610	.316	.223	.785	-.107	.198	60.9	2,222	.980	.899
NR	1.181	-.048	.117	.110	.773	1.230	.077	56.9	1,380	-1.200	1.682
NTS1	.841	1.168	.293	.302	.765	-.327	.204	51.3	2,457	1.020	1.076
NTS10	.927	1.047	.310	.370	.884	-.120	.174	68.6	2,152	1.270	1.237
NTS14	.732	.856	.386	.339	.787	-.124	.241	61.2	2,395	1.380	.756
OL1	-.059	-.090	.160	.121	.897	.031	.074	78.6	2,447	-.220	--
OT	.251	.149	.189	.160	.905	.102	.081	81.5	2,464	-.170	--
P33	1.509	1.532	.148	.104	.919	-.023	.067	79.6	2,406	1.230	1.024
P34	.419	.259	.213	.156	.855	.160	.113	71.6	2,428	.160	.119
P35	.118	.176	.171	.141	.947	-.058	.059	88.2	2,552	-.400	-.195
P36	.868	.888	.146	.109	.908	-.020	.066	79.7	2,407	.630	.530
P37	.002	.013	.155	.116	.866	-.012	.080	73.6	2,465	-.140	-.183
P38	.069	.049	.148	.115	.849	.020	.079	71.5	2,360	-.130	-.192
R127	.267	.362	.197	.147	.931	-.095	.081	83.3	2,384	.060	--
R158	.416	.664	.239	.380	.810	-.248	.233	4.8	2,445	.980	.927
R3110	.919	.999	.331	.349	.893	-.080	.159	77.0	2,456	1.240	1.094
RG1	1.242	1.589	.284	.128	.673	-.347	.219	40.4	1,941	1.460	1.061
RG2	1.138	1.357	.286	.278	.828	-.220	.166	66.4	2,108	1.450	1.390
Rutzke	.940	1.068	.260	.385	.800	-.128	.236	17.6	2,432	1.510	1.103
S12AT	2.182	2.069	.288	.173	.811	.113	.179	61.5	2,530	1.870	--
S12BT	2.205	2.051	.317	.172	.886	.154	.183	66.7	2,532	1.860	--
S12CT	2.239	2.182	.323	.184	.484	.057	.284	22.6	2,520	1.870	--
S12DT	2.209	2.064	.419	.222	.686	.144	.311	44.7	2,526	1.690	--
SP	.211	.262	.217	.180	.777	-.052	.137	60.0	2,188	.480	.280
SR	.886	-.097	.109	.216	.264	.983	.215	-290.6	1,354	-2.800	--
TE	1.242	.016	.127	.095	.858	1.226	.067	72.3	1,438	-.190	--
TMC	.902	.894	.239	.153	.885	.008	.126	72.3	2,232	.770	.732
TSB	.628	.852	.278	.247	.959	-.224	.082	91.4	1,327	.490	.610
TSH	.156	.176	.163	.142	.910	-.020	.068	82.6	2,445	.000	-.021
WE	1.611	-.054	.114	.122	.632	1.664	.101	20.5	1,461	-1.610	--
WP	1.365	-.031	.128	.167	.376	1.396	.168	-71.8	1,096	-1.870	--
WW	1.435	.043	.151	.145	.856	1.392	.080	72.1	1,461	-.230	--

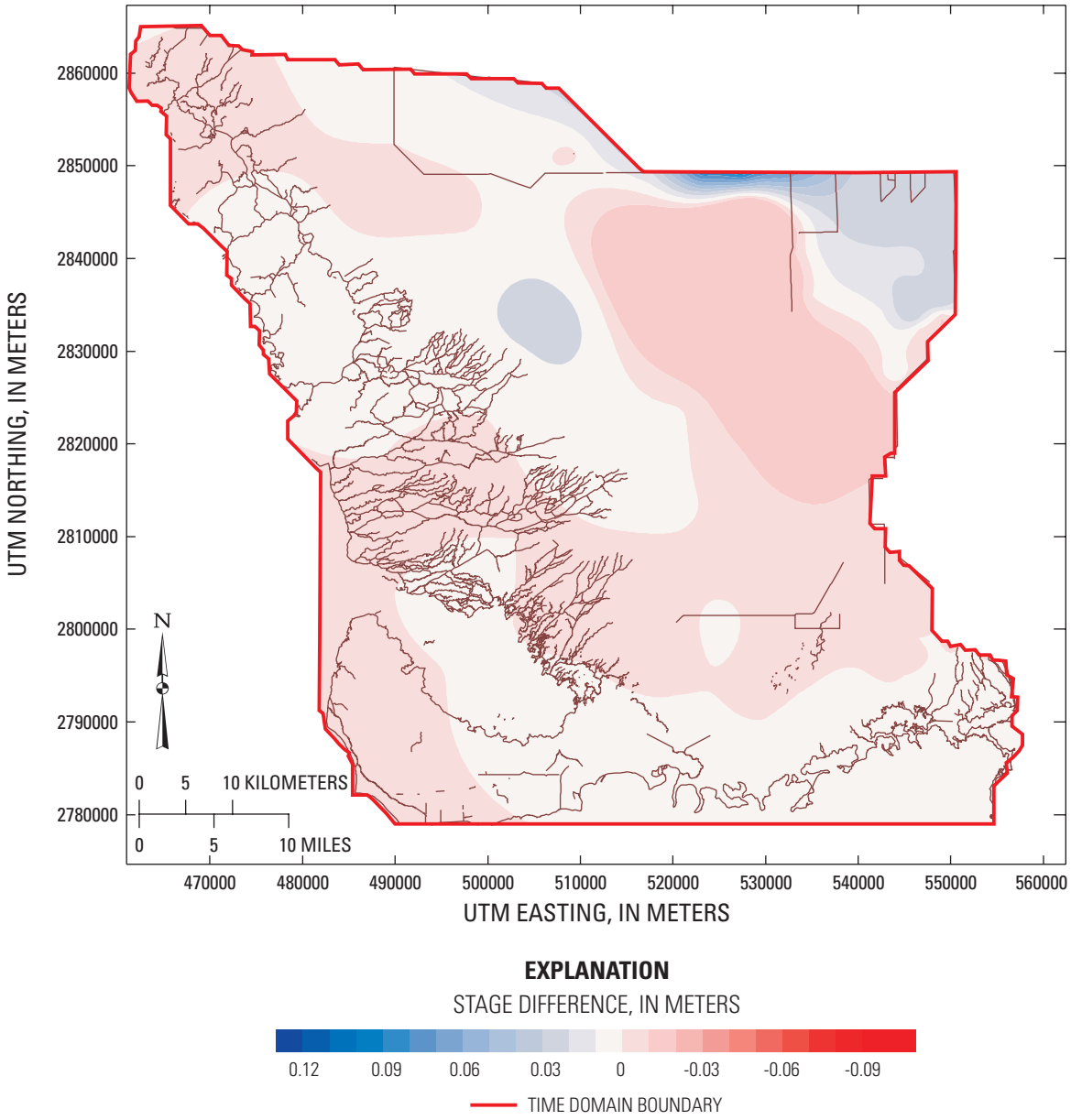

Figure 30. Spatial distribution of mean stage difference between simulations with adjusted Manning's *n*. Positive values indicate better fit, and negative values indicate a poorer fit.

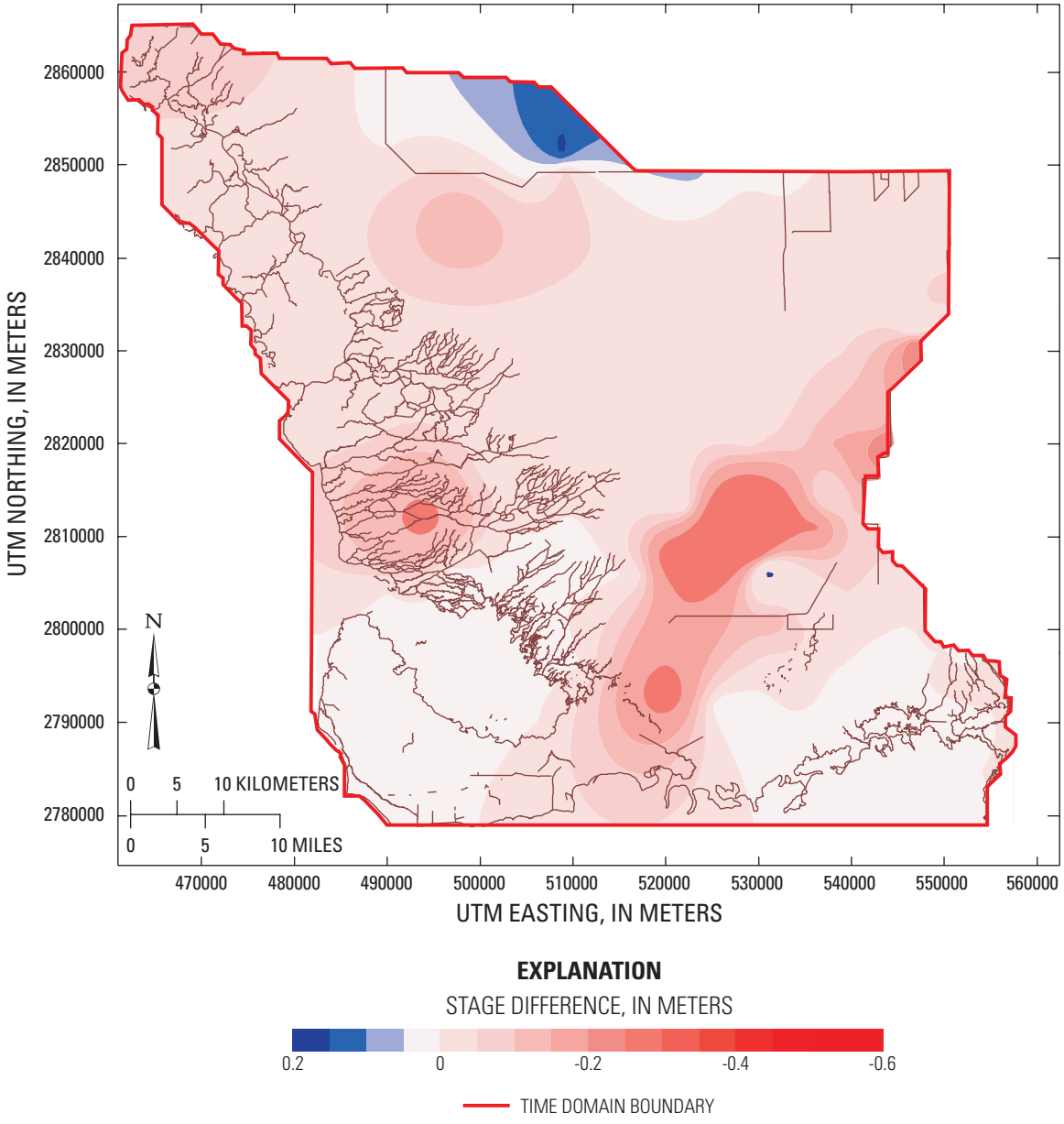

Figure 31. Spatial distribution of mean stage difference between simulations with and without leakage. Positive values indicate better fit, and negative values indicate a poorer fit.

Table 11. Water-level comparison statistics for run 145, leakage neglected.

[NAVD 88, North American Vertical Datum of 1988; n, number of points utilized from the time series]

Station	Mean stage (NAVD 88)		Stage standard deviation		Correlation coefficient	Mean difference between measured and computed values		Percentage of explained variance	n	Land surface altitude (NAVD 88)	
	Measured (meters)	Computed (meters)	Measured (meters)	Computed (meters)		Stage (meters)	Standard deviation (meters)			Model input (meters)	Measured (meters)
A13	0.968	1.093	0.259	0.221	0.664	-0.125	0.200	40.5	2,197	0.980	0.969
Angels	1.329	1.545	.264	.383	.656	-.216	.289	-19.9	2,557	1.730	1.451
BD	.826	-.006	.123	.247	.412	.832	.226	-240.6	1,945	.010	2.612
BICYA8	.215	.934	.328	.462	.283	-.718	.485	-119.3	1,959	.270	--
BICYA9	1.726	1.691	.211	.282	.614	.035	.225	-14.3	1,869	2.060	--
BICYA10	.718	.616	.303	.406	.633	.101	.317	-9.8	1,854	.890	--
BICYA11	.920	.932	.380	.208	.588	-.012	.308	34.4	1,883	.880	--
BR	1.074	.011	.131	.160	.767	1.063	.103	38.0	2,331	-.150	1.838
CN	.713	.017	.123	.123	.760	.696	.085	52.0	2,447	-.080	1.323
CP	-.056	-.053	.169	.101	.828	-.003	.102	63.4	2,479	-.440	-.503
CR2	1.121	1.409	.307	.237	.610	-.289	.248	34.7	2,161	1.330	1.231
CR3	1.119	1.335	.298	.266	.613	-.215	.249	29.8	2,212	1.310	1.234
CT27R	.143	.088	.148	.142	.593	.055	.131	21.5	1,903	-.060	-.085
CT50R	.106	.119	.140	.092	.853	-.013	.078	68.9	1,896	.010	.088
CV1NR	.121	.091	.149	.136	.455	.029	.149	-0.5	1,840	-.060	--
CV5S	.123	.128	.132	.119	.480	-.005	.129	5.5	601	-.060	--
CW	-.048	-.064	.103	.127	.485	.016	.119	-32.9	2,261	-1.830	--
CYP2	.235	.153	.206	.336	.603	.082	.268	-70.1	2,157	.480	1.643
CY3	.202	.001	.214	.323	.531	.201	.277	-67.3	2,206	.280	1.518
DK	-.207	-.177	.118	.096	.713	-.030	.083	49.8	1,317	-1.860	--
DO1	.349	.281	.267	.335	.548	.068	.292	-20.1	2,451	.560	.567
DO2	.432	.011	.278	.310	.354	.421	.335	-45.7	2,237	.700	.570
E112	.846	1.058	.301	.401	.870	-.212	.204	54.3	2,320	1.050	.527
E146	-.096	-.062	.147	.140	.768	-.034	.098	55.6	2,435	-.210	-.369
EP1R	.044	.076	.132	.130	.462	-.032	.136	-5.7	2,406	-.060	-.262
EP9R	-.159	-.118	.087	.070	.864	-.041	.044	74.3	366	-.160	-.314
EPGW/ SW	-.015	-.072	.099	.093	.758	.057	.067	54.0	2,387	-.110	-.158
EVER4	.170	.374	.145	.160	.881	-.204	.076	72.7	2,521	.240	.085
EVER5A	-.097	-.044	.153	.134	.899	-.053	.067	80.8	1,945	-.080	-.174
EVER6	.141	.033	.126	.096	.816	.108	.073	66.3	2,294	.000	-.006
EVER7	.201	.123	.120	.118	.872	.078	.060	74.8	2,342	.040	.131
G1251	.185	.245	.168	.208	.873	-.060	.102	63.2	2,026	.230	.390
G1502	1.485	1.736	.242	.103	.627	-.250	.195	35.2	2,453	1.580	2.060
G3272	1.491	1.744	.247	.144	.734	-.253	.172	51.6	2,528	1.570	1.612
G3273	1.476	1.732	.239	.151	.703	-.256	.171	48.9	2,557	1.600	1.667
G3353	-0.058	-0.020	0.137	0.142	0.891	-0.038	0.065	77.3	2,519	-0.020	1.149

Table 11. Water-level comparison statistics for run 145, leakage neglected.—Continued

[NAVD 88, North American Vertical Datum of 1988; n, number of points utilized from the time series]

Station	Mean stage (NAVD 88)		Stage standard deviation		Correlation coefficient	Mean difference between measured and computed values		Percentage of explained variance	n	Land surface altitude (NAVD 88)	
	Measured (meters)	Computed (meters)	Measured (meters)	Computed (meters)		Stage (meters)	Standard deviation (meters)			Model input (meters)	Measured (meters)
G3437	1.194	.968	.259	.353	.557	.226	.300	-34.3	2,510	1.850	1.615
G3576	1.562	1.747	.207	.092	.861	-.185	.136	56.7	1,965	1.370	1.353
G3577	1.426	1.750	.272	.089	.861	-.324	.201	45.5	2,014	1.360	1.356
G3578	1.520	1.757	.213	.088	.829	-.237	.148	51.4	2,494	1.370	1.356
G3619	.326	.431	.147	.149	.886	-.105	.071	76.9	2,446	.210	.579
G3622	.879	1.469	.239	.205	.515	-.591	.221	14.6	2,306	1.390	1.347
G3626	.975	1.095	.174	.345	.388	-.120	.321	-239.2	2,357	2.030	1.743
G3627	.860	1.166	.167	.391	.418	-.305	.355	-352.0	2,368	1.910	1.942
G3628	1.011	1.721	.203	.273	.342	-.710	.279	-88.4	2,336	1.730	1.667
G596	1.146	1.402	.197	.420	.531	-.256	.357	-227.0	2,546	1.810	1.753
G618	1.696	1.753	.146	.089	.783	-.058	.094	58.3	2,457	1.480	1.466
G620	1.574	1.545	.205	.247	.886	.029	.115	68.4	2,451	1.380	1.311
GI	1.363	-.079	.113	.179	.378	1.442	.172	-129.5	1,616	-2.500	--
HC	-.186	.184	.111	.241	.567	-.370	.200	-224.8	1,434	.560	--
HR	.931	-.320	.119	.422	.573	1.251	.367	-846.6	1,461	.120	--
L67XW	1.761	1.735	.237	.089	.694	.025	.187	38.0	1,883	1.350	--
LN	1.524	-.030	.120	.100	.821	1.554	.069	67.3	1,430	-.410	--
LO	.818	-.068	.119	.249	.147	.886	.260	-376.4	1,335	-2.000	--
LOOP1T	1.910	1.779	.158	.261	.682	.131	.192	-47.0	2,024	1.860	--
LOOP2T	1.540	1.480	.220	.250	.526	.060	.230	-9.9	2,086	1.480	--
LS	-.190	-.178	.106	.103	.786	-.011	.068	58.3	1,461	-1.520	--
NCL	-.015	-.051	.190	.153	.730	.036	.130	52.7	2,390	-.240	--
NE1	1.664	1.744	.131	.087	.805	-.081	.080	62.8	2,509	1.290	1.314
NE2	1.627	1.756	.156	.085	.801	-.129	.101	57.7	2,503	1.340	1.241
NE3	1.695	1.766	.115	.070	.718	-.071	.081	50.5	1,838	1.340	--
NE4	1.606	1.722	.158	.085	.788	-.116	.105	55.9	2,416	1.260	1.213
NE5	1.601	1.703	.146	.084	.810	-.103	.093	59.9	2,539	1.270	--
NMP	-.118	-.444	.151	.386	.683	.326	.304	-304.7	2,113	.010	--
NP201	1.869	1.807	.257	.205	.865	.061	.130	74.4	2,439	1.650	1.420
NP202	1.679	1.644	.196	.158	.957	.036	.064	89.4	2,309	1.350	1.164
NP203	1.471	1.471	.181	.126	.912	.000	.084	78.4	2,426	1.220	.890
NP205	1.478	1.448	.264	.260	.722	.031	.195	45.2	2,447	1.440	1.332
NP206	1.282	1.414	.272	.222	.614	-.133	.222	33.8	2,453	1.380	1.366
NP44	.636	.187	.351	.279	.050	.449	.438	-55.2	2,342	1.270	1.073
NP46	.018	-.241	.171	.322	.556	.259	.268	-145.0	2,429	.050	-.052
NP62	0.399	0.402	0.197	0.206	0.745	-0.003	0.144	46.3	2,229	0.310	0.835
NP67	.215	.302	.179	.172	.790	-.086	.114	59.4	2,406	.240	.582

Table 11. Water-level comparison statistics for run 145, leakage neglected.—Continued

[NAVD 88, North American Vertical Datum of 1988; n, number of points utilized from the time series]

Station	Mean stage (NAVD 88)		Stage standard deviation		Correlation coefficient	Mean difference between measured and computed values		Percentage of explained variance	n	Land surface altitude (NAVD 88)	
	Measured (meters)	Computed (meters)	Measured (meters)	Computed (meters)		Stage (meters)	Standard deviation (meters)			Model input (meters)	Measured (meters)
NP72	.503	.168	.316	.353	.277	.335	.403	-62.6	2,222	.980	.899
NR	1.181	-.046	.117	.110	.772	1.228	.077	56.8	1,380	-1.200	1.682
NTS1	.841	1.292	.293	.133	.920	-.451	.178	62.9	2,457	1.020	1.076
NTS10	.927	1.185	.310	.404	.748	-.258	.268	25.4	2,152	1.270	1.237
NTS14	.732	.591	.386	.540	.596	.141	.439	-28.9	2,395	1.380	.756
OL1	-.059	-.075	.160	.128	.863	.016	.081	74.1	2,447	-.220	--
OT	.251	.152	.189	.154	.877	.098	.092	76.5	2,464	-.170	--
P33	1.509	1.540	.148	.102	.902	-.031	.072	76.7	2,406	1.230	1.024
P34	.419	.240	.213	.197	.823	.179	.123	66.8	2,428	.160	.119
P35	.118	.187	.171	.141	.945	-.069	.059	87.9	2,552	-.400	-.195
P36	.868	.900	.146	.108	.889	-.032	.071	76.7	2,407	.630	.530
P37	.002	.040	.155	.105	.804	-.039	.094	63.0	2,465	-.140	-.183
P38	.069	.045	.148	.148	.802	.024	.093	60.4	2,360	-.130	-.192
R127	.267	.413	.197	.123	.902	-.146	.101	73.6	2,384	.060	--
R158	.416	.734	.239	.401	.735	-.319	.277	-34.6	2,445	.980	.927
R3110	.919	.986	.331	.497	.881	-.067	.259	38.8	2,456	1.240	1.094
RG1	1.242	1.644	.284	.073	.681	-.402	.240	28.3	1,941	1.460	1.061
RG2	1.138	1.464	.286	.289	.588	-.326	.261	16.7	2,108	1.450	1.390
Rutzke	.940	1.174	.260	.478	.754	-.234	.330	-61.0	2,432	1.510	1.103
S12AT	2.182	2.122	.288	.197	.514	.060	.252	23.5	2,530	1.870	--
S12BT	2.205	2.116	.317	.197	.480	.089	.282	21.1	2,532	1.860	--
S12CT	2.239	2.195	.323	.183	.411	.044	.299	14.4	2,520	1.870	--
S12DT	2.209	2.076	.419	.221	.607	.133	.335	36.2	2,526	1.690	--
SP	.211	-.089	.217	.283	.313	.299	.298	-88.8	2,188	.480	.280
SR	.886	-.096	.109	.216	.267	.982	.214	-288.9	1,354	-2.800	--
TE	1.242	.019	.127	.095	.856	1.223	.067	72.2	1,438	-.190	--
TMC	.902	.877	.239	.219	.759	.025	.160	55.1	2,232	.770	.732
TSB	.628	.950	.278	.186	.957	-.322	.114	83.2	1,327	.490	.610
TSH	.156	.216	.163	.136	.855	-.060	.085	73.1	2,445	.000	-.021
WE	1.611	-.052	.114	.122	.635	1.663	.101	20.9	1,461	-1.610	--
WP	1.365	-.029	.128	.169	.383	1.394	.169	-72.8	1,096	-1.870	--
WW	1.435	.047	.151	.143	.857	1.389	.079	72.7	1,461	-.230	--

westward and southward instead of recharging the aquifer and moving eastward. This "surplus" surface water primarily increases flows to Florida Bay and Ponce de Leon Bay (fig. 1). Mean stage improves locally near OIH and Forty-Mile Bend; these areas may have less conductive peat layers, which if confirmed, could be placed in the model.

3.7.4 - Sensitivity to Incorporation of Main Park Road as a Barrier

A scenario (run 143) was made to investigate the effect of Main Park Road (fig. 1) functioning as a complete barrier to flow. Redirection of Main Park Road flows caused TSB flows to increase by 10 percent; however, total flow to Florida Bay remained unchanged. The presence of the road influenced the local distribution and timing of flow; however, the changes in total flow and individual creekflows were negligible. The TSB flows are in better agreement with observations when the road is not included as a barrier in the model, indicating that the culverts convey enough flow to prevent the road from being an effective barrier. The model results are consistent with the earlier assumption that the road is not a substantial barrier to coastal flows. Stage comparison statistics are provided in table 12, and a comparison of all stage means with those from run 142 is shown in figure 32. The only noticeable changes occur near Main Park Road; therefore, including this road as a barrier has a negligible effect on overall model performance indices (table 12).

3.7.5 - Sensitivity to Lowering of Land-Surface Altitude

To test the sensitivity of model response to a vertical shift in topography, the model land surface was lowered by 0.1 m throughout the model domain in run 146. Subgrid-scale topographic variations could be on this order of magnitude. As expected, the stages also were lowered by about 0.1 m in most places, except near the coast where the prescribed sea-level conditions at the boundaries control stages. Although some stage differences showed substantial deterioration, others such as RG1 (location shown in fig. 3) improved. Overall, the stage comparison statistics in table 13 do not improve definitively compared to the base run. The spatial plot of the mean stage difference is more informative; lowering the land surface improves the predicted mean stage in the eastern and northwestern areas of the domain, and worsens mean stage in the Shark River Slough area (figs. 1 and 33). This result may indicate that the model topography does not match the true topography uniformly well around the study area. A better fit with recorded stages might be achieved with further adjustment of the model land-surface altitudes and friction coefficients; however, such adjustments were not made because an objective procedure has yet to be devised. The topographic shift affected flows by redistributing volumes between the different rivers, although total flow to the coast was minimally affected. Runoff from Chatham and Lostmans Rivers increased by about 10 percent, runoff to Ponce de Leon Bay decreased by 10 percent, and runoff to Florida Bay increased by 20 percent.

3.8 - Final Model Calibration – Run 157

Based on the results from the base run and sensitivity analyses, a final model calibration (run 157) was performed to improve model performance prior to scenario simulation. The final model calibration addressed the following problems with the initially calibrated TIME model (run 142): (1) underprediction of stage in the northwestern region of the TIME domain; (2) discrepancies in mean stage values and explained variances near parts of Levee 31N Canal, Levee-31W Canal and C-111 Canal; and (3) a tendency to underpredict the ground-water table decline during dry seasons, especially in areas where unsaturated zones of substantial depth, on the order of 1 m, are present.

3.8.1 - Northwestern Region

Few surface-water stage measurement sites exist in the northwestern region of the domain (fig. 9). Consequently, model comparison results in this area (fig. 16) are based entirely on measured data from gage BICYA8 (fig. 9) and indicate that model mean stage is higher than observed stage. Gage BICYA8 is located along Turner River just north of U.S. Highway 41. Turner River Road to the east (fig. 1) obstructs flow; and stage on the east side of the road is usually much higher (R. Sobczak, Big Cypress National Preserve, oral commun., 2005). The gage more closely represents river stage than wetland stage and thus, is lower because of the hydraulic connection between the river and ocean. Based on this information, Turner River was included in the model topography and the model cell used to compare computed stage to BICYA8 was placed in the river at row 168, column 24 of the model grid (fig. 3). The results in table 5 show a much better model fit in stage mean bias and explained variance.

3.8.2 - Levee 31 Area

In the area just west of Levee 31 (fig. 1), computed mean stage is too high (fig. 16). It is difficult to identify with complete certainty the factors that contribute to these discrepancies. Gage information taken from the station descriptions indicates that the model-input land-surface altitude used in the TIME application may be substantially higher than the actual land-surface altitude at the gage. This would allow standing surface water at a gage located in a dry model cell. If surface water was present, computed stage was used to compute statistics; however, some gages are believed to measure only ground water even when surface water is present (that is, G-prefix gages). In addition to these inherent problems, adequate data are not available to fully prescribe boundary stages.

Table 12. Water-level comparison statistics for run 143, Main Park Road as a barrier.

[NAVD 88, North American Vertical Datum of 1988; n, number of points utilized from the time series]

Station	Mean stage (NAVD 88)		Stage standard deviation		Correlation coefficient	Mean difference between measured and computed values		Percentage of explained variance	n	Land surface altitude (NAVD 88)	
	Measured (meters)	Computed (meters)	Measured (meters)	Computed (meters)		Stage (meters)	Standard deviation (meters)			Model input (meters)	Measured (meters)
A13	0.968	1.077	0.259	0.162	0.861	-0.110	0.145	68.6	2,197	0.980	0.969
Angels	1.329	1.534	.264	.285	.721	-.206	.206	39.2	2,557	1.730	1.451
BD	.826	.063	.123	.090	.405	.763	.119	5.4	1,945	.010	2.612
BICYA8	.215	.852	.328	.457	.219	-.637	.500	-133.3	1,959	.270	--
BICYA9	1.726	1.849	.211	.187	.760	-.123	.140	56.1	1,869	2.060	--
BICYA10	.718	.788	.303	.227	.777	-.070	.191	60.3	1,854	.890	--
BICYA11	.920	.939	.380	.170	.711	-.018	.285	43.6	1,883	.880	--
BR	1.074	.026	.131	.116	.836	1.048	.072	69.7	2,331	-.150	1.838
CN	.713	.026	.123	.082	.866	.688	.066	71.0	2,447	-.080	1.323
CP	-.056	-.078	.169	.122	.886	.022	.083	76.0	2,479	-.440	-.503
CR2	1.121	1.257	.307	.303	.897	-.136	.139	79.6	2,161	1.330	1.231
CR3	1.119	1.250	.298	.244	.870	-.130	.148	75.4	2,212	1.310	1.234
CT27R	.143	.083	.148	.126	.580	.060	.127	26.2	1,903	-.060	-.085
CT50R	.106	.100	.140	.090	.858	.006	.078	69.0	1,896	.010	.088
CV1NR	.121	.081	.149	.129	.401	.040	.153	-5.2	1,840	-.060	--
CV5S	.123	.116	.132	.103	.458	.007	.125	10.5	601	-.060	--
CW	-.048	-.065	.103	.126	.491	.017	.117	-29.0	2,261	-1.830	--
CYP2	.235	.292	.206	.206	.792	-.057	.133	58.2	2,157	.480	1.643
CY3	.202	.199	.214	.171	.791	.003	.131	62.6	2,206	.280	1.518
DK	-.207	-.177	.118	.096	.712	-.030	.083	49.6	1,317	-1.860	--
DO1	.349	.480	.267	.182	.845	-.131	.149	68.7	2,451	.560	.567
DO2	.432	.458	.278	.206	.833	-.026	.156	68.6	2,237	.700	.570
E112	.846	.981	.301	.408	.875	-.135	.205	53.8	2,320	1.050	.527
E146	-.096	-.081	.147	.134	.865	-.015	.074	74.7	2,435	-.210	-.369
EP1R	.044	.066	.132	.120	.414	-.022	.137	-7.2	2,406	-.060	-.262
EP9R	-.159	-.116	.087	.056	.837	-.042	.051	66.4	366	-.160	-.314
EPGW/SW	-.015	-.066	.099	.074	.694	.051	.072	47.9	2,387	-.110	-.158
EVER4	.170	.325	.145	.173	.924	-.155	.068	78.1	2,521	.240	.085
EVER5A	-.097	-.027	.153	.101	.828	-.070	.089	65.8	1,945	-.080	-.174
EVER6	.141	.033	.126	.083	.777	.108	.081	59.0	2,294	.000	-.006
EVER7	.201	.102	.120	.109	.891	.099	.054	79.3	2,342	.040	.131
G1251	.185	.229	.168	.177	.899	-.044	.078	78.5	2,02,6	.230	.390
G1502	1.485	1.700	.242	.132	.749	-.214	.168	51.9	2,453	1.580	2.060
G3272	1.491	1.716	.247	.144	.790	-.225	.160	58.2	2,528	1.570	1.612
G3273	1.476	1.705	.239	.139	.793	-.229	.154	58.3	2,557	1.600	1.667
G3353	-.058	-.002	.137	.107	.857	-.056	.071	72.9	2,519	-.020	1.149
G3437	1.194	1.117	0.259	0.275	0.680	0.077	0.214	31.8	2,510	1.850	1.615

Table 12. Water-level comparison statistics for run 143, Main Park Road as a barrier.—Continued

[NAVD 88, North American Vertical Datum of 1988; n, number of points utilized from the time series]

Station	Mean stage (NAVD 88)		Stage standard deviation		Correlation coefficient	Mean difference between measured and computed values		Percentage of explained variance	n	Land surface altitude (NAVD 88)	
	Measured (meters)	Computed (meters)	Measured (meters)	Computed (meters)		Stage (meters)	Standard deviation (meters)			Model input (meters)	Measured (meters)
G3576	1.562	1.725	.207	.105	.902	-.163	.121	65.8	1,965	1.370	1.353
G3577	1.426	1.728	.272	.096	.885	-.302	.193	49.8	2,014	1.360	1.356
G3578	1.520	1.733	.213	.094	.872	-.214	.139	57.4	2,494	1.370	1.356
G3619	.326	.388	.147	.152	.896	-.062	.068	78.4	2,446	.210	.579
G3622	.879	1.218	.239	.419	.669	-.339	.314	-72.8	2,306	1.390	1.347
G3626	.975	1.113	.174	.289	.424	-.138	.267	-135.0	2,357	2.030	1.743
G3627	.860	1.249	.167	.266	.551	-.389	.223	-77.7	2,368	1.910	1.942
G3628	1.011	1.466	.203	.398	.482	-.455	.349	-194.9	2,336	1.730	1.667
G596	1.146	1.330	.197	.334	.596	-.184	.268	-84.5	2,546	1.810	1.753
G618	1.696	1.740	.146	.087	.800	-.044	.092	60.0	2,457	1.480	1.466
G620	1.574	1.577	.205	.180	.927	-.004	.078	85.7	2,451	1.380	1.311
GI	1.363	-.081	.113	.179	.384	1.443	.171	-128.7	1,616	-2.500	--
HC	-.186	.158	.111	.221	.598	-.343	.179	-158.4	1,434	.560	--
HR	.931	.017	.119	.145	.623	.915	.117	4.3	1,461	.120	--
L67XW	1.761	1.720	.237	.090	.743	.040	.181	41.9	1,883	1.350	--
LN	1.524	-.033	.120	.101	.819	1.557	.069	66.9	1,430	-.410	--
LO	.818	-.069	.119	.249	.147	.887	.260	-376.8	1,335	-2.000	--
LOOP1T	1.910	1.837	.158	.170	.721	.073	.123	39.4	2,024	1.860	--
LOOP2T	1.540	1.495	.220	.179	.716	.045	.155	50.3	2,086	1.480	--
LS	-.190	-.174	.106	.099	.778	-.015	.069	58.0	1,461	-1.520	--
NCL	-.015	-.083	.190	.166	.850	.068	.100	72.2	2,390	-.240	--
NE1	1.664	1.727	.131	.088	.853	-.064	.072	69.4	2,509	1.290	1.314
NE2	1.627	1.737	.156	.087	.862	-.110	.092	65.2	2,503	1.340	1.241
NE3	1.695	1.748	.115	.069	.774	-.054	.075	56.9	1,838	1.340	--
NE4	1.606	1.705	.158	.086	.835	-.099	.098	61.4	2,416	1.260	1.213
NE5	1.601	1.687	.146	.085	.855	-.086	.086	65.6	2,539	1.270	--
NMP	-.118	-.097	.151	.171	.855	-.021	.089	65.1	2,113	.010	--
NP201	1.869	1.825	.257	.183	.855	.044	.139	71.0	2,439	1.650	1.420
NP202	1.679	1.646	.196	.156	.960	.033	.063	89.5	2,309	1.350	1.164
NP203	1.471	1.467	.181	.126	.920	.004	.082	79.7	2,426	1.220	.890
NP205	1.478	1.484	.264	.179	.828	-.006	.153	66.2	2,447	1.440	1.332
NP206	1.282	1.380	.272	.169	.846	-.098	.158	66.5	2,453	1.380	1.366
NP44	.636	.782	.351	.238	.769	-.145	.227	58.3	2,342	1.270	1.073
NP46	.018	.033	.171	.166	.751	-.015	.119	51.7	2,429	.050	-.052
NP62	.399	.420	.197	.127	.814	-.021	.119	63.4	2,229	.310	.835
NP67	0.215	0.273	0.179	0.151	0.898	-0.058	0.079	80.4	2,406	0.240	0.582
NP72	.503	.615	.316	.222	.786	-.111	.197	61.1	2,222	.980	.899

Table 12. Water-level comparison statistics for run 143, Main Park Road as a barrier.—Continued

[NAVD 88, North American Vertical Datum of 1988; n, number of points utilized from the time series]

Station	Mean stage (NAVD 88)		Stage standard deviation		Correlation coefficient	Mean difference between measured and computed values		Percentage of explained variance	n	Land surface altitude (NAVD 88)	
	Measured (meters)	Computed (meters)	Measured (meters)	Computed (meters)		Stage (meters)	Standard deviation (meters)			Model input (meters)	Measured (meters)
NR	1.181	-.049	.117	.110	.773	1.230	.077	56.9	1,380	-1.200	1.682
NTS1	.841	1.169	.293	.303	.767	-.328	.203	51.7	2,457	1.020	1.076
NTS10	.927	1.048	.310	.372	.887	-.121	.173	68.9	2,152	1.270	1.237
NTS14	.732	.863	.386	.345	.788	-.131	.241	61.0	2,395	1.380	.756
OL1	-.059	-.089	.160	.121	.897	.030	.074	78.6	2,447	-.220	--
OT	.251	.149	.189	.160	.905	.102	.081	81.6	2,464	-.170	--
P33	1.509	1.532	.148	.104	.919	-.023	.067	79.6	2,406	1.230	1.024
P34	.419	.259	.213	.156	.856	.160	.113	71.7	2,428	.160	.119
P35	.118	.176	.171	.141	.946	-.057	.059	88.0	2,552	-.400	-.195
P36	.868	.888	.146	.109	.908	-.020	.066	79.7	2,407	.630	.530
P37	.002	.014	.155	.117	.866	-.012	.079	73.8	2,465	-.140	-.183
P38	.069	.048	.148	.113	.851	.021	.079	71.6	2,360	-.130	-.192
R127	.267	.362	.197	.147	.932	-.095	.081	83.3	2,384	.060	--
R158	.416	.687	.239	.401	.834	-.272	.241	-1.6	2,445	.980	.927
R3110	.919	1.001	.331	.351	.890	-.082	.161	76.4	2,456	1.240	1.094
RG1	1.242	1.589	.284	.128	.673	-.347	.219	40.4	1,941	1.460	1.061
RG2	1.138	1.358	.286	.278	.829	-.220	.165	66.6	2,108	1.450	1.390
Rutzke	.940	1.067	.260	.385	.801	-.127	.236	17.9	2,432	1.510	1.103
S12AT	2.182	2.069	.288	.173	.809	.113	.179	61.1	2,530	1.870	--
S12BT	2.205	2.051	.317	.172	.887	.154	.183	66.7	2,532	1.860	--
S12CT	2.239	2.182	.323	.185	.480	.056	.285	22.2	2,520	1.870	--
S12DT	2.209	2.064	.419	.222	.685	.144	.312	44.5	2,526	1.690	--
SP	.211	.306	.217	.210	.788	-.095	.139	58.9	2,188	.480	.280
SR	.886	-.096	.109	.216	.265	.983	.214	-289.7	1,354	-2.800	--
TE	1.242	.017	.127	.095	.857	1.226	.067	72.2	1,438	-.190	--
TMC	.902	.894	.239	.153	.886	.008	.125	72.5	2,232	.770	.732
TSB	.628	.865	.278	.259	.962	-.237	.076	92.5	1,327	.490	.610
TSH	.156	.177	.163	.141	.909	-.021	.069	82.3	2,445	.000	-.021
WE	1.611	-.053	.114	.122	.636	1.664	.101	21.0	1,461	-1.610	--
WP	1.365	-.031	.128	.170	.383	1.396	.169	-73.6	1,096	-1.870	--
WW	1.435	.043	.151	.145	.855	1.392	.080	72.1	1,461	-.230	--

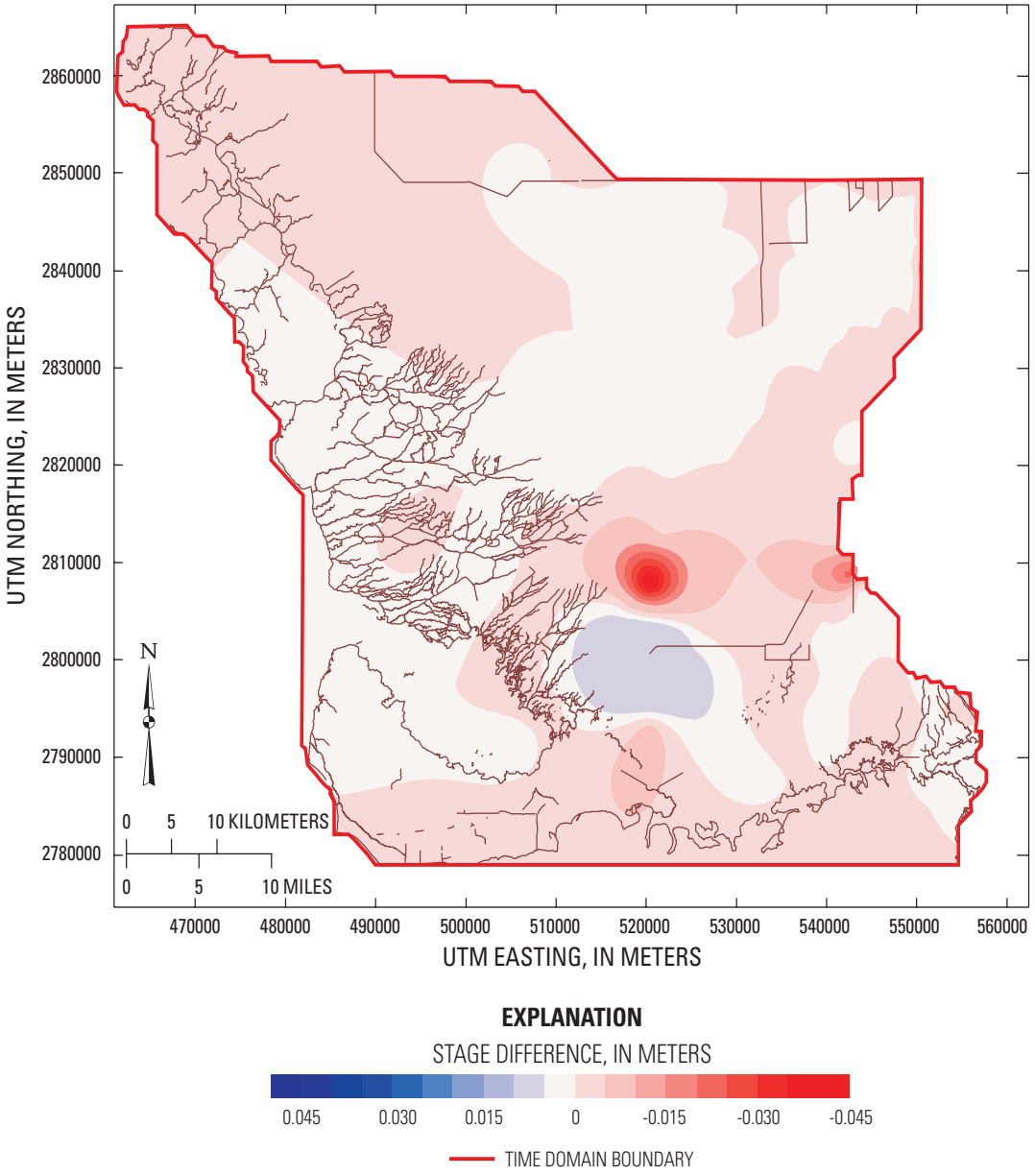

Figure 32. Spatial distribution of mean stage difference between simulations with and without the Main Park Road as a barrier. Positive values indicate better fit, and negative values indicate a poorer fit.

Table 13. Water-level comparison statistics for run 146, land-surface altitude lowered 0.1 meter.

[NAVD 88, North American Vertical Datum of 1988; n, number of points utilized from the time series]

Station	Mean stage (NAVD 88)		Stage standard deviation		Correlation coefficient	Mean difference between measured and computed values		Percentage of explained variance	n	Land surface altitude (NAVD 88)	
	Measured (meters)	Computed (meters)	Measured (meters)	Computed (meters)		Stage (meters)	Standard deviation (meters)			Model input (meters)	Measured (meters)
A13	0.968	0.259	0.985	0.157	0.861	-0.017	0.147	67.7	2,197	0.880	0.969
Angels	1.329	.264	1.493	.256	.726	-.165	.193	46.9	2,557	1.630	1.451
BD	.826	.123	.029	.099	.427	.797	.120	3.4	1,945	-.090	2.612
BICYA8	.215	.328	.764	.486	.099	-.549	.559	-190.9	1,959	.170	--
BICYA9	1.726	.211	1.763	.175	.784	-.036	.131	61.3	1,869	1.960	--
BICYA10	.718	.303	.693	.225	.775	.025	.192	60.0	1,854	.790	--
BICYA11	.920	.380	.844	.164	.719	.076	.286	43.5	1,883	.780	--
BR	1.074	.131	.018	.112	.844	1.056	.070	71.3	2,331	-.250	1.838
CN	.713	.123	-.005	.087	.864	.719	.065	72.0	2,447	-.180	1.323
CP	-.056	.169	-.106	.112	.792	.050	.105	61.0	2,479	-.540	-.503
CR2	1.121	.307	1.185	.278	.900	-.064	.134	81.0	2,161	1.230	1.231
CR3	1.119	.298	1.166	.230	.872	-.047	.149	75.0	2,212	1.210	1.234
CT27R	.143	.148	.085	.141	.597	.058	.130	23.0	1,903	-.160	-.085
CT50R	.106	.140	.020	.081	.785	.086	.092	57.3	1,896	-.090	.088
CV1NR	.121	.149	.003	.128	.109	.118	.185	-54.8	1,840	-.160	--
CV5S	.123	.132	.129	.109	.651	-.006	.103	39.5	601	-.160	--
CW	-.048	.103	-.067	.114	.520	.019	.107	-7.4	2,261	-1.930	--
CYP2	.235	.206	.205	.195	.790	.030	.130	59.9	2,157	.380	1.643
CY3	.202	.214	.116	.154	.782	.087	.134	60.7	2,206	.180	1.518
DK	-.207	.118	-.177	.096	.710	-.030	.084	49.4	1,317	-1.960	--
DO1	.349	.267	.390	.174	.843	-.041	.152	67.5	2,451	.460	.567
DO2	.432	.278	.360	.196	.828	.072	.159	67.1	2,237	.600	.570
E112	.846	.301	.908	.371	.888	-.062	.173	67.0	2,320	.950	.527
E146	-.096	.147	-.112	.113	.831	.016	.082	68.6	2,435	-.310	-.369
EP1R	.044	.132	-.005	.118	.093	.049	.169	-63.7	2,406	-.160	-.262
EP9R	-.159	.087	-.183	.061	.726	.024	.060	52.7	366	-.260	-.314
EPGW/ SW	-.015	.099	-.117	.077	.579	.102	.083	29.4	2,387	-.210	-.158
EVER4	.170	.145	.250	.149	.926	-.080	.057	84.8	2,521	.140	.085
EVER5A	-.097	.153	-.083	.091	.741	-.014	.105	52.9	1,945	-.180	-.174
EVER6	.141	.126	-.028	.071	.577	.169	.103	33.2	2,294	-.100	-.006
EVER7	.201	.120	.025	.091	.877	.176	.059	75.6	2,342	-.060	.131
G1251	.185	.168	.157	.153	.906	.028	.071	82.2	2,026	.130	.390
G1502	1.485	.242	1.613	.122	.760	-.128	.169	51.1	2,453	1.480	2.060
G3272	1.491	.247	1.633	.128	.797	-.142	.164	55.8	2,528	1.470	1.612
G3273	1.476	.239	1.621	.126	.792	-.145	.159	55.6	2,557	1.500	1.667
G3353	-.058	.137	-.060	.090	.794	.002	.086	61.1	2,519	-.120	1.149

Table 13. Water-level comparison statistics for run 146, land-surface altitude lowered 0.1 meter.—Continued

[NAVD 88, North American Vertical Datum of 1988; n, number of points utilized from the time series]

Station	Mean stage (NAVD 88)		Stage standard deviation		Correlation coefficient	Mean difference between measured and computed values		Percentage of explained variance	n	Land surface altitude (NAVD 88)	
	Measured (meters)	Computed (meters)	Measured (meters)	Computed (meters)		Stage (meters)	Standard deviation (meters)			Model input (meters)	Measured (meters)
G3437	1.194	0.259	1.089	0.259	0.704	0.105	0.199	40.9	2,510	1.750	1.615
G3576	1.562	.207	1.640	.096	.898	-.078	.128	61.9	1,965	1.270	1.353
G3577	1.426	.272	1.642	.093	.876	-.216	.196	48.1	2,014	1.260	1.356
G3578	1.520	.213	1.647	.090	.866	-.127	.142	55.4	2,494	1.270	1.356
G3619	.326	.147	.303	.142	.878	.024	.072	76.4	2,446	.110	.579
G3622	.879	.239	1.160	.375	.689	-.282	.273	-30.1	2,306	1.290	1.347
G3626	.975	.174	1.099	.267	.435	-.124	.248	-102.3	2,357	1.930	1.743
G3627	.860	.167	1.216	.242	.558	-.356	.203	-48.5	2,368	1.810	1.942
G3628	1.011	.203	1.410	.355	.496	-.399	.310	-132.4	2,336	1.630	1.667
G596	1.146	.197	1.312	.306	.603	-.165	.244	-53.0	2,546	1.710	1.753
G618	1.696	.146	1.652	.086	.773	.044	.096	56.5	2,457	1.380	1.466
G620	1.574	.205	1.482	.177	.924	.092	.080	85.0	2,451	1.280	1.311
GI	1.363	.113	-.079	.166	.414	1.442	.158	-93.3	1,616	-2.600	--
HC	-.186	.111	.147	.201	.605	-.332	.161	-109.3	1,434	.460	--
HR	.931	.119	.012	.099	.663	.919	.092	41.1	1,461	.020	--
L67XW	1.761	.237	1.633	.089	.743	.128	.181	41.6	1,883	1.250	--
LN	1.524	.120	-.046	.102	.823	1.570	.068	67.6	1,430	-.510	--
LO	.818	.119	-.072	.250	.152	.890	.260	-377.3	1,335	-2.100	--
LOOP1T	1.910	.158	1.747	.161	.715	.164	.120	42.1	2,024	1.760	--
LOOP2T	1.540	.220	1.399	.174	.705	.140	.157	48.9	2,086	1.380	--
LS	-.190	.106	-.173	.099	.813	-.017	.063	64.7	1,461	-1.620	--
NCL	-.015	.190	-.091	.119	.770	.076	.124	57.4	2,390	-.340	--
NE1	1.664	.131	1.639	.087	.849	.025	.073	68.5	2,509	1.190	1.314
NE2	1.627	.156	1.649	.085	.853	-.022	.094	63.4	2,503	1.240	1.241
NE3	1.695	.115	1.661	.068	.756	.033	.077	54.6	1,838	1.240	--
NE4	1.606	.158	1.616	.085	.832	-.010	.099	60.6	2,416	1.160	1.213
NE5	1.601	.146	1.597	.084	.852	.004	.087	64.8	2,539	1.170	--
NMP	-.118	.151	-.093	.124	.807	-.024	.089	65.2	2,113	-.090	--
NP201	1.869	.257	1.730	.178	.847	.139	.142	69.4	2,439	1.550	1.420
NP202	1.679	.196	1.550	.155	.958	.129	.065	89.0	2,309	1.250	1.164
NP203	1.471	.181	1.372	.126	.918	.099	.083	79.2	2426	1.120	.890
NP205	1.478	.264	1.389	.175	.827	.090	.155	65.7	2,447	1.340	1.332
NP206	1.282	.272	1.298	.155	.837	-.017	.166	62.8	2,453	1.280	1.366
NP44	.636	.351	.691	.231	.769	-.055	.228	57.9	2,342	1.170	1.073
NP46	.018	.171	-.056	.122	.742	.074	.115	55.0	2,429	-.050	-.052
NP62	.399	.197	.327	.129	.815	.072	.118	63.8	2,229	.210	.835
NP67	.215	.179	.185	.141	.899	.030	.081	79.7	2,406	.140	.582

Table 13. Water-level comparison statistics for run 146, land-surface altitude lowered 0.1 meter.—Continued

[NAVD 88, North American Vertical Datum of 1988; n, number of points utilized from the time series]

Station	Mean stage (NAVD 88)		Stage standard deviation		Correlation coefficient	Mean difference between measured and computed values		Percentage of explained variance	n	Land surface altitude (NAVD 88)	
	Measured (meters)	Computed (meters)	Measured (meters)	Computed (meters)		Stage (meters)	Standard deviation (meters)			Model input (meters)	Measured (meters)
NP72	0.503	0.316	0.527	0.217	0.790	-0.024	0.197	61.3	2,222	0.880	0.899
NR	1.181	.117	-.053	.106	.775	1.234	.075	58.4	1,380	-1.300	1.682
NTS1	.841	.293	1.083	.279	.786	-.242	.187	59.0	2,457	.920	1.076
NTS10	.927	.310	.997	.340	.888	-.070	.156	74.6	2,152	1.170	1.237
NTS14	.732	.386	.791	.328	.793	-.059	.236	62.6	2,395	1.280	.756
OL1	-.059	.160	-.126	.111	.833	.067	.091	67.6	2,447	-.320	--
OT	.251	.189	.091	.151	.864	.159	.096	74.2	2,464	-.270	--
P33	1.509	.148	1.438	.103	.916	.071	.068	79.0	2,406	1.130	1.024
P34	.419	.213	.177	.152	.852	.243	.115	70.7	2,428	.060	.119
P35	.118	.171	.113	.137	.950	.005	.059	88.0	2,552	-.500	-.195
P36	.868	.146	.794	.109	.905	.074	.066	79.4	2,407	.530	.530
P37	.002	.155	-.060	.113	.867	.062	.080	73.4	2,465	-.240	-.183
P38	.069	.148	.009	.109	.802	.060	.089	63.9	2,360	-.230	-.192
R127	.267	.197	.272	.141	.928	-.005	.085	81.6	2,384	-.040	--
R158	.416	.239	.612	.340	.812	-.196	.202	28.5	2,445	.880	.927
R3110	.919	.331	.940	.327	.896	-.021	.150	79.5	2,456	1.140	1.094
RG1	1.242	.284	1.504	.114	.692	-.262	.221	39.4	1,941	1.360	1.061
RG2	1.138	.286	1.299	.250	.817	-.161	.166	66.4	2,108	1.350	1.390
Rutzke	.940	.260	1.042	.357	.813	-.102	.210	34.9	2,432	1.410	1.103
S12AT	2.182	.288	1.971	.177	.779	.211	.186	58.0	2,530	1.770	--
S12BT	2.205	.317	1.947	.172	.913	.257	.175	69.7	2,532	1.760	--
S12CT	2.239	.323	2.103	.201	.337	.135	.317	3.2	2,520	1.770	--
S12DT	2.209	.419	1.974	.230	.609	.235	.333	36.7	2,526	1.590	--
SP	.211	.217	.184	.171	.779	.026	.136	60.7	2,188	.380	.280
SR	.886	.109	-.098	.215	.268	.984	.213	-285.4	1,354	-2.900	--
TE	1.242	.127	-.009	.101	.855	1.252	.066	72.8	1,438	-.290	--
TMC	.902	.239	.797	.150	.882	.105	.128	71.3	2,232	.670	.732
TSB	.628	.278	.766	.236	.965	-.138	.080	91.8	1,327	.390	.610
TSH	.156	.163	.089	.134	.903	.067	.072	80.8	2,445	-.100	-.021
WE	1.611	.114	-.056	.116	.642	1.667	.097	26.5	1,461	-1.710	--
WP	1.365	.128	-.026	.159	.414	1.391	.157	-50.8	1,096	-1.970	--
WW	1.435	.151	.027	.136	.872	1.408	.074	76.0	1,461	-.330	--

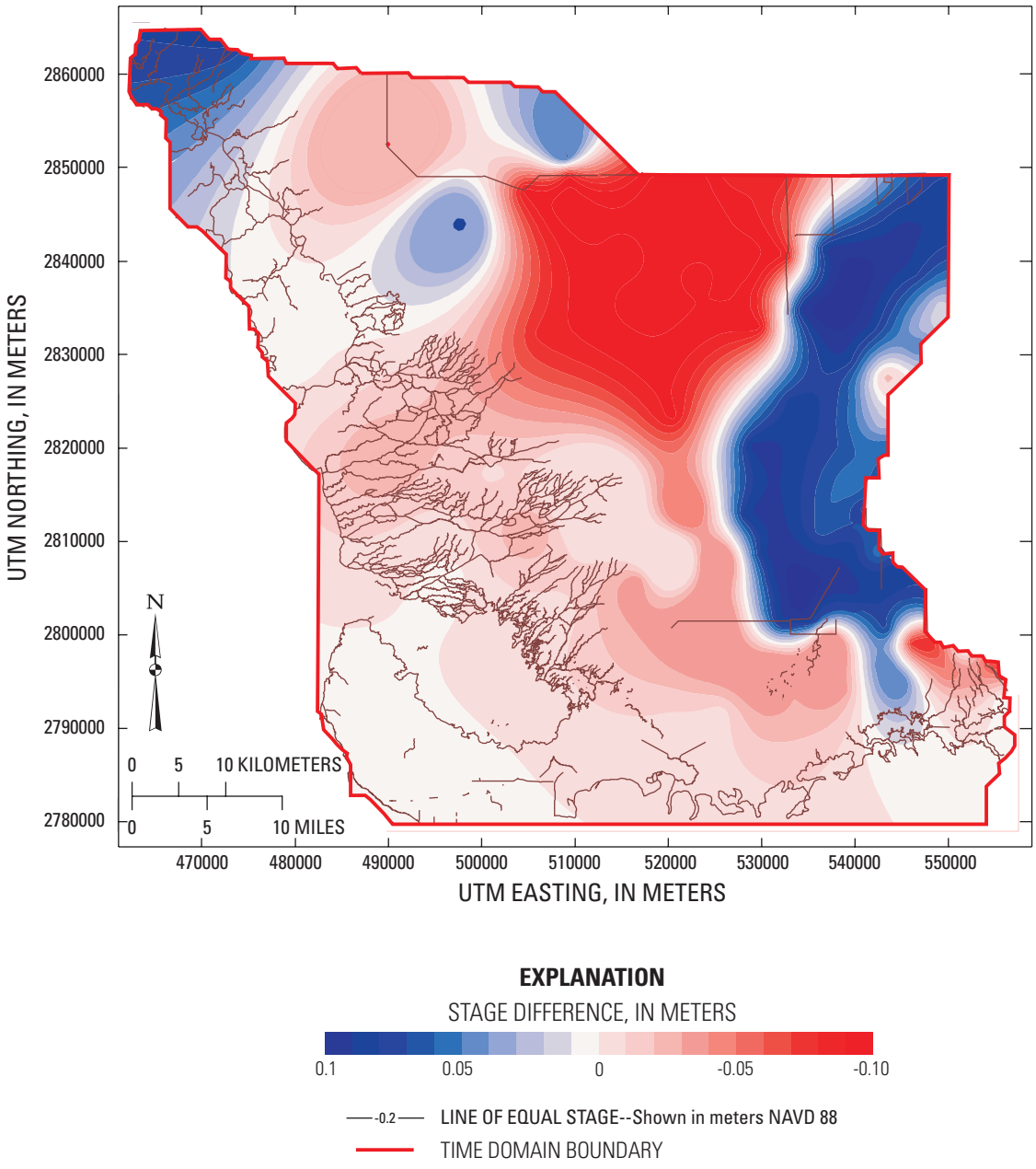

Figure 33. Spatial distribution of mean stage difference between simulations with and without lowered land surface. Positive values indicate better fit, and negative values indicate a poorer fit.

The station information for gage G-1502 (fig. 9) indicates the land-surface altitude near the gage is 2.06 m NAVD 88; therefore, the recorded water level for the entire data record is below land surface. The TIME application land-surface altitude at this location, however, is 1.58 m NAVD 88 based on the regional topography. Using this lower altitude, the TIME application shows surface water present most of the time, and consequently, the statistics routine compares mostly computed surface-water stage with measured groundwater head. This illustrates the problems that result from discrepancies between measured and model land-surface altitudes and from uncertainties in interpreting gage records. Similar discrepancies exist at other locations where the mean model and measured stage differ by 0.1 m; for example, CR2, CR3, RG1, RG2, and many of the G-prefix gages in the area.

Examples of how model results at many locations with substantial ponding could improve by lowering the model land-surface altitude can be seen by comparing the statistics for runs 142 and 146 (tables 10 and 13) for CR2, CR3, NTS10, NTS14, RG1, and RG2. In these cases, the simulated surface-water depth agrees reasonably well with the field data although stages are too high, indicating that land-surface altitude at the gage is higher in the model than measured in the field. Reducing stage by decreasing the frictional component is not feasible because stage at P33 is higher than RG1, indicating the flow gradient is to the southeast. The only apparent alternatives are to lower land-surface altitudes in the model and/or promote more flow through Taylor Slough. Because the model overestimates stage near TSB (figs. 9 and 16), an adjustment is made for the final calibration to facilitate flow through the slough, thereby lowering surface-water stages within it.

3.8.3 - C-111 Area

At gage HC (fig. 9) near the C-111 Canal (fig. 1), model response is controlled mainly by the prescribed ground-water head boundary because the water level is entirely below land surface. For previously reported runs, the prescribed ground-water head is equivalent to the measurement at EVER3 since there is a lack of other data. If data from HC were to be used to prescribe stage, the model fit likely would improve substantially; however, using HC to prescribe model boundary stage eliminates this gage as a calibration comparison site. Because these are boundary data issues in a calibration run using field-measured data, these issues should be nonexistent for model scenario runs that do not use field-measured data for boundaries.

The following calibration stations given in table 10 have: (1) an absolute value of mean bias (DIFMEAN) greater than 0.1 m, (2) a correlation of less than 0.8, and (3) an error standard deviation greater than 0.1 m or explained variance of less than 0.7 (DO1, DO2, E112, EP9R, EPGW/SW, EVER4, EVER5A, EVER6, EVER7, NCL, NMP, NP44, NP72, NTS10, NTS14, R127, and TSB). An examination of these statistics yields information that is useful for further calibration.

For run 142, mean biases at DO1, E112, EVER4, NP44, NP72, NTS10, NTS14, R127, and TSB are negative, which means the model overestimates mean stage (table 10). This indicates that statistics at these sites should improve if model land-surface altitudes are adjusted downward or friction is reduced; for EVER6 and EVER7, the opposite is true. It is undesirable to adjust land-surface altitudes without a careful field verification, however, and adjusting friction coefficients is considered more justifiable. At EVER4, computed stage is too high, but the model land-surface altitude is also high by 0.15 m. The neighboring station G-1251 shows a better fit, and the associated model land-surface altitude is below the corresponding observed altitude. The computed mean stage is reasonable at EPGW/SW, but the correlation and explained variance are lower than normal.

At stations EVER5A, EP9R, and G-3353, the model-input land-surface altitudes are higher than those measured at the stations. Model land-surface altitudes at EVER5A, EP9R, and G-3353 are higher by 0.09 m, 0.15 m, and 1.169 m, respectively. Figure 15 shows that the model reasonably simulates stage at these sites, except during periods of low water levels (below land surface), which may indicate inadequate simulated ground-water drainage or a combination of inadequate ET and an excessive aquifer specific yield.

The comparison at NCL in figure 15 is degraded by a relatively poor fit for the first 2 years, which also occurred at other locations in Everglades National Park. The model performance is substantially better for the later 5 years.

Assessing the fit between simulated and measured stage values at DO1, DO2, NMP, NP44, NP72, NTS10 and NTS14 (table 10) is problematic, owing to the difficulty of comparing simulated surface-water stage with measured data that most likely represent ground-water head. In this case, the water-table decline during the annual dry season is underestimated.

3.8.4 - Results of Final Calibration

A number of runs were made that incorporate the findings just described; specifically, the friction was reduced through TSB, the ET extinction function and depth were varied, and the friction coefficient was increased just south of the degraded portion of C-111 Canal. Additional stage data from stations CV1NR and HC were used for GHBs from east of EVER3 to Florida Bay. Finally, the friction coefficient was increased from 0.008 to 0.2 for Trout Creek to divert some of its flow to other creeks.

This final calibration (run 157) incorporates a modified ET extinction function for ground water in order to improve the model ground-water head response during the dry season. The actual ET equals $PET(1\text{-}DIST^2)$, if DIST is less than or equal to 1 m, where PET is potential ET and DIST is the distance between the land surface and water table. The open-boundary conditions are based on the hydrodynamic model of Florida Bay using the Environmental Fluid Dynamic Code (EFDC) (John Hamrick, Tetra Tech, written commun., 2005). Hydrographs for water-level stations based on model output are provided in figure 34.

Comparisons with measured data are quantified as in previous runs (table 14). Table 15, however, presents recalculated statistics using only computed ground-water head for every station where the computed land-surface altitude is higher than the mean observed stage. This is referred to as run 157GW and is an attempt to identify ground-water gages (as opposed to surface-water gages) and avoid comparisons between model surface-water stages with what may be measured ground-water heads. Statistics for run 157 indicate tangible model improvements and bring the majority of stations to the desired levels of correlation and explained variance. Figures 35 and 36 show the spatial distribution of the mean stage bias and PEV, respectively, for run 157. The degree of model improvement is illustrated also by the

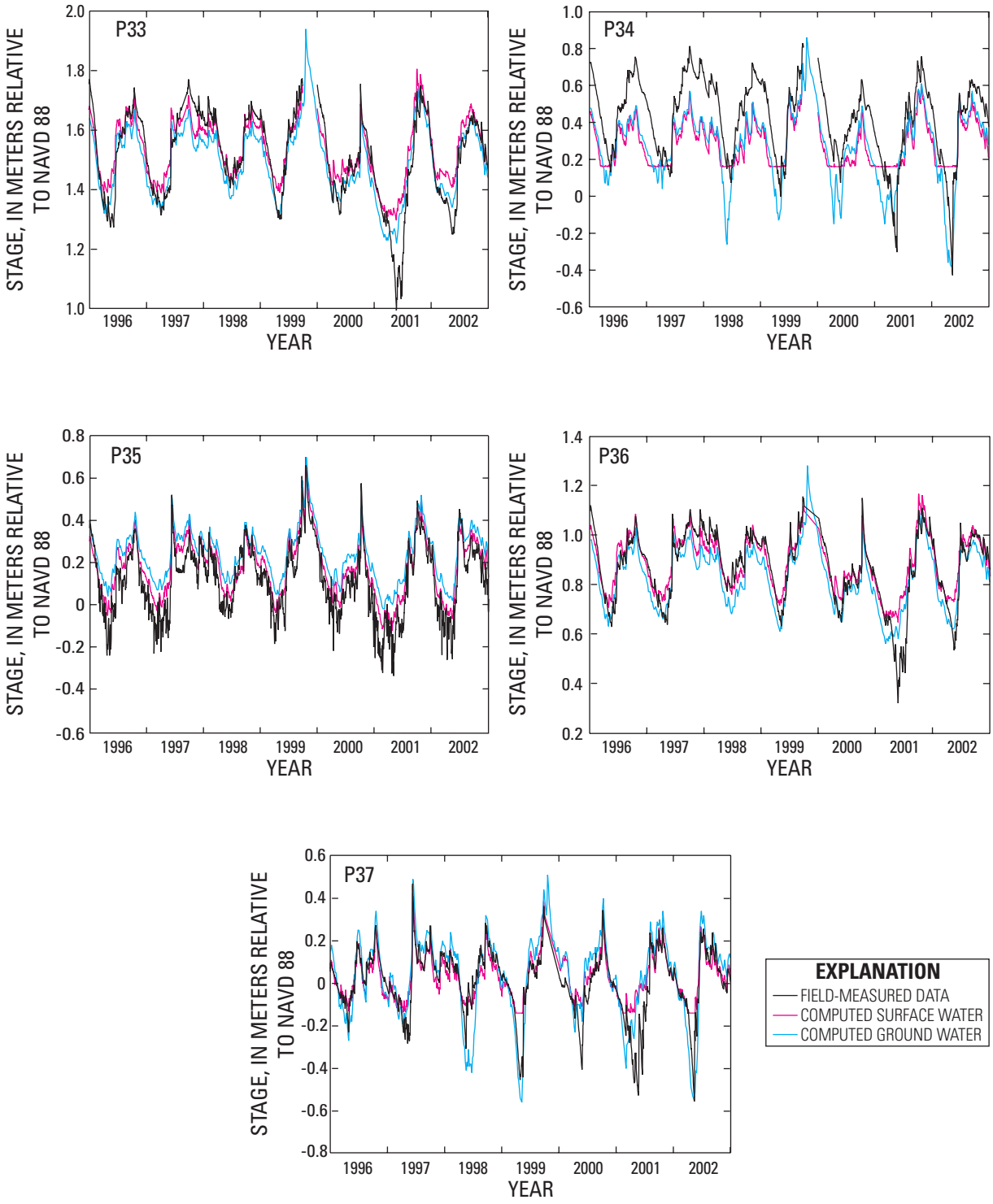

Figure 34. Comparison of water levels at selected stations in the TIME area for run 157.

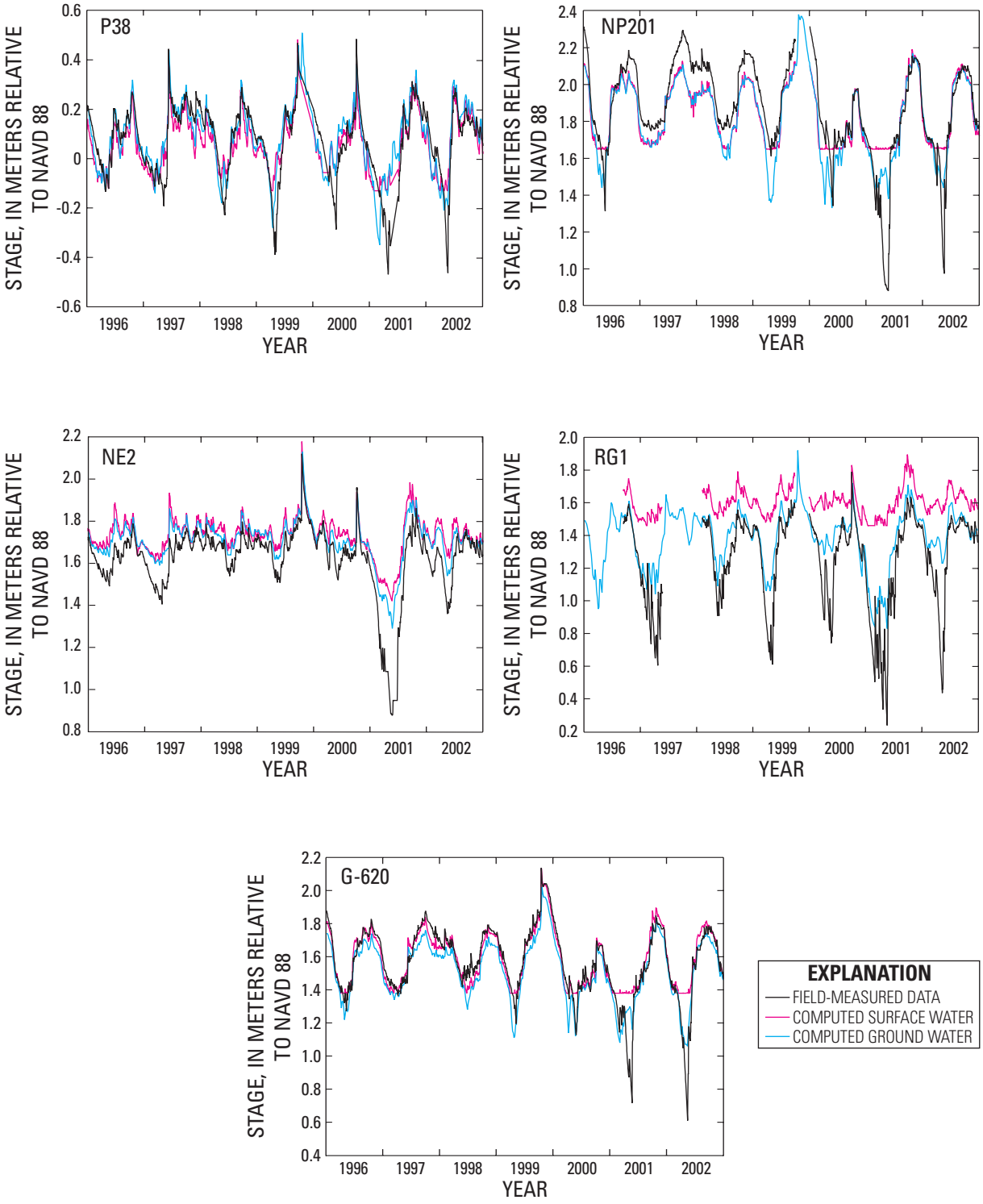

Figure 34. Comparison of water levels at selected stations in the TIME area for run 157.—Continued

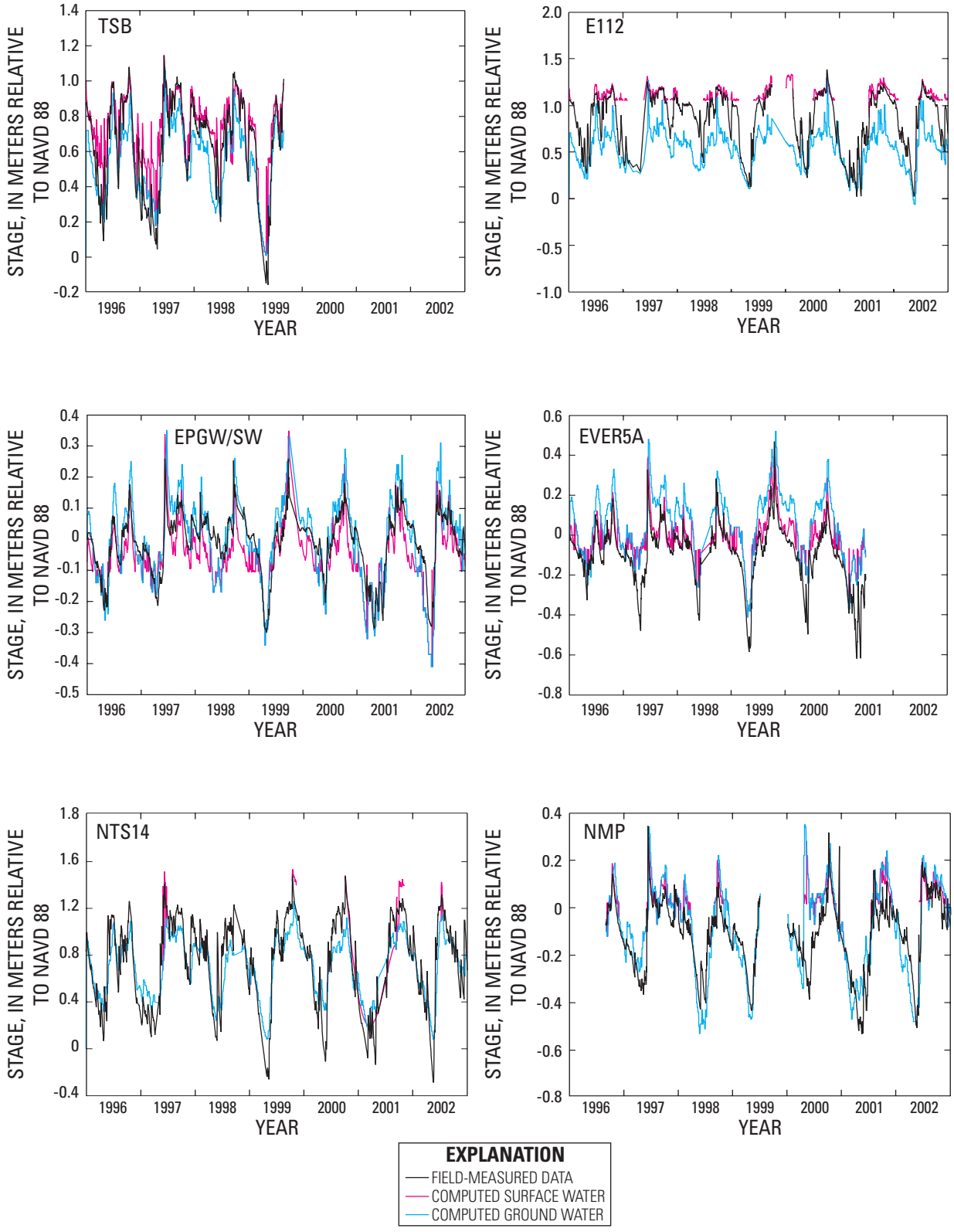

Figure 34. Comparison of water levels at selected stations in the TIME area for run 157.—Continued

Table 14. Water level comparison statistics for run 157, final calibration.

[NAVD 88, North American Vertical Datum of 1988; n, number of points utilized from the time series]

Station	Mean stage (NAVD 88)		Stage standard deviation		Correlation coefficient	Mean difference between measured and computed values		Percentage of explained variance	n	Land surface altitude (NAVD 88)	
	Measured (meters)	Computed (meters)	Measured (meters)	Computed (meters)		Stage (meters)	Standard deviation (meters)			Model input (meters)	Measured (meters)
A13	0.968	1.057	0.259	0.190	0.862	-0.090	0.135	72.7	2,197	0.980	0.969
Angels	1.329	1.302	.264	.122	.774	.026	.186	50.2	2,557	1.730	1.451
BD	.826	.090	.123	.095	.505	.736	.111	17.9	1,945	.010	2.612
BICYA10	.718	.721	.303	.286	.837	-.004	.169	68.8	1,854	.890	--
BICYA11	.920	.919	.380	.213	.727	.001	.268	50.1	1,883	.880	--
BICYA8	.215	-.008	.328	.159	.648	.223	.255	39.3	1,959	-1.000	--
BICYA9	1.726	1.803	.211	.215	.813	-.077	.130	61.8	1,869	2.060	--
BR	1.074	.040	.131	.117	.902	1.034	.056	81.4	2,331	-.150	1.838
CN	.713	.036	.123	.084	.900	.677	.060	76.3	2,447	-.080	1.323
CP	-.056	-.052	.169	.122	.826	-.004	.097	67.1	2,479	-.440	-.503
CR2	1.121	1.055	.307	.256	.925	.066	.120	84.7	2,161	1.330	1.231
CR3	1.119	1.219	.298	.282	.863	-.100	.152	73.8	2,212	1.310	1.234
CT27R	.143	-.005	.148	.096	.707	.148	.105	49.7	1,903	-.060	-.085
CT50R	.106	.120	.140	.142	.889	-.014	.067	77.5	1,896	.010	.088
CW	-.048	-.058	.103	.146	.754	.010	.096	12.8	2,261	-1.830	--
CY3	.202	.150	.214	.226	.810	.053	.136	59.7	2,206	.280	1.518
CYP2	.235	.206	.206	.222	.855	.029	.116	68.1	2,157	.480	1.643
DK	-.207	-.202	.118	.190	.861	-.005	.107	17.6	1,317	-1.860	--
DO1	.349	.395	.267	.230	.858	-.047	.137	73.6	2,451	.560	.567
DO2	.432	.361	.278	.221	.853	.071	.146	72.5	2,237	.700	.570
E112	.846	.907	.301	.356	.821	-.061	.203	54.5	2,320	1.050	.527
E146	-.096	-.059	.147	.140	.831	-.037	.084	67.7	2,435	-.210	-.369
EP1R	.044	-.033	.132	.093	.816	.077	.078	65.4	2,406	-.060	-.262
EP9R	-.159	-.107	.087	.070	.804	-.052	.052	64.7	366	-.160	-.314
EPGW/ SW	-.015	-.056	.099	.103	.841	.041	.057	66.9	2,387	-.110	-.158
EVER4	.170	.232	.145	.176	.894	-.062	.080	69.8	2,521	.240	.085
EVER5A	-.097	-.018	.153	.119	.838	-.079	.084	69.9	1,945	-.080	-.174
EVER6	.141	.023	.126	.101	.874	.118	.062	75.9	2,294	.000	-.006
EVER7	.201	.100	.120	.123	.891	.102	.057	77.5	2,342	.040	.131
G1251	.185	.173	.168	.193	.884	.012	.090	71.1	2,026	.230	.390
G1502	1.485	1.461	.242	.145	.821	.024	.148	62.4	2,453	1.580	2.060
G3272	1.491	1.471	.247	.111	.766	.020	.177	48.6	2,528	1.570	1.612
G3273	1.476	1.509	.239	.131	.818	-.033	.152	59.6	2,557	1.600	1.667
G3353	-.058	.000	.137	.127	.876	-.058	.066	76.5	2,519	-.020	1.149
G3437	1.194	1.048	.259	.184	.855	.146	.139	71.1	2,510	1.850	1.615
G3576	1.562	1.724	0.207	0.105	0.901	-0.161	0.121	65.9	1,965	1.370	1.353

Table 14. Water level comparison statistics for run 157, final calibration.—Continued

[NAVD 88, North American Vertical Datum of 1988; n, number of points utilized from the time series]

Station	Mean stage (NAVD 88)		Stage standard deviation		Correlation coefficient	Mean difference between measured and computed values		Percentage of explained variance	n	Land surface altitude (NAVD 88)	
	Measured (meters)	Computed (meters)	Measured (meters)	Computed (meters)		Stage (meters)	Standard deviation (meters)			Model input (meters)	Measured (meters)
G3577	1.426	1.726	.272	.096	.885	-.300	.192	50.0	2,014	1.360	1.356
G3578	1.520	1.732	.213	.095	.870	-.212	.138	57.8	2,494	1.370	1.356
G3619	.326	.390	.147	.162	.892	-.063	.073	75.2	2,446	.210	.579
G3622	.879	.735	.239	.205	.817	.144	.138	66.5	2,306	1.390	1.347
G3626	.975	1.034	.174	.118	.440	-.059	.162	13.7	2,357	2.030	1.743
G3627	.860	1.157	.167	.116	.618	-.296	.132	37.6	2,368	1.910	1.942
G3628	1.011	1.039	.203	.127	.732	-.028	.140	52.5	2,336	1.730	1.667
G596	1.146	1.141	.197	.109	.562	.005	.163	31.5	2,546	1.810	1.753
G618	1.696	1.739	.146	.087	.800	-.043	.092	60.0	2,457	1.480	1.466
G620	1.574	1.573	.205	.185	.931	.001	.075	86.5	2,451	1.380	1.311
GI	1.363	-.069	.113	.206	.627	1.432	.161	-101.5	1,616	-2.500	--
HC	-.186	-.212	.111	.114	.823	.027	.067	63.6	1,434	.560	--
HR	.931	.052	.119	.144	.668	.880	.110	15.5	1,461	.120	--
L67XW	1.761	1.719	.237	.090	.739	.042	.181	41.7	1,883	1.350	--
LN	1.524	-.019	.120	.104	.922	1.543	.047	84.7	1,430	-.410	--
LO	.818	-.045	.119	.283	.363	.864	.264	-393.3	1,335	-2.000	--
LOOP1T	1.910	1.818	.158	.203	.726	.092	.140	22.0	2,024	1.860	--
LOOP2T	1.540	1.474	.220	.225	.748	.066	.158	48.3	2,086	1.480	--
LS	-.190	-.156	.106	.131	.723	-.033	.091	25.8	1,461	-1.520	--
NCL	-.015	-.061	.190	.164	.775	.047	.121	59.3	2,390	-.240	--
NE1	1.664	1.726	.131	.088	.851	-.062	.073	69.2	2,509	1.290	1.314
NE2	1.627	1.736	.156	.087	.862	-.109	.092	65.3	2,503	1.340	1.241
NE3	1.695	1.747	.115	.069	.776	-.052	.075	57.2	1,838	1.340	--
NE4	1.606	1.704	.158	.087	.834	-.097	.099	61.3	2,416	1.260	1.213
NE5	1.601	1.686	.146	.085	.853	-.085	.086	65.4	2,539	1.270	--
NMP	-.118	-.087	.151	.190	.781	-.031	.118	38.4	2,113	.010	--
NP201	1.869	1.823	.257	.185	.857	.046	.137	71.5	2,439	1.650	1.420
NP202	1.679	1.645	.196	.156	.960	.034	.063	89.5	2,309	1.350	1.164
NP203	1.471	1.466	.181	.126	.921	.005	.082	79.8	2,426	1.220	.890
NP205	1.478	1.466	.264	.213	.827	.012	.148	68.4	2,447	1.440	1.332
NP206	1.282	1.280	.272	.186	.869	.002	.144	72.1	2,453	1.380	1.366
NP44	.636	.677	.351	.241	.864	-.041	.187	71.6	2,342	1.270	1.073
NP46	.018	-.029	.171	.170	.748	.047	.121	49.8	2,429	.050	-.052
NP62	.399	.399	.197	.148	.817	.000	.114	66.3	2,229	.310	.835
NP67	.215	.256	.179	.183	.895	-.041	.083	78.4	2,406	.240	.582
NP72	0.503	0.505	0.316	0.222	0.849	-0.002	0.173	70.0	2,222	0.980	0.899
NR	1.181	-.037	.117	.125	.907	1.218	.053	79.6	1,380	-1.200	1.682

Table 14. Water level comparison statistics for run 157, final calibration.—Continued

[NAVD 88, North American Vertical Datum of 1988; n, number of points utilized from the time series]

Station	Mean stage (NAVD 88)		Stage standard deviation		Correlation coefficient	Mean difference between measured and computed values		Percentage of explained variance	n	Land surface altitude (NAVD 88)	
	Measured (meters)	Computed (meters)	Measured (meters)	Computed (meters)		Stage (meters)	Standard deviation (meters)			Model input (meters)	Measured (meters)
NTS1	.841	.517	.293	.213	.768	.323	.188	58.8	2,457	1.020	1.076
NTS10	.927	.792	.310	.236	.902	.135	.141	79.3	2,152	1.270	1.237
NTS14	.732	.704	.386	.254	.909	.028	.188	76.2	2,395	1.380	.756
OL1	-.059	-.063	.160	.136	.864	.004	.080	74.7	2,447	-.220	--
OT	.251	.153	.189	.159	.902	.098	.082	81.0	2,464	-.170	--
P33	1.509	1.531	.148	.104	.919	-.022	.067	79.6	2,406	1.230	1.024
P34	.419	.251	.213	.171	.864	.168	.108	74.2	2,428	.160	.119
P35	.118	.179	.171	.139	.952	-.061	.057	88.8	2,552	-.400	-.195
P36	.868	.886	.146	.109	.909	-.018	.065	80.0	2,407	.630	.530
P37	.002	.014	.155	.134	.855	-.012	.080	73.0	2,465	-.140	-.183
P38	.069	.057	.148	.113	.823	.012	.085	67.4	2,360	-.130	-.192
R127	.267	.360	.197	.163	.922	-.093	.079	84.0	2,384	.060	--
R158	.416	.390	.239	.191	.867	.025	.120	74.7	2,445	.980	.927
R3110	.919	.826	.331	.261	.915	.093	.140	82.1	2,456	1.240	1.094
RG1	1.242	1.372	.284	.171	.855	-.130	.164	66.7	1,941	1.460	1.061
RG2	1.138	1.183	.286	.218	.894	-.045	.133	78.3	2,108	1.450	1.390
Rutzke	.940	.881	.260	.210	.866	.059	.131	74.6	2,432	1.510	1.103
S12AT	2.182	2.070	.288	.173	.807	.113	.180	60.9	2,530	1.870	--
S12BT	2.205	2.050	.317	.171	.889	.154	.182	66.9	2,532	1.860	--
S12CT	2.239	2.182	.323	.184	.480	.056	.285	22.2	2,520	1.870	--
S12DT	2.209	2.065	.419	.222	.684	.144	.312	44.4	2,526	1.690	--
SP	.211	.196	.217	.192	.831	.014	.121	68.8	2,188	.480	.280
SR	.886	-.076	.109	.247	.482	.962	.216	-296.9	1,354	-2.800	--
TE	1.242	.029	.127	.102	.933	1.213	.049	85.3	1,438	-.190	--
TMC	.902	.884	.239	.174	.892	.018	.115	76.8	2,232	.770	.732
TSB	.628	.709	.278	.214	.926	-.081	.114	83.2	1,327	.490	.610
TSH	.156	.169	.163	.164	.903	-.013	.072	80.5	2,445	.000	-.021
WE	1.611	-.044	.114	.142	.825	1.655	.081	49.6	1,461	-1.610	--
WP	1.365	-.052	.128	.203	.709	1.417	.144	-25.6	1,096	-1.870	--
WW	1.435	.060	.151	.142	.883	1.375	.071	77.7	1,461	-.230	--

Table 15. Water-level comparison statistics for run 157GW, model ground water only.

[NAVD 88, North American Vertical Datum of 1988; n, number of points utilized from the time series]

Station	Mean stage (NAVD 88)		Standard deviation of stage		Correlation coefficient	Mean difference between measured and computed values		Percentage of explained variance	n	Land surface altitude (NAVD 88)	
	Measured (meters)	Computed (meters)	Measured (meters)	Computed (meters)		Stage (meters)	Standard deviation (meters)			Model input (meters)	Measured (meters)
A13	0.968	1.017	0.259	0.210	0.881	-0.050	0.124	77.1	2,197	0.980	0.969
Angels	1.329	1.302	.264	.122	.774	.026	.186	50.2	2,557	1.730	1.451
BD	.826	.176	.123	.109	.513	.650	.115	11.9	1,945	.010	2.612
BICYA8	.215	.805	.328	.294	.873	-.590	.160	76.1	1,959	-1.000	--
BICYA9	1.726	1.803	.211	.215	.813	-.077	.130	61.8	1,869	2.060	--
BICYA10	.718	.721	.303	.286	.837	-.004	.169	68.8	1,854	.890	--
BICYA11	.920	.893	.380	.236	.801	.028	.237	61.0	1,883	.880	--
BR	1.074	.097	.131	.117	.744	.977	.090	53.0	2,331	-.150	1.838
CN	.713	.066	.123	.096	.810	.648	.072	65.6	2,447	-.080	1.323
CP	-.056	-.060	.169	.181	.816	.004	.107	60.0	2,479	-.440	-.503
CR2	1.121	1.055	.307	.256	.925	.066	.120	84.7	2,161	1.330	1.231
CR3	1.119	1.099	.298	.258	.901	.020	.129	81.1	2,212	1.310	1.234
CT27R	.143	.063	.148	.138	.885	.080	.069	78.1	1,903	-.060	-.085
CT50R	.106	.120	.140	.142	.889	-.014	.067	77.5	1,896	.010	.088
CW	-.048	.041	.103	.099	.640	-.089	.086	30.7	2,261	-1.830	--
CYP2	.235	.206	.206	.222	.855	.029	.116	68.1	2,157	.480	1.643
CY3	.202	.150	.214	.226	.810	.053	.136	59.7	2,206	.280	1.518
DK	-.207	-.149	.118	.159	.456	-.058	.148	-58.8	1,317	-1.860	--
DO1	.349	.395	.267	.230	.858	-.047	.137	73.6	2,451	.560	.567
DO2	.432	.361	.278	.221	.853	.071	.146	72.5	2,237	.700	.570
E112	.846	.542	.301	.208	.842	.304	.169	68.6	2,320	1.050	.527
E146	-.096	-.035	.147	.172	.836	-.061	.095	58.7	2,435	-.210	-.369
EP1R	.044	.000	.132	.117	.911	.044	.054	83.0	2,406	-.060	-.262
EP9R	-.159	-.057	.087	.122	.818	-.102	.072	32.4	366	-.160	-.314
EPGW/SW	-.015	-.006	.099	.136	.871	-.009	.069	51.1	2,387	-.110	-.158
EVER4	.170	.232	.145	.176	.894	-.062	.080	69.8	2,521	.240	.085
EVER5A	-.097	.050	.153	.166	.863	-.147	.084	69.4	1,945	-.080	-.174
EVER6	.141	.062	.126	.137	.914	.079	.056	80.5	2,294	.000	-.006
EVER7	.201	.106	.120	.154	.901	.095	.070	66.3	2,342	.040	.131
G1251	.185	.173	.168	.193	.884	.012	.090	71.1	2,026	.230	.390
G1502	1.485	1.461	.242	.145	.821	.024	.148	62.4	2,453	1.580	2.060
G3272	1.491	1.471	.247	.111	.766	.020	.177	48.6	2,528	1.570	1.612
G3273	1.476	1.509	.239	.131	.818	-.033	.152	59.6	2,557	1.600	1.667
G3353	-.058	.063	.137	.174	.867	-.122	.088	58.9	2,519	-.020	1.149
G3437	1.194	1.048	.259	.184	.855	.146	.139	71.1	2,510	1.850	1.615
G3576	1.562	1.601	0.207	0.143	0.916	-0.039	0.095	78.8	1,965	1.370	1.353

Table 15. Water-level comparison statistics for run 157GW, model ground water only.—Continued

[NAVD 88, North American Vertical Datum of 1988; n, number of points utilized from the time series]

Station	Mean stage (NAVD 88)		Standard deviation of stage		Correlation coefficient	Mean difference between measured and computed values		Percentage of explained variance	n	Land surface altitude (NAVD 88)	
	Measured (meters)	Computed (meters)	Measured (meters)	Computed (meters)		Stage (meters)	Standard deviation (meters)			Model input (meters)	Measured (meters)
G3577	1.426	1.227	.272	.144	.804	.198	.178	57.1	2,014	1.360	1.356
G3578	1.520	1.367	.213	.122	.852	.153	.127	64.7	2,494	1.370	1.356
G3619	.326	.332	.147	.185	.815	-.006	.107	46.6	2,446	.210	.579
G3622	.879	.735	.239	.205	.817	.144	.138	66.5	2,306	1.390	1.347
G3626	.975	1.034	.174	.118	.440	-.059	.162	13.7	2,357	2.030	1.743
G3627	.860	1.157	.167	.116	.618	-.296	.132	37.6	2,368	1.910	1.942
G3628	1.011	1.039	.203	.127	.732	-.028	.140	52.5	2,336	1.730	1.667
G596	1.146	1.141	.197	.109	.562	.005	.163	31.5	2,546	1.810	1.753
G618	1.696	2.122	.146	.176	.841	-.426	.096	56.9	2,457	1.480	1.466
G620	1.574	1.546	.205	.182	.905	.028	.088	81.8	2,451	1.380	1.311
GI	1.363	.088	.113	.106	.669	1.274	.089	38.0	1,616	-2.500	--
HC	-.186	-.212	.111	.114	.823	.027	.067	63.6	1,434	.560	--
HR	.931	.044	.119	.158	.642	.887	.123	-05.3	1,461	.120	--
L67XW	1.761	1.721	.237	.133	.898	.040	.132	69.3	1,883	1.350	--
LN	1.524	.046	.120	.121	.714	1.478	.091	42.5	1,430	-.410	--
LO	.818	.223	.119	.153	.661	.595	.116	4.4	1,335	-2.000	--
LOOP1T	1.910	1.767	.158	.200	.767	.144	.129	34.0	2,024	1.860	--
LOOP2T	1.540	1.414	.220	.248	.797	.126	.151	52.6	2,086	1.480	--
LS	-.190	-.252	.106	.125	.728	.063	.087	32.1	1,461	-1.520	--
NCL	-.015	-.061	.190	.197	.774	.046	.130	52.9	2,390	-.240	--
NE1	1.664	1.743	.131	.105	.835	-.079	.072	69.8	2,509	1.290	1.314
NE2	1.627	1.710	.156	.105	.868	-.083	.083	71.7	2,503	1.340	1.241
NE3	1.695	1.410	.115	.122	.733	.285	.087	43.0	1,838	1.340	--
NE4	1.606	1.659	.158	.109	.834	-.052	.090	67.4	2,416	1.260	1.213
NE5	1.601	1.622	.146	.110	.854	-.021	.077	72.0	2,539	1.270	--
NMP	-.118	-.087	.151	.190	.781	-.031	.118	38.4	2,113	.010	--
NP201	1.869	1.839	.257	.203	.850	.030	.136	72.0	2,439	1.650	1.420
NP202	1.679	1.623	.196	.148	.924	.057	.082	82.6	2,309	1.350	1.164
NP203	1.471	1.452	.181	.133	.898	.019	.085	77.8	2,426	1.220	.890
NP205	1.478	1.400	.264	.235	.852	.079	.138	72.4	2,447	1.440	1.332
NP206	1.282	1.280	.272	.186	.869	.002	.144	72.1	2,453	1.380	1.366
NP44	.636	.677	.351	.241	.864	-.041	.187	71.6	2,342	1.270	1.073
NP46	.018	-.029	.171	.188	.786	.047	.118	52.1	2,429	.050	-.052
NP62	.399	.423	.197	.185	.855	-.024	.104	72.3	2,229	.310	.835
NP67	.215	.236	.179	.206	.909	-.021	.086	76.8	2,406	.240	.582
NP72	0.503	0.505	0.316	0.222	0.849	-0.002	0.173	70.0	2,222	0.980	0.899
NR	1.181	.048	.117	.113	.674	1.133	.093	37.0	1,380	-1.200	1.682

Table 15. Water-level comparison statistics for run 157GW, model ground water only.—Continued

[NAVD 88, North American Vertical Datum of 1988; n, number of points utilized from the time series]

Station	Mean stage (NAVD 88)		Standard deviation of stage		Correlation coefficient	Mean difference between measured and computed values		Percentage of explained variance	n	Land surface altitude (NAVD 88)	
	Measured (meters)	Computed (meters)	Measured (meters)	Computed (meters)		Stage (meters)	Standard deviation (meters)			Model input (meters)	Measured (meters)
NTS1	.841	.517	.293	.213	.768	.323	.188	58.8	2,457	1.020	1.076
NTS10	.927	.792	.310	.236	.902	.135	.141	79.3	2,152	1.270	1.237
NTS14	.732	.704	.386	.254	.909	.028	.188	76.2	2,395	1.380	.756
OL1	-.059	-.021	.160	.172	.864	-.037	.087	70.2	2,447	-.220	--
OT	.251	.201	.189	.168	.912	.050	.078	83.2	2,464	-.170	--
P33	1.509	1.508	.148	.115	.877	.001	.073	75.8	2,406	1.230	1.024
P34	.419	.292	.213	.199	.890	.127	.097	79.1	2,428	.160	.119
P35	.118	.263	.171	.126	.905	-.145	.078	79.2	2,552	-.400	-.195
P36	.868	.867	.146	.120	.891	.001	.067	78.9	2,407	.630	.530
P37	.002	.048	.155	.193	.827	-.047	.109	50.8	2,465	-.140	-.183
P38	.069	.103	.148	.142	.861	-.034	.077	73.3	2,360	-.130	-.192
R127	.267	.315	.197	.198	.919	-.049	.080	83.7	2,384	.060	--
R158	.416	.390	.239	.191	.867	.025	.120	74.7	2,445	.980	.927
R3110	.919	.826	.331	.261	.915	.093	.140	82.1	2,456	1.240	1.094
RG1	1.242	1.372	.284	.171	.855	-.130	.164	66.7	1,941	1.460	1.061
RG2	1.138	1.183	.286	.218	.894	-.045	.133	78.3	2,108	1.450	1.390
Rutzke	.940	.881	.260	.210	.866	.059	.131	74.6	2,432	1.510	1.103
S12AT	2.182	2.436	.288	.242	.689	-.254	.213	45.2	2,530	1.870	--
S12BT	2.205	2.436	.317	.242	.760	-.232	.206	57.8	2,532	1.860	--
S12CT	2.239	2.436	.323	.243	.795	-.197	.196	63.0	2,520	1.870	--
S12DT	2.209	2.438	.419	.241	.811	-.229	.264	60.2	2,526	1.690	--
SP	.211	.196	.217	.192	.831	.014	.121	68.8	2,188	.480	.280
SR	.886	.076	.109	.112	.637	.811	.094	24.9	1,354	-2.800	--
TE	1.242	.080	.127	.106	.758	1.163	.083	56.9	1,438	-.190	--
TMC	.902	.837	.239	.195	.909	.065	.102	81.8	2,232	.770	.732
TSB	.628	.538	.278	.207	.896	.090	.131	77.9	1,327	.490	.610
TSH	.156	.169	.163	.193	.896	-.013	.086	72.0	2,445	.000	-.021
WE	1.611	.071	.114	.201	.390	1.540	.188	-174.6	1,461	-1.610	--
WP	1.365	.132	.128	.139	.639	1.233	.114	21.2	1,096	-1.870	--
WW	1.435	.122	.151	.145	.801	1.314	.094	61.5	1,461	-.230	--

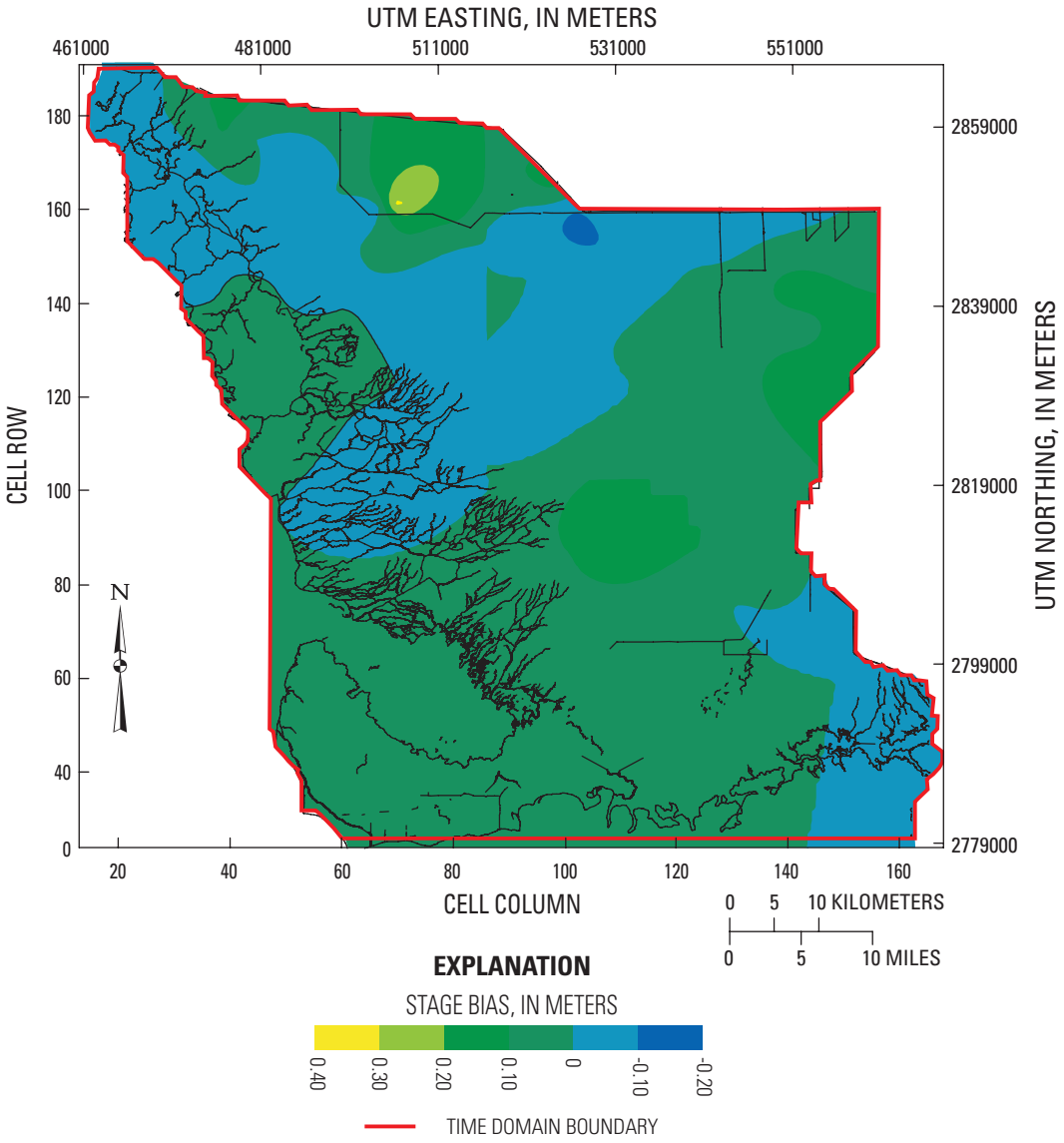

Figure 35. Spatial distribution of model mean stage bias in the TIME area for run 157.

summary statistics for 103 sites in table 5; run 157GW shows substantial improvement in each category. In figures showing the spatial distribution of statistical properties, the contour shapes are partly dependent upon the location and spacing of the field sites used for comparison. For example, an apparent horizontal offset of figure 36 contours can be explained by the interpolation between field sites and does not correspond to a distinct hydrologic feature.

The changes from run 142 to 157 decrease the total average flow to northeastern Florida Bay from 16.0 to 13.4 m^3/s. This reduction in flow, partly caused by reduced boundary seepage and increased ET, improves the agreement between model discharge to Florida Bay and measured flows of 10.2 m^3/s. The redistribution of flows through rivers and creeks is shown in figure 25.

Improvements in water-level representation are evident at a number of sites, especially TSB, E112, EPGW/SW, EVER5A, and NTS14 (fig. 34); however, EVER4, EVER6, and EVER7 are nearly unchanged. The computed surface-water values are actually a composite of model surface water (when present) and model ground water when land surface is dry. NTS14 is an example where model land-surface altitude is substantially (0.6 m) higher than the corresponding measured altitude. An altitude adjustment is probably necessary to obtain

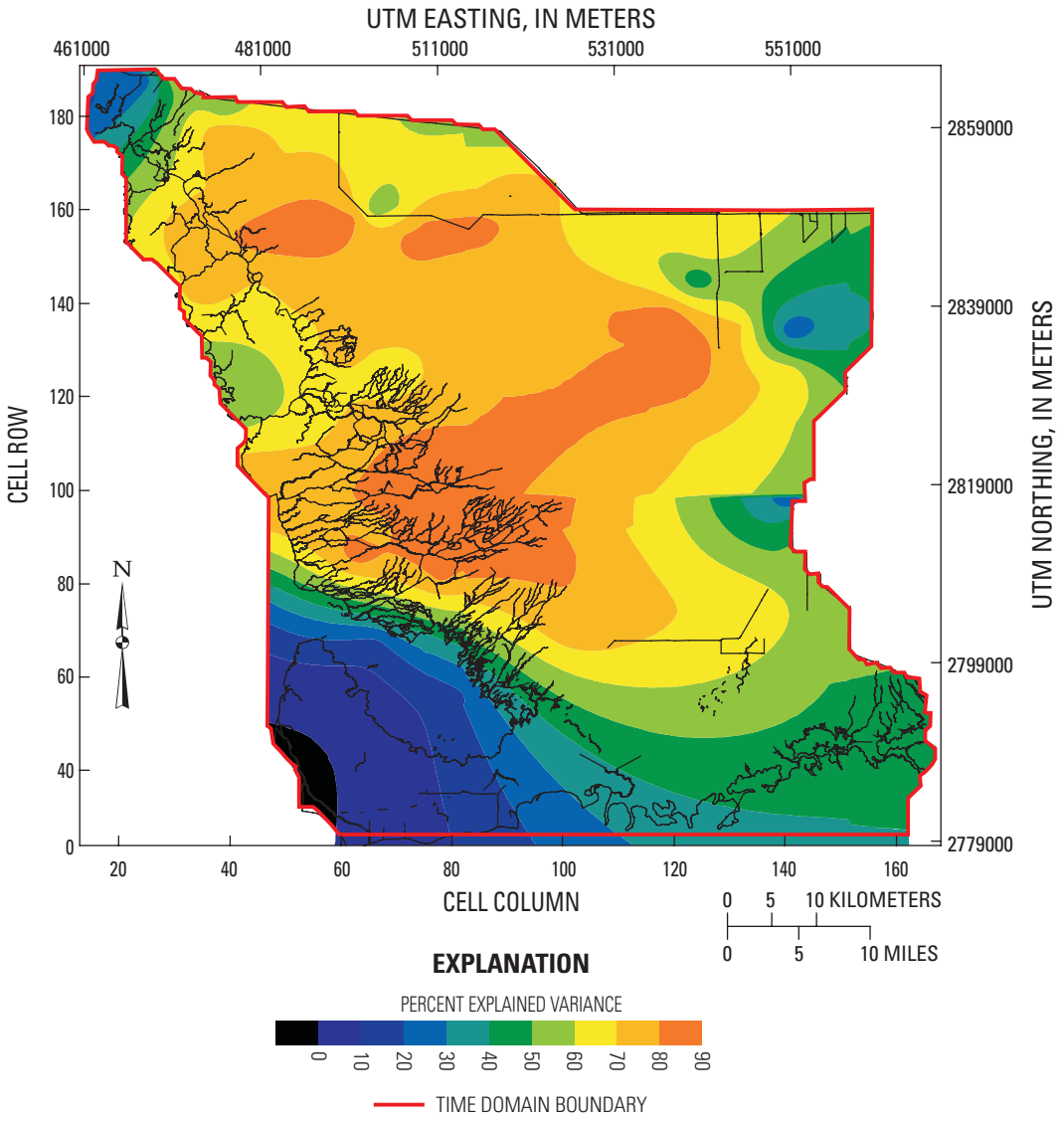

Figure 36. Spatial distribution of percentage of explained variance in the TIME area for run 157.

further improvement at sites were substantial land-altitude discrepancies exist. The EPGW/SW station is noteworthy because the data are bracketed by model ground water and surface water and because ground-water head is above the surface-water stage, indicating upward leakage.

The predicted salinities at Trout Creek for runs 142 and 157 are shown in figure 37. The open-boundary prescribed salinity of 36 psu for incoming flow in run 142 caused substantial phase errors and a range compression compared to observations. Using the EFDC model salinity boundary conditions improves the phase and also expands the range to reproduce more closely the data. Hypersalinity (greater than 36 psu) extremes are still underpredicted, which is related directly to the Florida Bay model representation. In contrast, the overestimation of low salinities primarily is due to a lack of sufficient resolution in the TIME model directly adjacent to creeks where spatial gradients in salinity are large; however, this should have little effect on predicted freshwater outflows.

3.9 - Future Uses of TIME application

In order to use the TIME application to evaluate the effects of proposed restoration scenarios on the coastal Everglades, boundary conditions for TIME must be developed from a linkage to the South Florida Water Management

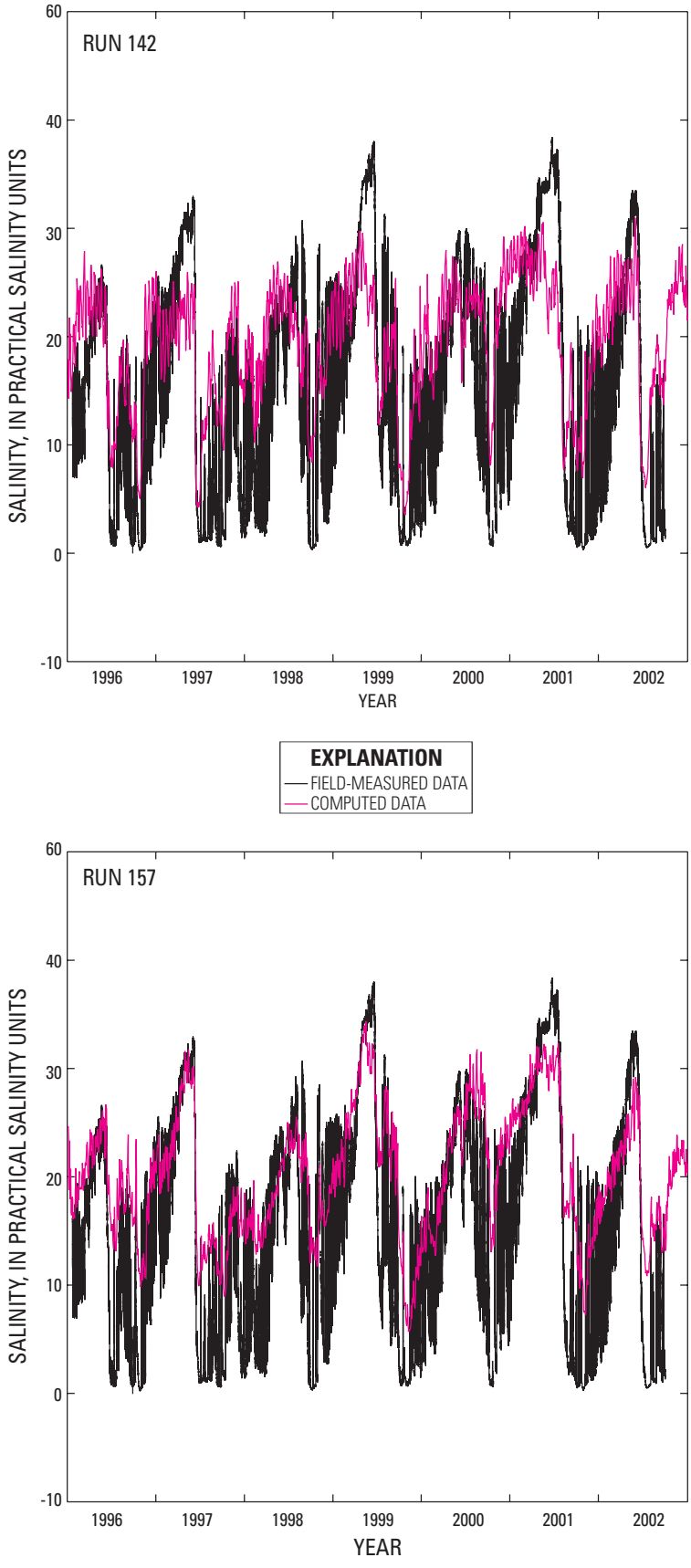

Figure 37. Comparison of salinities at Trout Creek for runs 142 and 157.

Model (SFWMM). This is implemented in a similar fashion to the SFWMM/SICS application link described in Wolfert and others (2004) and shown in appendix 1. The effects of restoration changes on stages, flows, and hydroperiods in the TIME domain can then be evaluated and ecologic implications determined. As shown in figure 2, the results of the TIME simulated scenarios can be used to supply coastal freshwater flow information for the Florida Bay Hydrodynamic model. The TIME application functions as an important representation of the interface between the inland region, represented by the SFWMM, and Florida Bay.

4 - Summary

The effort to develop numerical models to represent the inland and coastal areas of the Everglades has led to the development of the FTLOADDS model code, which couples the surface-water model SWIFT2D with the ground-water model SEAWAT. After a preliminary application to a small region of the coastal Everglades called SICS, the FTLOADDS code was applied, with further modifications, to the TIME domain—a larger region that includes practically all of Everglades National Park and the coastal waters. One purpose of developing TIME is to represent the complex coastal regime that lies between the South Florida Water Management Model (SFWMM), which represents restoration scenarios for the South Florida inland areas, and the Florida Bay hydrodynamic model.

A total of 157 seven-year TIME application runs were made for calibration and sensitivity analyses. Model output values used to evaluate calibration included: (1) wetlands water levels; (2) river stages and flows; (3) wetland surface-water depths, flows, and salinities; and (4) ground-water heads and salinities. Evaluations were made using statistics (mean bias, correlation, and percentage of explained variance), which indicated that the calibration fit is within the allowable error. This finding supports the use of the TIME application as a suitable tool to utilize input of boundary conditions developed from the regional SFWMM ecosystem restoration scenarios to determine the effects of these proposed changes to the hydrologic system.

Sensitivity studies of the TIME application were conducted by comparing output statistics between the calibrated application and a simulation with: (1) the model-code version used for SICS, (2) local adjustment of frictional resistance, (3) no leakage, (4) a road barrier removed, and (5) lowered land surface. The following were observed:

- The TIME application has improved capabilities compared to SICS, particularly in the representation of coastal flows. This result probably is due to a more computationally stable representation of the coastal creek outlets.
- Empirically manipulating frictional resistance values in inland areas improved water-level representation locally, but had a negligible effect on area-wide values. Because these changes have only local effects and are not physically based, they are not considered a valid representation of frictional resistance in the model.
- Neglecting leakage caused ground-water heads to differ substantially from measured values and reduced the overall accuracy of the model simulations. Surface-water stages changed slightly at most sites, indicating minimal ground-water influence, although substantial differences occurred occasionally.
- The incorporation of a major road as a complete barrier to flow influenced the local distribution and timing of flow; however, the differences in total flow and individual creekflows were negligible compared to simulations without the road barrier.
- Lowering the model land-surface altitude by 0.1 m produced mixed results; overall, the stage representation did not improve definitively.

These sensitivity tests led to a final calibration to improve the model fit at several locations. Incorporating the topography of Turner River and reporting computed stage in the river for comparison improved the fit in the northwestern corner of the TIME domain. An improved water-level fit was achieved by reducing the friction coefficient at the Taylor Slough Bridge boundary inflow point and increasing the coefficient just south of C-111 Canal. The ET extinction function was modified to improve the ground-water head response of the model during the dry season. Additional data were used for the ground-water head boundary along the southeastern part of C-111 Canal and the frictional resistance of Trout Creek outlet was increased; both steps improved the model fit to measured data for the total flow to Florida Bay and coastal salinities. Improved agreements also were obtained at the majority of water-level sites throughout the model domain. This final calibration also supports the use of the TIME application as a suitable tool for representing restoration scenarios.

5 - References Cited

Abtew, W., 1996, Evapotranspiration measurements and modeling for three wetland systems in South Florida: Water Resources Bulletin, v. 32, no. 3, p. 465-473.

Abtew, W., and Obeysekera, Jayantha, 1995, Lysimeter study of evapotranspiration of cattails and comparison of three estimation methods: Transactions of the American Society of Agricultural Engineers, v. 38, no. 1, p. 121-129.

Abtew, W., Obeysekera, Jayantha, Irizarry-Ortiz, M., Lyons, D., and Reardon, A., 2003, Evapotranspiration estimation for South Florida, *in* Bizier P., and DeBarry P.A., eds., World water environmental resources congress 2003: American Society of Civil Engineers and Environmental Water Resources Institute, Philadelphia, Pennsylvania, June 23-26, 2003.

Cohen, A.D., and Spackman, Jr., William, 1984, The petrology of peats from the Everglades and coastal swamps of southern Florida, *in* Gleason, P.J., ed., Environments of South Florida, present and past II: Miami Geological Society, p. 352-374.

Desmond, Greg, 2003, Measuring and mapping the topography of the Florida Everglades for ecosystem restoration: U.S. Geological Survey Greater Everglades science program: 2002 biennial report: U.S. Geological Survey Open-File Report 03-54, p. 31-32.

Eagleson, P.S., 1970, Dynamic Hydrology: New York, McGraw-Hill, 462 p.

Fish, J.E., and Stewart, M.T., 1991, Hydrogeology of the surficial aquifer system, Dade County, Florida: U.S. Geological Survey Water-Resources Investigations Report 90-4108, 53 p.

Fitterman, D.V., and Deszcz-Pan, M., 1998, Helicopter EM mapping of saltwater intrusion in Everglades National Park, Florida: Exploration Geophysics, v. 29, p. 240-243.

Fitterman, D.V., and Deszcz-Pan, M., 2002, Helicopter electromagnetic data from Everglades National Park and surrounding areas, Florida: Collected 9-14 December 1994: U.S. Geological Survey Open-File Report 02-101, 38 p.

Fitterman, D.V., Deszcz-Pan, Maria, and Stoddard, C.E., 1999, Results of time-domain electromagnetic soundings in Everglades National Park, Florida: U.S. Geological Survey Open-File Report 99-426.

German, E.R., 2000, Regional evaluation of evapotranspiration in the Everglades: U.S. Geological Survey Water-Resources Investigations Report 00-4217, 48 p.

Guo, Weixing, and Langevin, C.D., 2002, User's guide to SEAWAT: A computer program for simulation of three-dimensional variable-density ground-water flow: U.S. Geological Survey Techniques of Water-Resources Investigations, book 6, chap. A7, 77 p.

Hamrick, J.M., and Moustafa, M.Z., 2003, Florida Bay hydrodynamic and salinity model analysis: Joint Conference on the Science and Restoration of the Greater Everglades and Florida Bay Ecosystem "From Kissimmee to the Keys", April 13-18, 2003, Palm Harbor, Florida.

Hansen, M., and DeWitt, N.T., 1999, Modern and historical bathymetry of Florida Bay *in* Proceedings of the 1999 Florida Bay and Adjacent Marine Systems Science Conference, November 1-5 1999, Key Largo, Fla.

Harvey, J.W., Jackson, J.M., Mooney, R.H., and Choi, J., 2000, Interaction between ground water and surface water in Taylor Slough and vicinity, Everglades National Park, South Florida: Study methods and appendixes: U.S. Geological Survey Open-File Report 00-483, 67 p.

Holmes, C.W., Robbins, John, Halley, R.B., Bothner, Michael, Tenbrink, Marilyn, and Marot, M., 2000, Sediment dynamics of Florida Bay mud banks on a decadal time scale: U.S. Geological Survey Program on the South Florida Ecosystem: 2000 Proceedings of the Greater Everglades Ecosystem Restoration (GEER) Conference, December 11-15, 2000: U.S. Geological Survey Open-File Report 00-449.

Intergovernmental Panel on Climate Change, 2001, Climate change 2001: The scientific basis: United Kingdom and New York, Cambridge University Press, 881 p.

Jacobs, J.M., and Sudheer, R.S., 2001, Evaluation of reference evapotranspiration methodologies and AFSIRS crop water use simulation model. Final report John M. Fitzgerald, Water Use Data Manager Division of Water Supply Management St. Johns River Water Management District Palatka, Florida. Department of Civil and Coastal Engineering University of Florida Gainesville, Florida. SJRWMD Contract Number: SD325AA. UF Contract Number: 4504771, April 2001.

Langevin, C.D., Swain, E.D., and Wolfert, M.A., 2004, Simulation of integrated surface-water/ground-water flow and salinity for a coastal wetland and adjacent estuary: U.S. Geological Survey Open-File Report 2004-1097, 30 p.

Langevin, C.D., Swain, E.D., and Wolfert, M.A., 2005, Simulation of integrated surface-water/ground-water flow and salinity for a coastal wetland and adjacent estuary: Journal of Hydrology v. 314, p. 212-234.

Large, W.G., and Pond, S., 1981, Open ocean momentum flux measurements in moderate to strong winds: Journal of Physical Oceanography, v. 11, p. 324-336.

Lee, J.K., and Carter, Virginia, 1999, Field measurement of flow resistance in the Florida Everglades: Proceedings of the South Florida Restoration Science Forum: May 17-19, 1999, Boca Raton, Florida: U.S. Geological Survey Open File Report 99-181.

Linsley, R.K. Jr., Kohler, M.A., and Paulhus, J.L.H., 1982, Hydrology for Engineers: New York, McGraw-Hill, p. 162-163.

Nemeth, M.S., Wilcox, W.M., and Solo-Gabriele, H.M., 2000, Evaluation of the use of reach transmissivity to quantify leakage beneath Levee 31N, Miami-Dade County, Florida: U.S. Geological Survey Water-Resources Investigations Report 00-4066.

Oke, T.R., 1978, Boundary Layer Climates: London, Methuen, 350 p.

Perrier A., and Tuzet A., 1991, Land surface processes: description, theoretical approaches, and physical laws underlying their measurements, *in* Schmugge. J., and Andre, J-C., eds., Land surface evaporation: Measurement and parameterization: New York, Springer, p. 145-155.

Prager, E.J., and Halley, R.B., 1997, Florida Bay bottom types: U.S. Geological Survey Open-File Report 97-526, 1 sheet.

Reese, R.S., and Cunningham, K.J., 2000, Hydrogeology of the gray limestone aquifer in southern Florida: U.S. Geological Survey Water-Resources Investigations Report 99-4213, 244 p.

Schaffranek, R.W., 2004, Simulation of surface-water integrated flow and transport in two dimensions: SWIFT2D user's manual: U.S. Geological Survey Techniques and Methods, book 6, chap B-1, 115 p.

Scheidt, D., Stober, J., Jones, R., and Thorton, K., 2000, South Florida Ecosystem Assessment: Everglades Water Management, Soil Loss, Eutrophication, and Habitat: U.S. Environmental Protection Agency Report 904-R-00-003.

Shoemaker, W.B., Sumner, D.M., Castillo, A., 2005, Estimating changes in heat energy stored within a column of wetland surface water and factors controlling their importance in the surface energy budget: Water Resources Research, v. 41, W10411.

Stannard, D.I., 1993, Comparison of Penman-Monteith, Shuttleworth-Wallace, and modified Preistley-Taylor evapotranspiration models for wildland vegetation in semiarid rangeland: Water Resources Research, v. 29, no. 5, p. 1379-1392.

Stewart, M.A., Bhatt, T.N., Fennema, R.J., and Fitterman, D.V., 2002, The road to flamingo: An evaluation of flow pattern alterations and salinity intrusion in the lower glades, Everglades National Park: U.S. Geological Survey Open-File Report 02-0059, 36 p.

Swain, E.D., 2005, A model for simulation of Surface-Water Integrated Flow and Transport in Two Dimensions: User's guide for application to coastal wetlands: U.S. Geological Survey Open-File Report 2005-1033, 88 p.

Swain, E.D., Wolfert, M.A., Bales, J.D., and Goodwin, C.R., 2004, Two-dimensional hydrodynamic simulation of surface-water flow and transport to Florida Bay through the Southern Inland and Coastal Systems (SICS): U.S. Geological Survey Water-Resources Investigations Report 03-4287, 56 p., 6 pls.

U.S. Army Corps of Engineers, 1999, CORPSCON v4.1 Technical documentation and operating instructions: Accessed on Nov. 2, 2006, at *http://www.iep.ca.gov/pub/corpscon/corpscon.doc*

U.S. Army Corps of Engineers and South Florida Water Management District, 2003, A Vision Statement for the Comprehensive Everglades Restoration Plan: accessed on Oct. 1, 2006, at *http://www.evergladesplan.org/pm/program_docs/cerp_vision_statement.cfm*

Wolfert, M.A., Langevin, C.D., and Swain, E.D., 2004, Assigning boundary conditions to the Southern Inland and Coastal Systems (SICS) model using results from the South Florida Water Management Model (SFWMM): U.S. Geological Survey Open-File Report 2004-1195, 30 p.

Worth, Dewey, Weaver, Cecella, and Trulock, Shelly, 2002, Florida Bay and Florida Keys Feasibility Study Overview: Accessed on Oct. 1, 2006, at *http://www.evergladesplan.org/docs/fs_fl_bay_feas_hires.pdf*